Title
Preclinical Studies on Viro-Immunotherapy for Brain Tumors

Author
Kato, Yuki

Publication Date
2016

Peer reviewed|Thesis/dissertation

UNVERSITY OF CALIFORNIA

Los Angeles

Preclinical Studies on Viro-Immunotherapy for Brain Tumors

A dissertation submitted in partial satisfaction of the requirements for the degree

Doctor of Philosophy in Molecular and Medical Pharmacology

by

Yuki Kato

2016

ABSTRACT OF THE DISSERTATION

Preclinical Studies on Viro-Immunotherapy for Brain Tumors

By

Yuki Kato

Doctor of Philosophy in Molecular and Medical Pharmacology

University of California, Los Angeles, 2016

Professor Noriyuki Kasahara, Co-Chair

Professor Robert M. Prins, Co-Chair

Retroviral replicating vectors (RRV) are capable of tumor-selective replication and stable integration into the cancer cell genome, and are currently under investigation for prodrug activator gene therapy of recurrent high grade glioma in phase II/III clinical trials. In preclinical studies evaluating RRV gene therapy in intracranial glioma models, we showed effective long-term tumor control in human glioma xenograft models as long as prodrug administration was continued. In contrast, tumor eradication was achieved even after cessation of prodrug administration in immunocompetent syngeneic glioma models. Accordingly, my research has focused on investigating the immunological mechanisms involved in RRV gene therapy, and evaluating combined viro-immunotherapy approaches to improve RRV-mediated tumor transduction and therapeutic efficacy, as well as to confer a dominant foreign antigen to be targeted by adoptively transferred T cells.

RRV replication may be delayed at lower inoculation doses, if initial distribution is confined to the area surrounding an intratumoral injection site. More rapid tumor transduction may be achieved if the inoculum is distributed more evenly within the tumor. Alloreactive cytotoxic T lymphocytes (alloCTL) are migratory cells trained to react to major histocompatibility complex (MHC) that are selectively displayed on gliomas. Combining alloCTL and RRV gene therapy as individual therapies showed added benefit compared to either modality alone. We further tested the use of alloCTL as vector producer cells to deliver marker and suicide genes to tumors after their transduction with RRV (alloCTL/RRV). When compared against either therapy alone in a subcutaneous glioma model, the greatest benefit was achieved by alloCTL/RRV. This suggests that alloCTL/RRV can serve as anti-tumor effector cells targeting endogenous antigens, as well as motile 'carriers' that facilitate spread of RRV to tumor cells.

Aside from MHC, there are few well-characterized / immunogenic tumor-associated antigens with defined epitopes in glioblastoma. The efficient spread and permanent genomic integration of RRV can be utilized to induce stable expression of viral antigens that may represent useful immunotherapeutic targets. We developed an RRV displaying the lymphocytic choriomeningitis virus glycoprotein gp33-43 (gp33) epitope fused to the viral *env* gene. Target cell-specific cytotoxicity by transgenic lymphocytes engineered with a T cell receptor recognizing the gp33 epitope (P14 cells) was observed in vitro and in vivo. P14 adoptive transfer in immunocompetent hosts increased survival. Thus, the use of RRV to deliver highly immunogenic viral antigens to glioma could enable more effective immunotherapy for this disease.

The dissertation of Yuki Kato is approved.

Samson A. Chow

Ting-ting Wu

Jerome A. Zack

Robert M. Prins, Committee Co-Chair

Noriyuki Kasahara, Committee Co-Chair

University of California, Los Angeles

2016

DEDICATION

For my parents and relatives, who gave me endless support to let me pursue my goals far away from home. Thank you for everything.

TABLE OF CONTENTS

LIST OF FIGURES AND TABLES

CHAPTER ONE

CHAPTER TWO

CHAPTER THREE

ACKNOWLEDGEMENTS

The work for this dissertation was performed under the direction of Dr. Noriyuki Kasahara, the late Dr. Carol Kruse, and Dr. Robert Prins

Chapter One

Chapter One is adapted from Hiraoka K,* Inagaki A,* Kato Y, Huang T, Kamijima S, Takahashi M, Matsumoto H, Hacke K, Kruse CA, Ostertag D, Gruber HE, Jolly DJ, Robbins JM, Kasahara N. Retroviral Replicating Vector-Mediated Prodrug Conversion Achieves Long-Term Control of Tumor Recurrence and Leads to Durable Anti-Cancer Immunity (manuscript in preparation).

*K. Hiraoka and A. Inagaki contributed equally to this paper.

Authors' Contributions: KH and AI designed, performed, and analyzed experiments, and wrote manuscript. YK, TTH, SK, MT, HM, and KH performed and analyzed experiments. CAK, DO, HEG, and DJJ supervised analysis and edited manuscript. JMR and NK designed, oversaw and interpreted experiments and wrote manuscript.

Chapter Two

Chapter Two is adapted from:

Hickey MJ, Malone CC, Erickson KL, Lin A, Soto H, Ha ET, Kamijima S, Inagaki A, Takahashi M, Kato Y, N Kasahara, Mueller BM, Kruse CA. Combined Alloreactive CTL Cellular Therapy With Prodrug Activator Gene Therapy in a Model of Breast Cancer Metastatic to the Brain. *Clinical Cancer Research.* 19(15): 4137-4148 (2013).

Authors' Contributions: MJH designed, performed, analyzed experiments, and wrote manuscript. HS, KLE, CCM, AL, EH, SK, MT, AI, and YK supervised analysis, performed and analyzed experiments,

and edited manuscript. CAK, NK, and BMM designed, oversaw and interpreted experiments and wrote manuscript.

Erickson KL, Hickey MJ, Kato Y, Malone CC, Owens GC, Prins RM, Liau LM, Kasahara N, Kruse CA. Radial Mobility and Cytotoxic Function of Retroviral Replicating Vector Transduced, Non-Adherent Alloresponsive T Lymphocytes. *Journal of Visual Experiments.* (96) (2015).

Authors' Contributions: KLE and MJH designed, performed, analyzed experiments, and wrote manuscript. YK and CCM supervised analysis, performed and analyzed experiments, and edited manuscript. GCO, RMP, LML, NK, and CAK oversaw and interpreted experiments and wrote manuscript.

Haga K, Lin A, Hickey MJ, Gomez GG, Malone CC, Erickson KL, Kimura T, Hiraoka K, Kato Y, Kamijima S, Logg CR, Kruse CA, Kasahara N. Improving Therapeutic Efficacy in Experimental Glioma by Combining Alloreactive T Cell-Mediated Adoptive Immunotherapy with Retroviral Replicating Vector-Mediated Gene Therapy (manuscript in preparation).

Authors' Contributions: KH and AL designed, performed, analyzed experiments, and wrote manuscript. GGG, CCM, KLE, TK and KH supervised analysis, performed and analyzed experiments. YK and SK analyzed and wrote manuscript. CRL, CAK, and NK oversaw and interpreted experiments and wrote manuscript.

Chapter Three

Chapter Three is adapted from Kato Y, Scharnweber R, Inagaki A, Soto H, Sedighim S, Hermann K, Kamijima S, Hickey MJ, Treger J, Lisiero D, Everson R, Antonios J, Liau LM, Klatzmann D, Prins R,

Kasahara N. Retroviral Replicating Vector-Mediated Delivery of an Immunodominant Neo-antigen Epitope Target for Viro-Immunotherapy in Experimental Glioma (manuscript in preparation).

We would like to thank Dr. David Brooks for providing us with P14 T cell receptor transgenic mice.

I would like to thank Japan Student Services Organization (JASSO) for tuition funds and scholarship throughout my entire graduate career.

VITA

Education

2013 B.A., Biology

International Christian University

Mitaka City, Tokyo, Japan

Publications and presentations

Erickson KL, Hickey MJ, Kato Y, Malone CC, Owens GC, Prins RM, Liau LM, Kasahara N, Kruse CA. Radial mobility and cytotoxic function of retroviral replicating vector transduced non-adherent alloresponsive T lymphocytes. *J Vis Exp.* 2015 Feb 11;(96).

Hickey MJ, Malone CC, Erickson KL, Lin A, Soto H, Ha ET, Kamijima S, Inagaki A, Takahashi M, Kato Y, Kasahara N, Mueller BM, Kruse CA. Combined alloreactive CTL cellular therapy with prodrug activator gene therapy in a model of breast cancer metastatic to the brain. *Clin Cancer Res.* 2013 Aug 1;19(15):4137-48.

Yuki Kato, Rudi Scharnweber, Akihito Inagaki, Horacio Soto, Shaina Sedighim, Kip Hermann, Shuichi Kamijima, Michelle Hickey, Janet Treger, Dominique Lisiero, Richard Everson, Joe Antonios, Hideho Okada, Linda Liau, David Klatzmann, Robert Prins, Noriyuki Kasahara. Retroviral replicating vector-mediated delivery of an immunodominant neo-antigen epitope target for viro-immunotherapy in experimental glioma (manuscript in preparation).

*Kei Hiraoka, *Akihito Inagaki, Yuki Kato, Shuichi Kamijima, Hiroshi Matsumoto, Carol A. Kruse, Harry E. Gruber, Derek Ostertag, Tiffany T. Huang, Douglas J. Jolly, Joan M. Robbins, Noriyuki Kasahara. Retroviral replicating vector-mediated prodrug conversion achieves long-term control of tumor recurrence and leads to durable anti-cancer immunity (manuscript in preparation) (*authors contributed equally).

Kazunori Haga, Amy H. Lin, Michelle J. Hickey, German G. Gomez, Colin C. Malone, Kate E. Erickson, Takahiro Kimura, Kei Hiraoka, Yuki Kato, Shuichi Kamijima, Christopher R. Logg, Carol A. Kruse, Noriyuki Kasahara. Improving therapeutic efficacy in experimental glioma by combining alloreactive T cell-mediated adoptive immunotherapy with retroviral replicating vector-mediated gene therapy (manuscript in preparation).

Kato Y, Scharnweber R, Inagaki A, Kamijima S, Hickey M, Lisiero D, Hermann K, Soto H, Antonios J, Sedighim S, Okada H, Liau L, Klatzmann D, Prins R, Kasahara N. "Retroviral replicating vector-mediated delivery of an immunodominant neo-antigen epitope target for viro-immunotherapy in experimental glioma." Society for Neuro-Oncology. San Antonio, TX, 2015.

Kato Y, Hickey MJ, Treger J, Erickson KL, Haga K, Malone CC, Inagaki A, Kruse CA, Kasahara N. "RRV-mediated prodrug activator gene therapy combined with alloreactive T cell immunotherapy for malignancies in the CNS." International Society of Cellular Therapy. Las Vegas, NV, 2015.

Kato Y, Hickey MJ, Erickson KL, Haga K, Malone CC, Inagaki A, Kruse CA, Kasahara N. "Adoptive T cell immunotherapy using alloreactive CTL combined with RRV-mediated prodrug activator gene therapy in experimental glioma." Japan Society of Gene Therapy. Tokyo, Japan, 2014.

Introduction

Glioblastoma is the most common form of primary brain cancer, with over 16,000 people diagnosed every year in the United States [1]. The disease is extremely aggressive; newly diagnosed patients have a five-year survival rate of less than 5 percent, and the tumor typically recurs following standard-of-care (SOC) treatment of surgery, radiation, and chemotherapy. There is no SOC for recurrent disease, and the median survival following recurrence is approximately eight months. Drugs approved by the U.S. Food and Drug Administration (FDA) include temozolomide, bevacizumab, and lomustine, which only modestly extend survival or improve disease related symptoms at best. The lack of effective therapies makes development of new approaches most critical.

One new therapeutic approach that shows promise is oncolytic virotherapy, which involves the use of tumor-selectively replicating viruses. Recently, *talimogene laherparepvec* (T-VEC; Imlygic), an oncolytic Herpes simplex virus engineered to express the immunocytokine GM-CSF, showed a statistically significant survival benefit compared to GM-CSF alone in Phase III clinical trials for advanced stage melanoma, and became the first oncolytic virus product to be approved in the United States.

Most viruses currently being clinically evaluated as oncolytic agents have some tumor specificity due to cancer cell-intrinsic defects in innate immunity and local suppression of adaptive immunity in the tumor microenvironment [2, 3, 4]. As wild type strains of these viruses can infect and lyse normal cells as well as tumor cells, many of these oncolytic agents are attenuated or tumor-targeted at the level of cell entry and/or viral replication. As these immunogenic viruses spread by cytolysis, they also destroy the tumor microenvironment that was shielding them from the immune system as they replicate, and this ends in a race to try to cause as much damage to the tumor as possible, and induce anti-tumor immunity, before viral clearance occurs [5].

Unique among replicating viruses being developed as anticancer agents, gamma retroviruses, specifically murine leukemia virus (MLV)-based retroviral replicating vectors (RRV) maintain viral persistence in tumors through the combined characteristics of non-lytic replication, stable integration into the cancer cell genome, and reduced viral immunogenicity [6, 7, 8]. As an integrating virus, MLV replicates without causing cytolysis, and while neutralizing immune responses can occur systemically, injection of MLV into brain causes only minor local inflammation without any associated neuropathology [9, 10]. Also, MLV lacks signals for active uptake into nuclei in quiescent cells, and only integrates into the host genome when the nuclear membrane dissolves during mitosis[11]. In fact, this absolute selectivity for actively dividing cells was the original rationale for using gamma retroviral vectors in cancer gene therapy, particularly in the context of tumors within the quiescent brain[12].

We [13, 14, 15, 16, 17, 18, 19, 20, 21, 22] and others [23, 24, 25, 26] have found that RRV can efficiently transduce and stably propagate in a variety of cancer cell lines in vitro and tumor models in vivo, resulting in tremendous in situ amplification from a small inoculum. After intratumoral injection of RRV at multiplicities of infection (MOI, i.e., virus:glioma cell ratios) as low as 0.01 into pre-established intracranial brain tumor models, >98% transduction can be achieved throughout the entire tumor mass after a few weeks [17, 19, 20, 24, 25]. In contrast, tumor transduction levels were ≤ 1% after injecting the same dose of conventional non-replicating retroviral vectors [20, 25].

The use of retroviral replicating vectors (RRV) represents a novel gene delivery platform technology that achieves a significant enhancement in transduction efficiency and therapeutic efficacy of gene therapy for cancer. The feasibility of engineering RRV to achieve highly efficient gene delivery has already been established, and due to the intrinsic inability of the virus to infect post-mitotic normal cells, as well as innate and adaptive immunity which are intact in normal tissues but suppressed in tumors, RRV spread after injection is highly restricted to the tumor tissue itself in immunocompetent hosts. This holds true not only for intratumorally injected RRV but also when injected locoregionally and intravenously.

Furthermore, RRV achieve persistent infection of solid tumors in vivo, thereby allowing the virus to track tumor cells even as they migrate and form invading tumor foci.

Since retroviruses are not intrinsically cytolytic, RRV can be engineered with a prodrug activator ("suicide") gene such as yeast cytosine deaminase (yCD), which generates 5-fluorouracil (5-FU) directly within cancer cells from its precursor 5-fluorocytosine (5-FC), an anti-fungal agent approved for clinical use and commonly used to treat CNS fungal infections. The specific tumor transduction achieved by these replicating vectors then translates into significant therapeutic benefit after 5-FC administration in both human xenograft intracranial tumor models [19, 20, 21] and syngeneic rodent intracranial tumor models [17, 22]. The prodrug activator gene is stably seeded throughout the tumor as the virus replicates unimpeded, as anti-viral immune responses are not triggered by its non-lytic replication, and simultaneous killing of infected cancer cells is activated by administration of the prodrug.

Since the anti-cancer drug is generated directly within the infected cancer cells, systemic side effects seen with systemic chemotherapy such as myelotoxicity are avoided, and the immune system remains intact. Furthermore, generation of 5-FU locally within the tumor microenvironment should not only achieve direct killing of cancer cells and release of tumor antigens, but bystander effects should also result in destruction of immunosuppressive components of the tumor, such as myeloid-derived suppressor cells. Theoretically, therefore, this should facilitate the development of anti-tumor immunity.

Notably, the induction of anti-tumor immunity by highly immunogenic cytolytic viruses used as oncolytic agents has increasingly been recognized as playing a major role in their mechanism of action. However, a detailed analysis of whether immunological anti-tumor responses contribute to the therapeutic efficacy of RRV-mediated prodrug activator gene therapy has been lacking.

Here, the role of the immune system in RRV suicide gene therapy was dissected, in order to better understand the mechanism by which the treatment achieves long-term therapeutic benefit, and to

determine whether anti-tumor immunity and immunological memory are induced. First, RRV-mediated prodrug activator gene therapy was compared between orthotopic intracranial gliomas in immunodeficient vs. immunocompetent hosts, established using human xenograft tumors in nude mice vs. syngeneic murine tumors in B6/C3 F1 mice. This study was unique compared to previously published studies in employing bioluminescence imaging at serial time points, and demonstrated that, in the immunodeficient model, long-term tumor control could be achieved with successive prodrug cycles, but tumors could not be completely eradicated. In contrast, in the immunocompetent model, tumor signals became undetectable, and no recurrence was observed even after cessation of prodrug, indicating that complete tumor eradication had been achieved. This was also the first study to perform further detailed immunological analysis, indicated the role of CD4+ effector cells in mediating anti-tumor immunity.

Based on this and other encouraging preclinical results, the use of RRV in high grade glioma (HGG), which includes glioblastomas and anaplastic astrocytomas, is being investigated in the clinical setting. More than 100 HGG patients have been injected with RRV to this date, and all have tolerated the treatment well, as no significant drug-related toxicity was observed. Due to highly promising results from Phase I dose escalation trials including radiological evidence of tumor responses and increased overall survival, it is currently being tested in pivotal phase II/III clinical trials looking at overall survival as its primary endpoint, and is expected to enroll 170 patients across 80 sites globally (NCT02414165).

RRV replication may be delayed, however, especially at lower inoculation doses, if initial distribution is confined to the immediate area surrounding a single intratumoral injection site. Furthermore, dose-response studies have shown that an adequate initial inoculum of vector needs to be delivered to sustain robust virus replication, and intratumoral spread is more efficient if the virus is distributed more evenly throughout the tumor at the outset. The Kruse laboratory has developed an immunotherapy approach employing intratumoral administration of alloreactive cytotoxic T lymphocytes (alloCTL). AlloCTL are trained to react to patient human leukocyte antigens (HLA) that are absent on normal neuroglia [27, 28, 29], but displayed on gliomas [27, 30, 31]. Thus, alloCTL adoptively transferred intratumorally at a high effector to

target (E:T) cell ratio can achieve selective allorecognition and efficient killing of glioma cells, mediating a localized immunorejection effect. In addition, alloCTL are motile and may act as RRV producers when transduced. These alloCTL/RRV should not only be capable of directly attacking tumor cells at high E:T ratios through their natural mechanisms of allo-rejection, but even at very low E:T ratios should still release RRV and mediate multifocal dissemination of virus within the tumor cell population, thereby initiating rapid viral propagation. While these two therapies are each potently cytoreductive by themselves, the combination of the two, timed appropriately, may achieve enhanced efficacy.

However, alloCTL may still have a limited lifespan in the host, and also is ineffective towards HLA-downregulated glioma. Aside from HLA, there are few well-characterized, highly immunogenic tumor-associated antigens with defined epitopes in glioblastoma. The Prins laboratory has previously identified how a prototypic viral antigen expressed by one glioblastoma patient's tumor lysate could effectively prime a tumor-viral T cell response when such lysate was used to pulse dendritic cells [32]. The highly efficient spread of RRV throughout the tumor can be utilized to induce stable expression and robust presentation of viral antigens that may represent useful immunotherapeutic targets, in effect "xenogenizing" the tumor. Thus, the use of RRV to deliver highly immunogenic viral antigens to glioma could enable more effective immunotherapy for this disease.

Some of the advantages of using immunotherapy for treating brain tumors include its high specificity and its ability to access infiltrating tumor cells. Here, we explored the use of alloCTL as motile RRV producer cells, as well as the ability of RRV to deliver foreign epitopes to target tumor cells.

Chapter One: Retroviral replicating vector-mediated gene therapy achieves long-term control of tumor recurrence and leads to anti-cancer immunity

Introduction

For clinical trials, a new retroviral replicating vector (RRV) construct, Toca 511 (*vocimagene amiretrorepvec*), containing multiple modifications in the virus backbone and a codon-optimized and temperature-stabilized yCD transgene [33], has been developed. This new RRV was found to exhibit higher level of genomic stability over serial infection cycles, and showed a 3-fold higher level of 5-FC to 5-FU conversion activity than the original RRV vector expressing yCD, further enhancing therapeutic potency. Toca 511 and Toca FC, an extended release formulation of 5-FC, is currently being evaluated in first-in-human clinical trials of RRV-mediated prodrug activator gene therapy in patients with recurrent high-grade glioma (HGG), with the vector administered in one of three ways: via stereotactic intra-tumoral injection; via injection into the walls of the resection cavity; or most recently, via intravenous infusion (clinicaltrials.gov: NCT01156584, NCT01470794, NCT01985256, respectively). Current outcomes show the treatment is well tolerated to date and has encouraging signs of clinical activity, including radiological and functional improvement, and an increase in median overall survival compared to historical controls[34, 35]. An international phase 2/3 randomized trial studying Toca 511 and Toca FC versus standard of care in recurrent HGG is now underway (NCT02414165).

In the studies reported herein, we have further investigated the mechanisms underlying the therapeutic efficacy of Toca 511 followed by 5-FC (Toca 511+5-FC) in both subcutaneous and intracranial xenograft models of human glioma and syngeneic models of murine glioma. Previous studies in immunodeficient xenograft models suggested that, although long-term tumor control could be achieved, this was dependent upon continued administration of prodrug using a cyclic dosing schedule.

In contrast, prodrug could be discontinued after a few cycles without further recurrence in immunocompetent syngeneic models.

Our results definitively demonstrate that, although RRV itself is not highly immunogenic [7], the therapeutic efficacy of direct tumor cell killing after Toca 511+5-FC treatment as demonstrated in the immunodeficient tumor model is significantly augmented by induction of anti-cancer immunity in the immunocompetent tumor model. In this model, the ability of RRV-mediated local intratumoral production of a cytotoxic drug to mediate tumor mass reduction without systemic myelotoxicity permits the development of durable immunorejection responses directed against endogenous tumor antigens, contributing to apparent complete eradication of residual disease.

Materials and Methods

Cell culture

Transformed human embryonic kidney cell line 293T and human glioma cell line U-87 MG (U-87) were obtained from American Type Culture Collection, and murine glioma cell line Tu-2449 was kindly provided by Dr. Walter Günzburg (University of Veterinary Medicine, Vienna). Tu-2449, derived from a spontaneous tumor in GFAP-v-src-transgenic mice, has morphological features and growth characteristics of intracranial gliomas [36, 37], as does Tu-2449SC derived by subcutaneous passage of Tu-2449. All cell lines were maintained in Dulbecco's modified Eagle's medium (DMEM) supplemented with 10% fetal bovine serum and 1% penicillin–streptomycin, and maintained in a humidified atmosphere with 5% CO_2.

Viral vector plasmid, virus production, and titer determination

The plasmids pAC3-GFP and pAC3-yCD2 have been described previously [33] (Fig. 1A). AC3-GFP virus production in 293T cells has been described [13, 14]. Toca 511 virus production in a human fibrosarcoma cell line, purification and concentration has been described [17]. Viral titers were determined as described previously [33]. Viral titers were determined on PC-3 human prostate adenocarcinoma cells (purchased from American Type Culture Collection) as described previously [33] and calculated according to the formula: transducing units (TU) /ml = (number of cells counted immediately before infection × percentage of transduced cells reported from qPCR analysis)/dilution factor of viral supernatant, and typical titers were around 5x10^6 transduction units (TU)/ml in supernatant media after transient transfection.

The self-inactivating (SIN) lentiviral vector in this study was derived from the pRRL-sin-cPPT-hCMV-MCS-pre vector and firefly luciferase cDNA was inserted in the multiple cloning site of the vector

as described previously [13]. Virus was produced by transient cotransfection of 293T cells and titers were determined by measuring viral p24 antigen concentration by ELISA (Coulter Immunotech).

Replication kinetics of RRV in vitro

For analysis of replication kinetics in vitro, 2x10^3 TU of AC3-GFP or Toca 511 virus vector was used for infection of 4x10^5 cells of U-87 or Tu-2449 cells at MOI of 0.005. Polybrene (4 μg/ml; Sigma) was added to all cultures before infection. At serial time points, the cells were trypsinized, one-fourth was replated, and the remainder analyzed for GFP expression by flow cytometry and for viral copy number by genomic qPCR. As nonreplicating controls, 50 μmol AZT was added to the culture medium on day 3 of RRV infected cells to prevent virus spread. A stably transduced cell population that reached 100% transduction with AC3-GFP or Toca 511 was maintained for further experiments.

Quantitative real-time PCR analysis

The quantitative analysis of RRV copy number in the infected cells was performed as described previously [13]. For quantitative analysis of RRV copy number in the infected cells, genomic DNA was extracted from cultured cells, tissues, and tumors using the DNeasy tissue kit (Qiagen). To detect integrated RRV proviral sequences, qPCR was done in a reaction mixture containing TaqMan Universal PCR Master Mix (PE Applied Biosystems) using a My-iQ2 (BIO-RAD) thermal cycler. A reference curve for retrovirus copy number was prepared by amplifying serial dilutions of plasmid pAC3-yCD2 in a background of genomic DNA from untransduced cells. The threshold for vector detection was determined by a control sample with no viral DNA. The primers and probe were designed to target the 4070A amphotropic env gene, and human RNase P or mouse β-actin was also quantified as an internal control gene. To evaluate Toca 511 biodistribution in normal organs, tissues (lung, heart, liver, spleen,

kidney, esophagus, intestine, ovary, bone marrow, left forebrain and right forebrain) were harvested from all of the cured mice (Toca 511+5-FC group in Fig.2A and D) from the intracranial survival study. Detection limit of less than 40 copies per 1x10^5 cells was determined based on non-specific copy number of individual uninfected control organ. Relative copy number = 4070A copy number / cell equivalent as measured by mouse β-actin or RNase P copy number. Additionally, qPCR analysis of firefly luciferase sequences to detect the presence of any residual tumor cells was performed on left and right forebrain genomic DNA. Firefly luciferase primers: Left CTAAGGTGGTGGACTTGGACA, Right CGATGAGAGCGTTTGTAGCC, HYB Oligo CATGAGCGGCTACGTTAACA FAM.

Cytotoxicity assay in vitro

Cell viability was determined using a tetrazolium dye conversion MTS assay (Promega). To assess drug cytotoxicity in glioma cell lines, triplicate wells containing parental glioma cells, cells fully transduced with AC3-GFP, or cells fully transduced with Toca 511 (2x10^3 cells / well) were cultured in 96-well plates with various concentrations of 5-FC. On day 9, dye conversion was measured using an ELISA plate reader at 490 nm after 2 h incubation at 37ºC. Cytotoxicity was determined by calculation of the absorbance of viable cells as measured against wells without 5-FC.

Major Histocompatibility Complex (MHC) expression in Tu-2449 cells

Prior to analyses, Tu-2449 cells were cultured for 24hr with or without murine IFN-γ (10ng/mL). Cells were then dissociated with 10mM EDTA, washed, and stained with antibodies directed against MHC class I H-2Db (BD Pharmingen), H-2Kb (eBioscience), or respective isotype controls, and analyzed on a FACScanto flow cytometer (Becton-Dickinson). MHC-positive populations were gated based on isotype

controls. Percentage of positive cells and median fluorescence intensity (MFI) were calculated using the FlowJo software.

U-87 or Tu-2449 subcutaneous tumor models

Six to eight-week-old female nude mice (Hsd:Athymic Nude-Foxn1nu , Harlan, IN) or B6C3F1/J immunocompetent mice (Jackson laboratory, ME) were bred and maintained under specific pathogen-free conditions, and all studies conducted under protocols approved by the UCLA Animal Research Committee. For subcutaneous (s.c.) tumor models, 2% U-87 or Tu-2449SC (s.c. growth adapted subline) cells fully transduced with RRV were mixed with 98% uninfected parental cells, and these cell mixtures (2x10^6 cells) in 100 µl PBS were injected s.c. into the right dorsal flanks of athymic nude or B6C3F1/J mice, respectively.

For quantification of transduction efficiency in vivo, tumor tissues were excised, minced, separated from extraneous tissue under sterile conditions, and digested with collagenase/dispase (1 mg/mL; Roche Diagnostics) for 2 h at 37ºC. Dissociated cells were passed through a 100-µm cell strainer, washed in PBS, and plated on 6-well plates. After 24 h culture with AZT, the cells were trypsinized and analyzed by flow cytometry for GFP expression or by genomic qPCR for viral copy number. As control cells, tumor cells from mice injected with parental non-transduced cells were used.

For prodrug-activator gene therapy in s.c. tumor models, intraperitoneal i.p. administration of 5-FC (500 mg/kg, daily) or PBS (800 µl, daily) was started 17 days after tumor cell inoculation. Tumor sizes were measured every 3-4 days and tumor volumes were calculated by this formula: volume (mm3) = length x width2/2. These experiments were terminated once at least one of the s.c. tumors in each group reached >15 mm in diameter per institutional guidelines.

Optical imaging analysis

Bioluminescence in cultured cells or live mice was examined by optical imaging using a CCD system (IVIS Lumina II; Caliper Life Sciences). Gray-scale background photographic images of the tissues were overlaid with color images of bioluminescent signals using Living Image software (Caliper Life Sciences). For in vitro imaging, firefly luciferase expression in U-87 or Tu-2449 cells after lentiviral vector transduction (MOI 10) was confirmed with the IVIS system after addition of D-luciferin (150 µg/well). For in vivo imaging, mice were anesthetized with ketamine (100 mg/kg) and xylazine (10 mg/kg), and 5 min after i.p. administration with D-luciferin (126 mg/kg), bioluminescent signals were analyzed with the IVIS system with a 1 min acquisition time.

Prodrug activator gene therapy in intracranial tumor models

To establish intracranial gliomas, U-87 (1x10^5 cells / 2 µl) or Tu-2449 (1x10^4 cells / 2 µl) were stereotactically injected into the right frontal lobe in nude mice or B6C3F1/J mice, respectively, as described previously [20]. In U-87 tumor models, Toca 511 vector (low dose: 3.4x10^4 TU or high dose: 2x10^6 TU / 10 µl) was given by stereotactic injection 5 days after tumor cell inoculation, and daily intraperitoneal (i.p.) administration of 5-FC (500 mg/kg once-daily or twice-daily) or PBS was started 18 days after tumor cell inoculation for 7 consecutive days. This 7-day cycle of prodrug or vehicle administration was repeated at intervals of every 1-2 weeks. In Tu-2449 tumor model studies conducted at UCLA, Toca 511 vector (2x10^6 TU / 10 µl) was given by stereotactic injection 4 days after tumor cell inoculation, and daily i.p. administration of 5-FC or PBS was started 10 days after tumor cell inoculation for 7 consecutive days. This cycle was repeated at intervals of every 10 days. To evaluate tumor growth inhibition, the mice were analyzed every 7 days by optical imaging as described above. In independent Tu-2449 studies conducted at Tocagen, Toca 511 was administered as above at 3x10^6 TU/ 5 µl followed

by 4 cycles of 5-FC administered twice a day for 4 days every two weeks, or at a lower dose (1.6x10^4 TU / 5 µl), and continuous 5-FC administered once a day for 14 or 21 consecutive days.

Tumor re-challenge and immunological assays

Tumor re-challenge was performed on all cured mice from intracranial Tu-2449 tumor long-term survival studies, by either: 1) s.c. implantation of 2x10^6 Tu-2449SC cells in 100 µl of PBS into each mouse on day 0 (Day 303); or 2) s.c. implantation of 1x10^5 Tu-2449SC cells in 100 µl of PBS into each mouse on day 0 (Day 105 for high dose Toca 511/cyclic 5-FC mice and day 182 for low dose Toca 511/continuous 5-FC mice). As a control, Tu-2449SC cells were implanted into naïve B6C3F1/J mice. Tumor measurements were performed twice a week.

For the cellular immunity assays, splenocytes were isolated from cured mice (after the re-challenge assay was completed), and purified using Lympholyte-M (Cat# CL5030, CEDARLAEN, Canada). Purified splenocytes were then stimulated on anti-CD3ε coating 96 well plates for 2 days. After stimulation, splenocytes were cultured with recombinant human Interleukin-2 (rhIL-2,100 U/ml) for 3 days. The number of IFN-γ-producing cells was measured using an ELISPOT assay. Mouse IFN-γ ELISPOT Kit plates were coated with anti-mouse IFN-γ Ab (Cat# 552569, BD Bioscience). Splenocytes (1x10^4 cells/well) were cultured for 18 h at 37°C in a 5% CO_2 humidified incubator. The number of spots per 10^4 splenocytes, which represented the number of IFN-γ-producing cells, was enumerated automatically using an ELISPOT plate reader (CTL Laboratories, Shaker Heights, OH) at the Immuno/BioSpot & Cytometrics Core, UCLA.

Lymphocyte subset depletions were performed by i.p. injection of antibodies targeting specific populations. 50 µg of anti-CD4 (GK1.5) or anti-CD8 (2.43), or 25 µg of anti-NK1.1 (PK136) was administered on day -1, 1, 3 and then twice a week in previously cured animals. Depletion was verified in

one animal from each group on day -1 and 8 before or after re-challenge and analyzing splenocytes by flow cytometry. All antibodies were purchased from Bio X cell, New Lebanon, NH.

xCELLigence analysis

Cytotoxicity of stimulated or unstimulated splenocytes derived from previously cured mice or naïve B6C3F1/J mice against Tu-2449SC cells were determined by xCELLigence real-time cell analysis (Acea Biosciences Inc). For stimulation of naïve splenocytes, 10 ng/ml IFN-γ was added to Tu-2449SC cells cultured in complete DMEM (10% FBS) 24 hours before irradiation at 70 Gy or addition of mitomycin (25 μg/ml, 1 hour). Freshly isolated splenocytes from naïve B6C3F1/J mice were co-cultured with the Tu-2449SC cells at a 50, 30, 10 to 1 ratio in a MLTR with 60 IU/ml rhIL-2 in complete X-VIVO (2% FBS and 50 μM β-mercaptoethanol) at 2x10^6 cells/ml. On day 1 post MLTR, half of the media was changed with 60 IU/ml rhIL-2 supplement. On day 2 post MLTR, Tu-2449SC cells were plated on E-Plate 96 at 5x10^3 cells / 100 μl complete X-VIVO after the plate was zeroed by adding 50 μl complete X-VIVO and running a one minute sweep. Up to 100 sweeps were run at 15 minute intervals until effector cell addition the next day.

As non-stimulated controls, splenocytes were freshly isolated from a B6C3F1/J female mouse and cultured in complete X-VIVO at 2x10^6 cells/ml without rhIL-2 for one day. Next day, non-stimulated splenocytes were plated in triplicates with the target cells on E-Plate 96 at effector to target ratios (E:T) of 50, 30, 10 to 1 in 10 μl complete X-VIVO cell suspensions. 2 μl Triton-X was added to target cells for maximum kill wells and 10 μl complete X-VIVO was added for target only wells. Up to 400 sweeps were run at 2 minute intervals until data collection 24 hours later. The collected data was analyzed by RTCA software.

For an immune boost, previously cured mice were implanted 2x10^6 cells of Tu-2449SC cells subcutaneously on day 0. On day 8, Tu-2449SC cells were plated, then harvested splenocytes from

immune-boosted cured mice were cultured without rhIL-2 for one day. On day 9, these splenocytes were plated in triplicates with the target cells on E-Plate 96 at effector to target ratios (E:T) of 50, 30, 10 to 1 in 10 µl complete X-VIVO cell suspensions. 2 µl Triton-X was added to target cells for maximum kill wells and 10 µl complete X-VIVO was added for target only wells. Up to 400 sweeps were run at 2 minute intervals until data collection 24 hours later.

Statistical analysis

Statistical analyses were done with Student's t test, one-way or two-way ANOVA to determine significance. Survival data were analyzed according to the method of Kaplan–Meier. P values of <0.05 were considered statistically significant in all analyses, which were done with Prism 5 statistical software (GraphPad Software).

Results

RRV-mediated efficient delivery and functional expression of yCD gene in glioma cells

In preliminary studies, AC3-GFP, an RRV expressing the GFP reporter gene (**Figure 1-1A**) was used to evaluate the equivalence of MLV-based RRV replication and gene transfer efficiency *in vitro* in both human U-87 and murine Tu-2449 glioma cells, and *in vivo* in subcutaneous tumors established with both cell lines. In both cell lines, RRV transduction levels increased from 0.5% to >90% within 5-10 days in vitro (**Figure 1-2**), and from 2% to >85% within 7 days in vivo (**Figure 1-3**), stably maintaining 1-2 integrated vector copies per cell (**Figure 1-2, 3**).

For prodrug activator gene therapy, we employed Toca 511 (AC3-yCD2) [33], a vector designed for clinical use which expresses an improved yeast CD prodrug activator gene (yCD2) (**Figure 1-1A**). To evaluate possible differences in replication kinetics between AC3-GFP and Toca 511, we also analyzed the integrated vector copy number by genomic quantitative PCR (qPCR) analysis of cells initially infected with Toca 511 at an MOI of 0.005, using primers targeting the amphotropic envelope gene, at serial time points after infection in the presence or absence of 3'-azide-3'-deoxythymidine (AZT) in vitro. In both U-87 and Tu-2449 glioma cells, the time course of changes in Toca 511 vector copy numbers was similar to that of AC3-GFP, showing an initial rapid increase followed by gradual decrease to a plateau level (**Figure 1-1B**). In U-87 human glioma cells, the vector copy number increased rapidly to reach >10 copies/cell by day 6, followed by gradual decrease to plateau at ~2 copies/cell within 15 days. In Tu-2449 murine glioma cells, the viral copy number increased rapidly to reach >4 copies/cell within 9 days, followed by a gradual decrease to plateau at ~3 copies/cell within 15 days.

As the CD enzyme converts the well tolerated prodrug 5-FC into the antimetabolite 5-FU intracellularly within infected cancer cells, in vitro cytotoxicity was then examined by 3-(4-5-dimethylthiazol-2-yl)-5-(3-carboxymethoxyphenyl)-2-(4-sulfophenyl)-2H-tetrazolium (MTS) assay after exposure of fully transduced glioma cell populations to 5-FC prodrug at various concentrations (**Figure**

1-1C). Control U-87 cells transduced with AC3-GFP or no vector showed no loss of viability at lower concentrations of 5-FC up to 10 mM 5-FC treatment. In contrast, the viability of Toca 511 transduced cells was reduced to below 40% even after exposure to only 0.1 mM 5-FC, and complete cell killing was observed after 9 days of exposure to 10 mM 5-FC. Similar results were obtained in Tu-2449 cells transduced with the Toca 511 vector. Control Tu-2449 cells showed no loss of viability up to concentrations of 1 mM, whereas, the viability of Toca 511 transduced cells was reduced over 70% even after exposure to only 0.01 mM of 5-FC, and 95% cell killing was achieved at 1 mM 5-FC.

Toca 511 + 5-FC prodrug activator gene therapy shows potent anti-tumor effects in both human and murine subcutaneous glioma models *in vivo*.

The replicative spread of Toca 511 was first compared between human U-87 and murine Tu-2449 subcutaneous tumor models by genomic qPCR for integrated viral copy number as described above. To reduce animal-to-animal variability of vector transduction levels in these models, U-87 and Tu-2449 cell mixtures consisting of 2% pretransduced cells mixed with 98% naïve uninfected cells were subcutaneously inoculated in, respectively, athymic nude or syngeneic B6C3F1/J mice on day 0, and tumors were excised on day 7. Genomic DNA was extracted from the infected cells immediately prior to injection on day 0 and from the infected tumor on day 7, and the copy numbers of integrated Toca 511 vector were quantitated by genomic qPCR (Fig. 1-3C). Consistent with the results of AC3-GFP replicative spread in subcutaneous tumors, vector copy numbers of Toca 511 integrated into the genomic DNA of tumor cells increased efficiently in both models, reaching >1.5 - 2.5 copies/cell in U-87 or Tu-2449 tumor, respectively, within 7 days.

The therapeutic efficacy of Toca 511 + 5-FC treatment was then compared in these two subcutaneous glioma models. Seventeen days after tumor cell inoculation, intraperitoneal 5-FC administration (daily at 500 mg/kg) was initiated (Fig. 1-4). As expected, mice receiving PBS vehicle or 5-FC treatment without

virus transduction showed no obvious inhibition of tumor growth compared with control mice bearing non-transduced tumors. Interestingly, in the U-87 model, significant differences were observed between the vector-only transduced group (receiving PBS instead of 5-FC) and the non-transduced control groups on Day 28 when the latter control groups had to be terminated due to excessive tumor volume ($p < 0.0001$; Fig. 1-4A). The overall curves for the vector-only transduced groups suggested that transient tumor growth delay had occurred in these groups as compared to non-transduced controls.

Nonetheless, in both models, the growth of tumors transduced with Toca 511 was significantly inhibited by 5-FC treatment after Day 17 as compared to the other control groups (no vector + PBS or no vector + 5-FC) on Day 28 ($p<0.0001$, Fig. 1-4A; $p=0.0005$, Fig. 1-4B).

Toca 511 plus repeated cycles of 5-FC achieve long-term survival in intracranial glioma models

We next performed Toca 511+5-FC gene therapy in intracranial glioma models. We previously showed in the intracranial U-87 xenograft model in athymic nude mice that a single dose of a preclinical prototype RRV expressing the CD prodrug activator gene followed by continuous administration of 5-FC for over 2 weeks resulted in doubling of median survival time, but animals all eventually succumbed to tumor recurrence [19]. In contrast, multiple cycles of 5-FC could achieve prolonged survival, which we confirmed using the clinical vector Toca 511. After establishment of intracranial U-87 gliomas, a total dose of 2x10^6 Transducing Units (TU) of Toca 511 was given by stereotactic injection at the same coordinates, and multicycle daily 5-FC prodrug treatment was commenced on day 18 for 7 consecutive days at 1-2-week intervals. As expected, none of the mice in the control groups, which were untreated or treated with vector only without prodrug, survived longer than 38 days. In contrast, the group treated with Toca 511+5-FC showed significant survival benefit ($p<0.0001$) and 87.5% survival for more than 120 days (**Figure 1-5A**).

We then evaluated the survival benefit of Toca 511+5-FC in the intracranial Tu-2449 syngeneic model in immunocompetent B6C3F1/J mice. We hypothesized that the local intratumoral production of 5-FU avoids the drug induced myelosuppression caused by systemic 5-FU treatment, and allows induction of anti-tumor immune responses. However, while the 5-FC prodrug itself is well tolerated in man and only extended high-level exposure can result in clinically relevant bone marrow toxicity, it is also possible that prolonged production of 5-FU from the tumor might be counterproductive. Therefore we investigated different dosing regimens for efficacy and induction of anti-tumor immunity. First, we examined Toca 511 at a low dose (10^4 TU), followed by continuous daily 5-FC for 14 or 21 days. This is equivalent to the dose used in previous U-87 studies with the preclinical vector followed by continuous 5-FC, and as there is a dose response effect for Toca 511 in the Tu-2449 model, this lower vector dose enables us to see either improvement or detriment compared to our previous 5-FC dosing regimens. Results in Fig. 1-5B show that these continuous dosing regimens give similar outcomes: significantly improved survival compared to control ($p<0.005$) and 40% survival for >240 days after a continuous 14- or 21-day single course of 5-FC. It should be noted that these results are significantly different from those seen after the equivalent dose of virus followed by continuous 5-FC in the U-87 model, again indicating the critical role of an intact immune system in achieving long-term survival, and suggesting that the 5-FC dosing regimen or Toca 511 dose can impact the induction of anti-tumor immunity.

We next investigated a shorter and more intense cyclic dosing regimen with high dose Toca 511 (3x10^6 TU) followed by 5-FC for twice-daily 4-day cycles, spaced 10 days apart. This regimen also results in significantly improved survival compared to controls ($p<0.0001$) and 82% survival for more than 160 days without further prodrug treatment after the fourth cycle (**Figure 1-5C**). Notably, previously published results from a 4-day on/10-day off dosing regimen using a lower dose of virus also showed long-term survival benefit, but in a lower percentage of animals [17], again suggesting that the initial effectiveness of prodrug activator gene therapy can impact subsequent development of anti-tumor immunity.

Finally, we also evaluated the survival benefit of prodrug activator gene therapy in the Tu-2449 model using the same cyclic 5-FC dosing regimen employed in the confirmatory U-87 studies described above, i.e., 2x10^6 TU Toca 511 injected into pre-established intracranial tumors followed by multi-cycle daily 5-FC prodrug treatment for 7 days at 1-2-week intervals. As expected, both control groups (no vector and Toca 511 followed by saline vehicle instead of 5-FC) showed similar results and neither control group survived longer than 28 days. However, the group treated with Toca 511 plus 5-FC for 7-day cycles showed significantly longer survival than the control groups ($p<0.0001$) achieving 100% survival for more than 360 days even without further prodrug treatment after the third cycle (**Figure 1-5D**).

In vivo bioluminescence imaging of tumor response

To enable real-time assessment of the therapeutic effect of Toca 511 followed by multi-cycle 5-FC in individual animals, U-87 and Tu-2449 cells used in the optimized cyclic 5-FC administration studies above had been pre-transduced with a conventional replication-defective lentivirus vector expressing firefly luciferase. Stable expression of luciferase in these cells was confirmed by optical imaging in vitro (**Figure1-6A**), which showed a quantitative correlation between cell number and luminescent signal intensity (**Figure 1-6B**). After establishment of intracranial U-87 gliomas and intratumoral injection of Toca 511, each mouse was analyzed by optical imaging every week. In both tumor models, control mice that received PBS vehicle only instead of 5-FC showed tumor progression, as evidenced by increasing bioluminescence signal intensities. However, animals treated with Toca 511 followed by 5-FC administration exhibited stable disease or decreased tumor burden, and overall, average tumor growth was significantly inhibited compared with the control groups after the initial cycle of 5-FC treatment in both U-87 ($p<0.0001$) and Tu-2449 ($p<0.0001$) tumor models (**Figure 1-7B and C, Figure 1-8**).

Subsequently, in the U-87 human glioma xenograft tumor model, the Toca 511+5-FC treated mice repeatedly showed re-emergence of increased luminescence signal intensities during the intervals between 5-FC treatment cycles, indicating tumor recurrence upon cessation of prodrug treatment after each cycle (**Figure 1-7B, 1-8AB**). Increased tumor burden as indicated by live luminescence imaging was associated with characteristic behavioral changes including hunched posture, and reduced feeding and grooming activity, while reduction of tumor burden with each prodrug cycle restored normal activity without any obvious ill effects. Thus, with repeated cycles of prodrug treatment, long-term tumor control was possible without incurring any adverse effects. Consistent with imaging results, qPCR for both human genomic and RRV sequences showed residual signals in brain tissues in this immunodeficient model, supporting the existence of a reservoir of stably-infected glioma cells enabling continued therapeutic benefit with prodrug administration upon tumor recurrence for at least 125 days until study termination (**Figure 1-9**).

In contrast, in the immunocompetent Tu-2449 model, bioluminescent signals of all treated tumors decreased rapidly after the initial cycle of 5-FC prodrug, stayed below detection threshold after the second cycle of treatment, and never recurred even without further prodrug treatment after the third cycle (**Figure 1-7C, 1-8CD**). At the molecular level, firefly luciferase and RRV sequences were both undetectable by qPCR analysis of brain tissues from long-term surviving animals even 280 days after the last prodrug injection (i.e., at study termination on day 361 after initial tumor establishment) (**Figure 1-7D**, **Figure 1-9**).

Immunological memory induced in long-term survivors after Toca 511+5-FC treatment

Major histocompatibility complex (MHC) antigens are not highly expressed on Tu-2449 cells at baseline, but MHC Class I expression can be upregulated by interferon-ɣ (**Figure 1-10**), and it was previously reported that while tumor engraftment is robust in naïve syngeneic hosts, pre-immunization

leads to rejection, indicating that anti-tumor immunity can be elicited in this model [36]. To evaluate whether anti-tumor immunity had developed in immunocompetent hosts with Tu-2449 intracranial gliomas after administration of different doses of vector and schedules of 5-FC, we challenged surviving animals with a low-dose subcutaneous inoculum (1x10^5 cells) of uninfected Tu-2449SC cells (previously passaged as subcutaneous tumors) on Day 105 or 182 post-establishment of the original intracranial tumors (**Figure1-11A**). Some of the mice that had shown long-term survival with low-dose Toca 511 and continuous 5-FC (**Figure 1-5B**) completely controlled growth of subcutaneous tumors (4/8 treated vs. 0/4 control), although the mean tumor volume difference did not reach significance (**Figure 1-11B**). In contrast, mice that had been cured of brain tumor after receiving high-dose Toca 511 and cyclic 5-FC (**Figure 1-5C**) controlled the growth of subcutaneous tumors significantly better than naïve animals ($p<0.005$, **Figure 1-11B**). To further evaluate long-term anti-tumor immunity after high-dose Toca 511 treatment, we challenged mice with a higher-dose inoculum (2x10^6 cells) of uninfected Tu-2449SC cells (i.e., uninfected with either RRV or lentiviral firefly luciferase marking vector) injected into the flanks of naïve control mice, or cured mice from long-term survival studies on Day 303 after the original tumor implantation (**Figure 1-11A**). Tumors successfully engrafted in all control animals, which had not previously been exposed to Tu-2449 tumors and were naïve to any prior treatment. In contrast, in the previously cured mice, although subcutaneous tumors were observed initially on day 7 after challenge, these tumors all spontaneously disappeared by day 14 without any recurrence (**Figure 1-11C**).

Cellular immunity was further evaluated in splenocyte populations obtained from these previously cured mice by measuring the number of IFN-γ producing cells with enzyme-linked immuno spot (ELISPOT) assay. Target cell-stimulated IFN-γ responses of splenocytes derived from cured mice were significantly higher than splenocytes obtained from naïve control mice ($p=0.0005$), indicating the presence of cellular immune memory responses in mice that had been cured after tumor establishment more than 300 days prior (**Figure 1-12A**).

After stimulating splenocytes from naïve animals with interferon-ɣ treated Tu-2449 cells, mixed lymphocyte-target cell reactions (MLTR) monitored in real-time by xCELLigence electrical impedance analysis confirmed robust killing of Tu-2449 target cells over time in an effector:target (E:T) ratio-dependent manner (**Figure 1-13**). Next, the antitumor response using splenocytes from previously cured animals was also examined by xCELLigence analysis after subcutaneous re-challenge with parental Tu-2449 cells and tumor rejection. Again, robust E:T ratio-dependent killing of Tu-2449SC target cells was seen over time compared to splenocytes from naïve mice (**Figure 1-12B, C**), suggesting that RRV-mediated prodrug activator gene therapy had stimulated endogenous antitumor responses in immunocompetent mice that could be re-activated over 300 days later.

Specific lymphocyte subsets that contribute to tumor eradication and rejection upon tumor re-challenge were assessed by antibody-mediated depletion of CD4+, CD8+ and NK cells. Depletion was verified by flow cytometry of splenocytes isolated from a randomly selected animal from each depletion group, and tumor establishment vs. rejection was compared between lymphocyte subset-depleted groups and non-depleted controls. Notably, tumors were still rejected in all previously cured animals subjected to NK or CD8+ T cell depletion, as in non-depleted controls. In contrast, CD4+ T cell or combination CD4+/CD8+ T cell depletion prevented tumor rejection in previously cured animals (**Figure 1-14**).

Discussion

The results of the present study underscore the advantages of RRV therapy, which integrates a prodrug activator transgene into the cancer cell genome non-lytically, thereby converting infected cancer cells permanently into virus-producing cells. In our previous studies, survival analysis was used to evaluate the efficacy of multiple cycle prodrug treatment in intracranial brain tumor models [17, 19, 20]. In these studies, end-point immunohistochemical analyses suggested that stably integrated virus in glioma cells that had escaped previous prodrug conversion cycles could persist and mediate reinfection of recurring tumors, enabling continued therapeutic benefit upon further cycles of prodrug treatment, and that tumor eradication could be achieved in the immunocompetent Tu-2449 model but not the immunodeficient U-87 model. In the present study, we employed live bioluminescence optical imaging to monitor the responses of tumors to each treatment in real time, by sequentially visualizing and quantifying tumors in the same individual. To our knowledge, this is the first report to use live imaging to monitor RRV-mediated prodrug activator gene therapy in intracranial glioma models. Our results show that this bioluminescence imaging system allowed more sensitive and detailed assessment of tumor response to each cycle of treatment in an intracranial glioma model than conventional survival analysis, and enabled adjustments in the timing of prodrug administration cycles based on the level of tumor burden, essentially achieving cytoreduction on demand.

In the U-87 immunodeficient intracranial tumor model, the group treated with Toca 511 followed by 5-FC administration showed a significant reduction of tumor burden compared with control groups after the initial cycle of 5-FC. However, luminescence imaging revealed the continual presence of residual disease, resulting in periodic tumor recurrence, and after repeated cycles of prodrug treatment, variable responses to 5-FC were observed in individual animals, i.e. tumor responses were either attenuated, lost, or recovered. Theoretically, the response to prodrug treatment depends on the number of RRV-transduced tumor cells undergoing division at the time of prodrug administration. Although the transduction efficiency of the treated tumor was relatively uniform among the infected tumors at the

initial cycle of 5-FC treatment, each animal varied in the number of residual infected cells at later time points and this might have caused the variations in response to prodrug treatment. Nonetheless, relatively consistent control of tumor burden could be achieved over a long-term duration by prodrug administration as needed, whenever recurrence was observed by real-time imaging.

Despite viral replication kinetics and overall transduction levels being relatively equivalent, the contrast between the U-87 xenograft model, where the tumor could be controlled with continued prodrug cycles but not completely eliminated, and the Tu-2449 intracranial glioma model in which tumor signals were completely undetectable even after cessation of prodrug, is intriguing. Previously we reported that tumor eradication could be achieved by Toca 511+5-FC treatment in the Tu-2449 model [17], and we confirmed that observation here by qPCR analysis for luciferase sequences as a marker for residual tumor cells in the brain tissue of long-term survivors. An obvious difference is the lack of a functioning cellular immune system in the nude mouse xenograft host as compared to the immunocompetent syngeneic host. However, as we have found that baseline levels of MHC expression are low in Tu-2449 cells (**Figure 2-S7**), and that intact RRV particles cause inhibition of Type I interferon responses [7], the extent to which anti-tumor immunity could be induced by RRV-mediated gene therapy was not clear. Our results indicate that, in fact, the strong therapeutic efficacy with apparent tumor clearance observed in the immunocompetent model was achieved not only by Toca 511+5-FC treatment, but also by the development of immune responses against viral proteins and/or tumor antigens released by Toca 511+5-FC induced cell killing. Furthermore, once denatured, RRV particles show immunostimulatory activity [7] and hence may act as an adjuvant. Notably, tumor re-challenge experiments on long-term survivors after Toca 511+5-FC therapy used uninfected parental tumor cells, so rejection responses observed in these experiments were not directed against viral or luciferase reporter gene epitopes, but presumably were directed against innate tumor antigens.

ELISPOT and xCELLigence assays confirmed the presence of cellular immunity against the parental tumor cells. As these responses were observed in animals that had survived for over 300 days without

further prodrug treatment beyond the 3rd cycle, the responses may be mediated by memory T cells. Interestingly, lymphocyte subset depletion studies demonstrated that the CD4+ T cell subset was required for tumor rejection, while depletion of NK and CD8+ T cell subsets alone did not prevent rejection. CD4+ T cells are the source of regulatory T cells (Tregs) induced by the tumor, but can also serve as helper cells for antibody production from B cells and to generate cytotoxic CD8+ T cells [38]. Furthermore, recent data indicates that effector functions of CD4+ T cells may be important in both anti-tumor and anti-viral immunity, and in some cases CD4+ T cells may be even more efficient as cytolytic effector cells than CD8+ T cells [39, 40, 41].

Therapeutic results in the Tu-2449 model were robust with respect to 5-FC dosing schedules as results at high dose vector with a 5-FC dosing schedule of either once-a-day 7 days on 10 days off, or twice-a-day 4 days on 10 days off gave indistinguishable efficacy and immune induction. As we have previously observed [17], there is a dose-response effect in this model with fewer animals showing long-term survival with low-dose Toca 511. This is likely because there is a race between virus spread and tumor growth, or a threshold for effective RRV infection. Furthermore, while longer-term continuous dosing of 5-FC (14 or 21 days continuously) for one cycle yielded some long-term survivors, the data suggest that cyclic 5-FC dosing schedules may be more effective at inducing long term immune memory, analogous to classic prime boost vaccination.

In summary, one major advantage of the use of a replicative integrating vector compared to other therapies is the ability to trigger repeated cycles of cytoreduction at will upon tumor recurrence, simply by systemic administration of a well-tolerated prodrug. A second major advantage of the Toca 511+5-FC treatment demonstrated here is the ability to induce anti-tumor immune responses after Toca 511+5-FC mediated tumor ablation. Importantly, prodrug conversion is intracellular and 5-FU metabolic inactivation is rapid, so that cytotoxicity is confined locally to the tumor. Hence, the adverse side effects characteristic of conventional chemotherapy are avoided, and the host immune system remains intact, as opposed to systemic treatment with 5-FU which can cause marked myelosuppression. It is possible that

development of anti-tumor immunity is further augmented by local production of 5-FU leading to preferential ablation of myeloid derived suppressor cells within the tumor [42].

Toca 511 combined with cycles of Toca FC (an extended release formulation of 5-FC) is showing evidence of clinical activity in several clinical trials for recurrent HGG [34, 35, 43, 44], and a phase 2/3 trial is enrolling subjects with recurrent HGG. We are currently investigating in these trials whether there is the same kind of anti-cancer immunity induced. Given the recent increased understanding of the nature of anti-cancer immune responses, their individual-specific profiles [45], and the generalizable nature of the RRV-mediated prodrug conversion method of inducing anti-cancer cell immunity, this raises the possibility that Toca 511 and 5-FC may be widely useful as an anti-cancer strategy, with the possibility of treating disseminated tumors by local or systemic RRV administration [13, 22, 46].

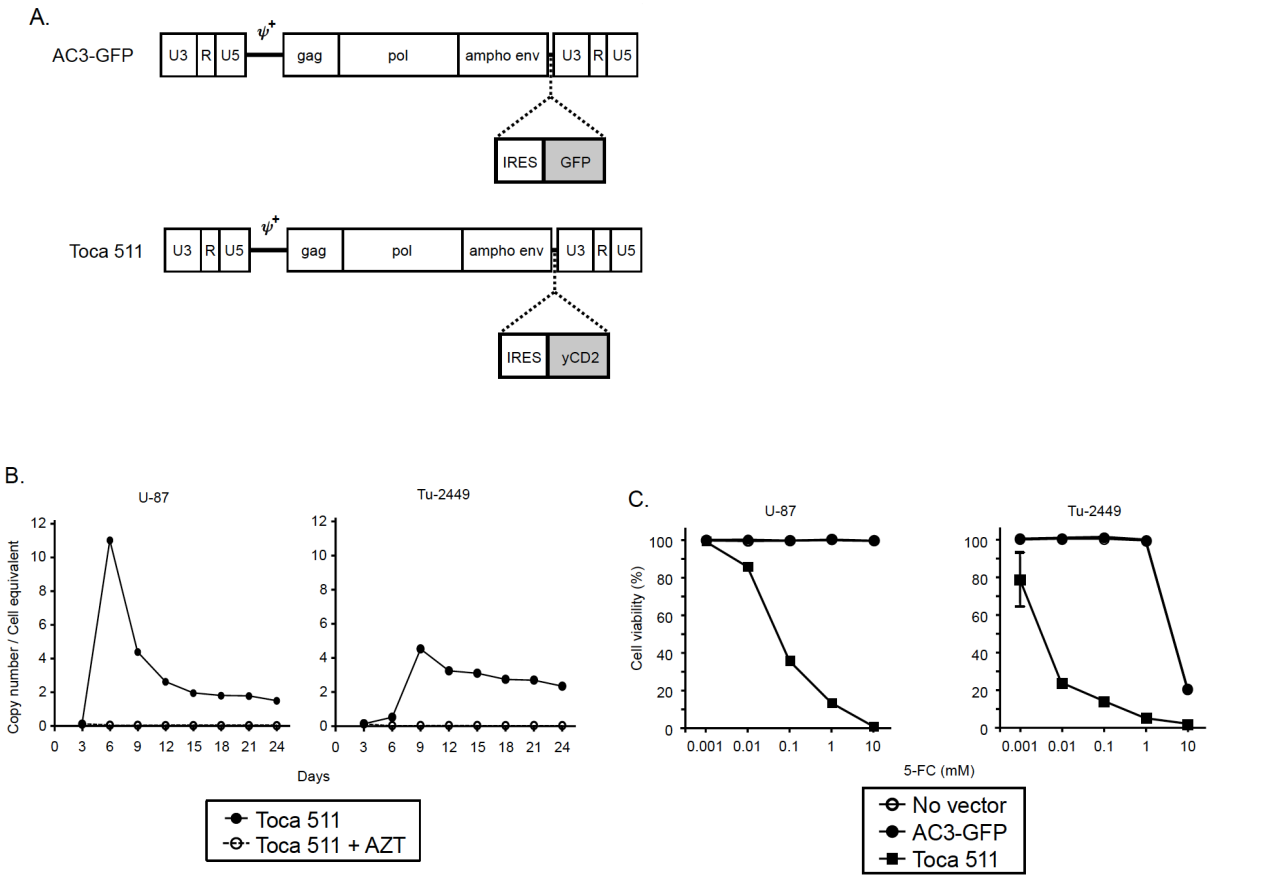

Fig. 1-1. Vector design, replication, and functionality. (A) Design of RRV AC3-GFP and Toca 511. The integrated proviral version of these vector are shown; U3/R/U5, domains of viral long terminal repeat; gag/pol/ampho env, coding sequences of amphotropic virus. **(B)** Replication kinetics of Toca 511 in glioma cell lines. U-87 and Tu-2449 (4x10^5) cells were infected with Toca 511 (5x10^3 TU / 5 µl, MOI 0.005) on day 0. Infected cells were analyzed for integrated viral copy number by genomic qPCR every third day after virus infection. **(C)** MTS assay to assess 5-FC drug cytotoxicity. U-87 and Tu-2449 were fully transduced with AC3-GFP or Toca 511 before plating. Cell viability was measured by MTS dye conversion after exposure to 5-FC at the indicated concentrations and normalized to nontreated cells. "No vector" almost completely coincides with the "AC3-GFP" for both cell lines.

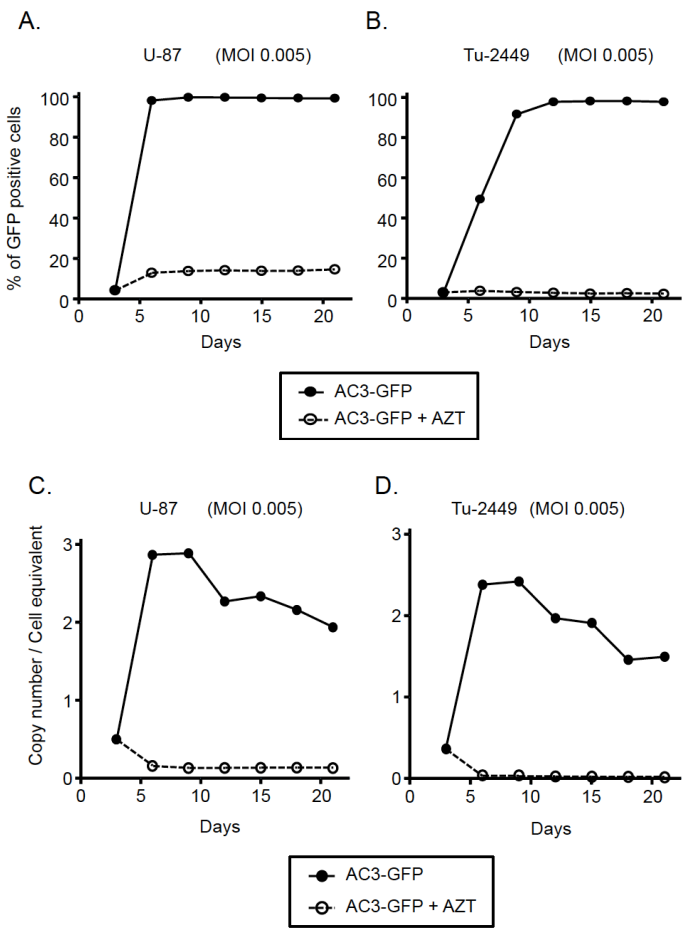

Figure 1-2. RRV AC3-GFP robust replication, spread, and stable transmission of transgenes, in both human and murine glioma cell lines in vitro. GFP expression was monitored by flow cytometry at serial time points after infection with AC3-GFP in the presence or absence of AZT. **(A),** U-87 and **(B),** Tu-2449 glioma cells, the initial percentage of GFP positive cells was less than 10% at day 3 after infection and increased rapidly to reach >95% by day 6 or by day 9, respectively. The integrated viral copy number was determined by genomic qPCR in **(C),** U-87 and **(D),** Tu-2449, the integrated viral copy number increased rapidly and reached the peak (2-3 copies / cell equivalent) by day 9 followed by gradual decrease to about 1-2 copies / cell equivalent within 21 days.

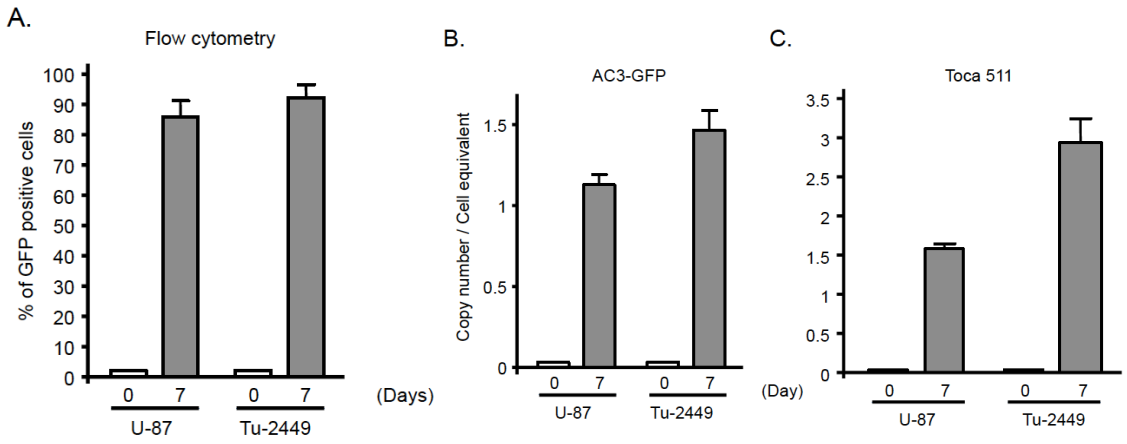

Figure 1-3. RRV replication in subcutaneous tumor models. The transduction efficiency of AC3-GFP or Toca 511 was quantitated in both human U-87 and mouse Tu-2449 glioma subcutaneous tumor models by flow cytometric analysis of GFP transmission **(A)** or by genomic qPCR for integrated viral copy number (**B** and **C**). Initial transduction levels of only 2% AC3-GFP **(B)** or Toca 511 **(C)**-infected tumor cells at the time of tumor implantation was confirmed to achieve >85% transduction efficiency throughout the subcutaneous tumor masses and copy numbers of RRV over 1 copy / cell equivalent in less than 7 days in both U-87 and Tu-2449 tumors.

A.

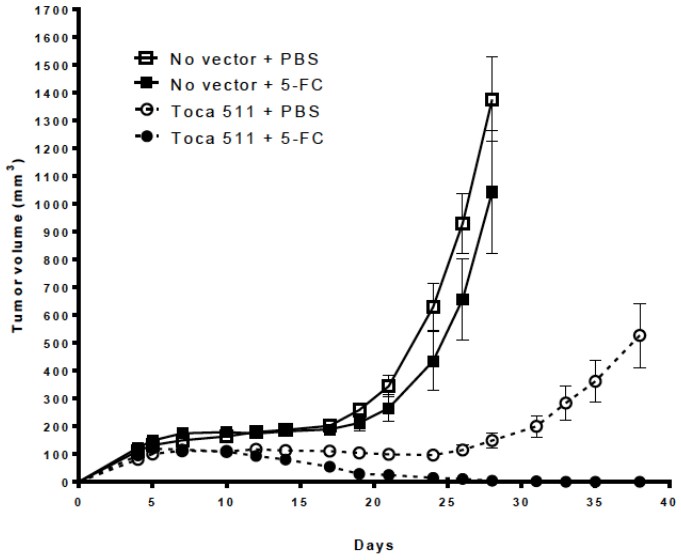

B.

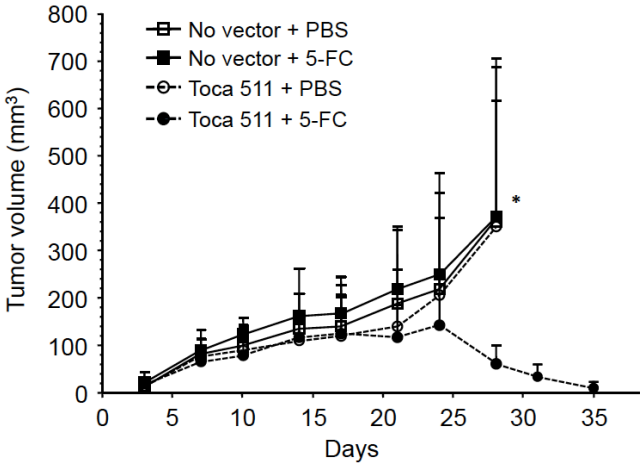

Figure 1-4. Tumor growth inhibition in subcutaneous tumor models. Uninfected glioma cells (100%), or mixtures of uninfected (98%) and cells transduced with Toca 511 (2%), were s.c. injected into mice. **(A)** U-87 cells were subcutaneously injected into immunodeficient athymic nude mice. On day 28, significant differences were observed between the Toca 511+5-FC group and the other control groups ($p = 0.0005$). **(B)** Tu-2449SC cells were subcutaneously injected into immunocompetent B6C3F1/J mice. On day 28, significant differences were observed between the Toca 511+5-FC group and the other control groups ($p = 0.0005$). 5-FC or PBS was administered i.p starting 17 days after tumor cell inoculation.

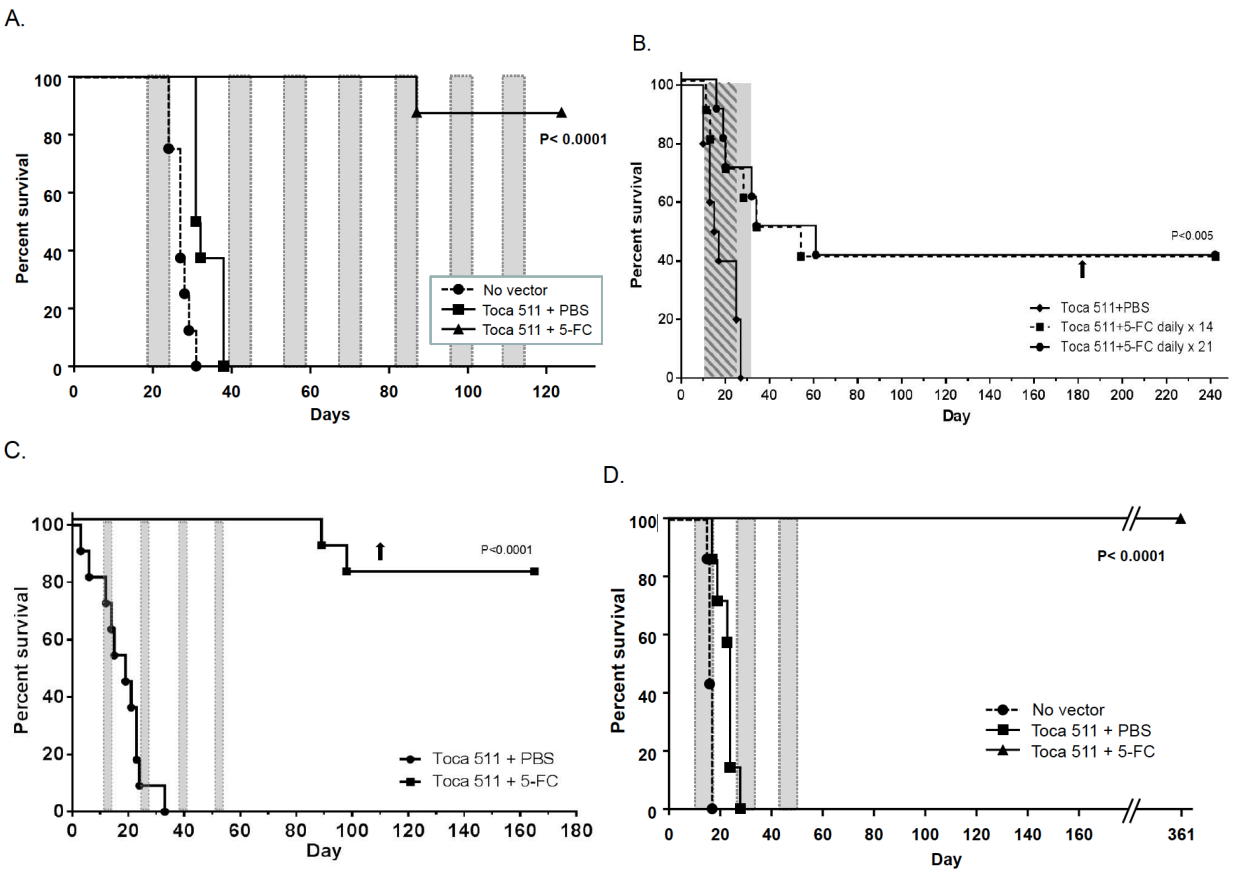

Fig. 1-5. Survival benefit of prodrug activator gene therapy in intracranial glioma models. (A) U-87 glioma model. Toca 511+5-FC showed significant survival benefit compared to control groups ($p < 0.0001$) and 87.5% survival for more than 120 days. Gray area, daily 5-FC treatment. (B to D) Tu-2449 glioma models. **(B)** Low dose: 1.6x10^4 TU. Daily 5-FC administration was commenced on day 10 for a single course of either 14 or 21 consecutive days (Toca 511+5-FC x 14 or 21). Toca 511+5-FC showed significant improvement in survival compared to Toca 511+PBS ($p < 0.005$) and 40% survival for more than 240 days. Hatched area, daily 5-FC x 14 days, gray area, daily 5-FC x 21 days treatment. **(C)** High dose: 3x10^6 TU. Twice-daily 5-FC treatment was commenced on day 10 for 4 consecutive days at 2-week intervals (Toca 511+5-FC). Toca 511+5-FC showed significant improvement in survival compared to Toca 511+PBS ($p < 0.0001$) and 82% survival for more than 160 days. Gray area, twice-daily 5-FC treatment. **(D)** High dose: 2x10^6 TU. Daily 5-FC administration was commenced on day 10 for 7 consecutive days at 10 day intervals (Toca 511+5-FC). Toca 511+5-FC survived significantly longer than the control groups ($p < 0.0001$) and 100% survival for more than 300 days. Gray area, daily 5-FC treatment.

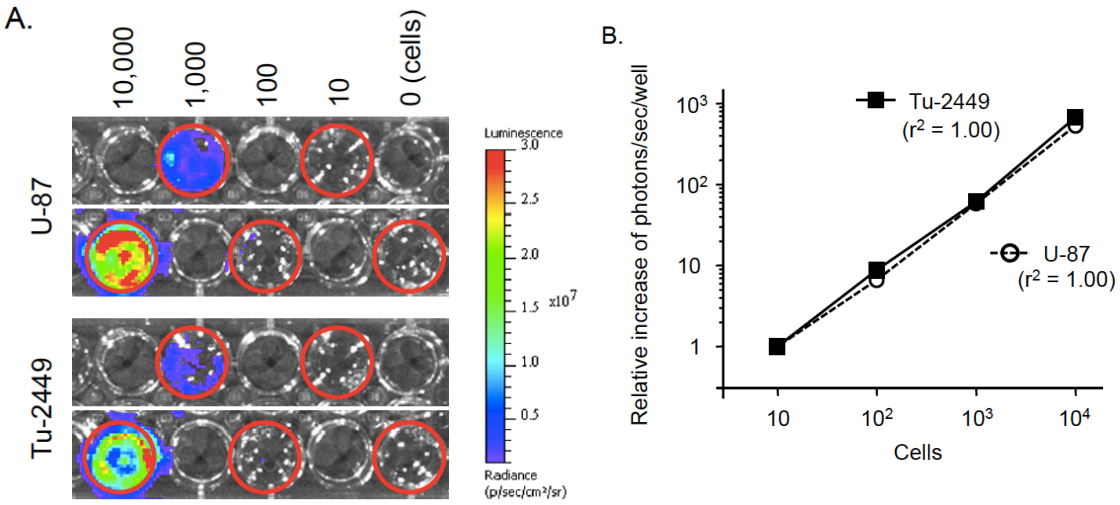

Figure 1-6. Bioluminescence imaging of glioma tumor cells in vitro. After plating different number of the cells expressing firefly luciferase into each well, **(A)** the signal intensities (photons/sec/well) were measured under optical imaging and **(B)** the relative increases were plotted against cell numbers. Solid line, linear regression curve in Tu-2449. Dashed lines, linear regression curve in U-87 (r2 = 1.00; P < 0.0001 in both cell lines).

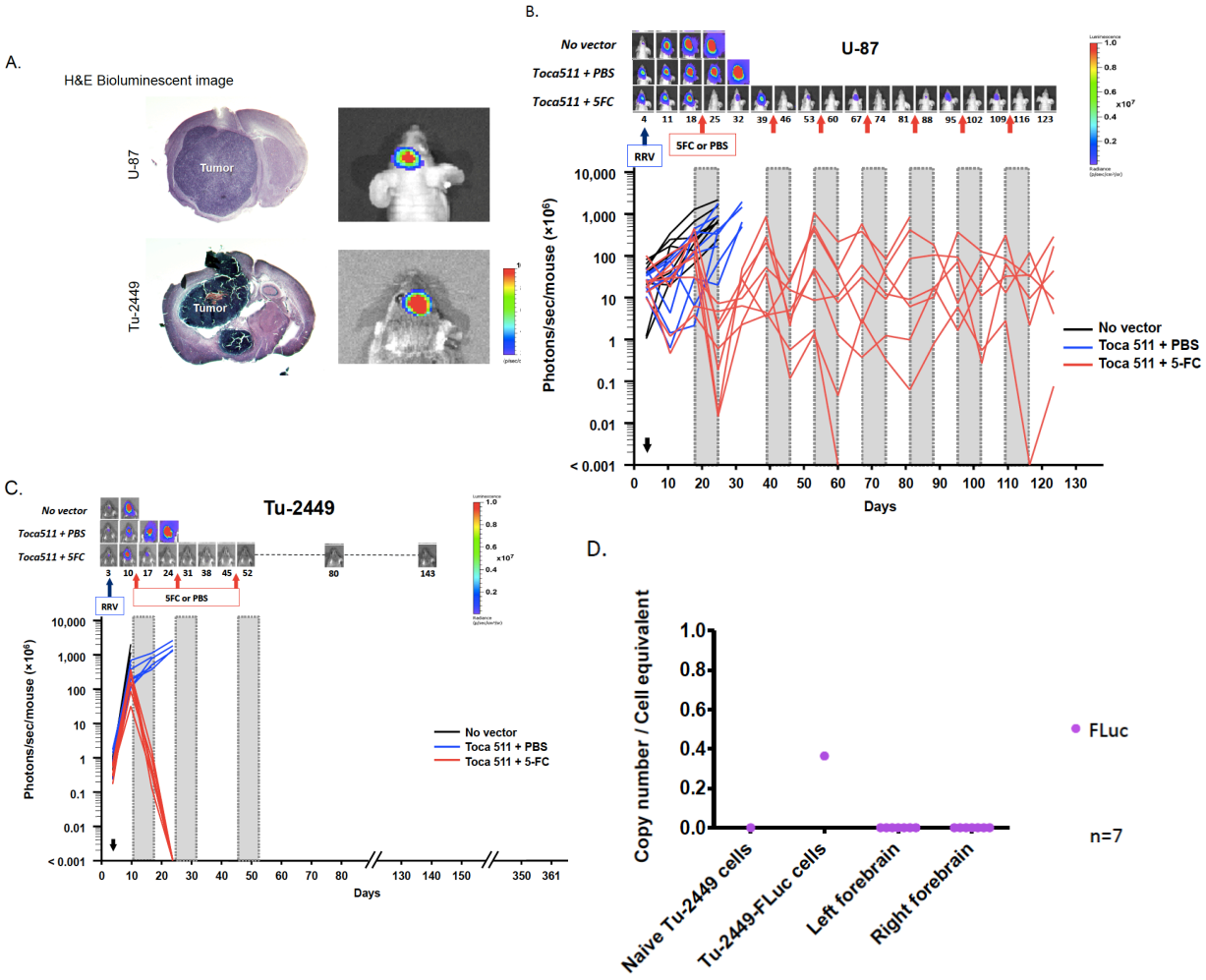

Fig. 1-7. Bioluminescence imaging of glioma tumors in vivo. U-87 and Tu-2449 cells expressing firefly luciferase were examined by optical imaging in vivo. **(A)** Representative examples comparing bioluminescence imaging results and the H&E stained brain tumor sections in the same animal. (**B** and **C**, upper panels) Imaging results from representative animals bearing U-87 **(B)** or Tu-2449 **(C)** intracranial tumors at different time points (Fig. 1-5A and D). (**B** and **C**, lower panels) Signal intensities (photons/sec/mouse) from each animal at different time points. **(D)** qPCR analysis to detect firefly luciferase sequences from residual tumor cells in brain after Toca 511+5-FC in Tu-2449 model on day 361 (Fig. 1-5D). Detection limit was determined based on non-specific copy number of naïve Tu-2449 cells. Copy number/Cell equivalent = firefly luciferase copy number/1x10^5 cells of mouse β-actin copy number.

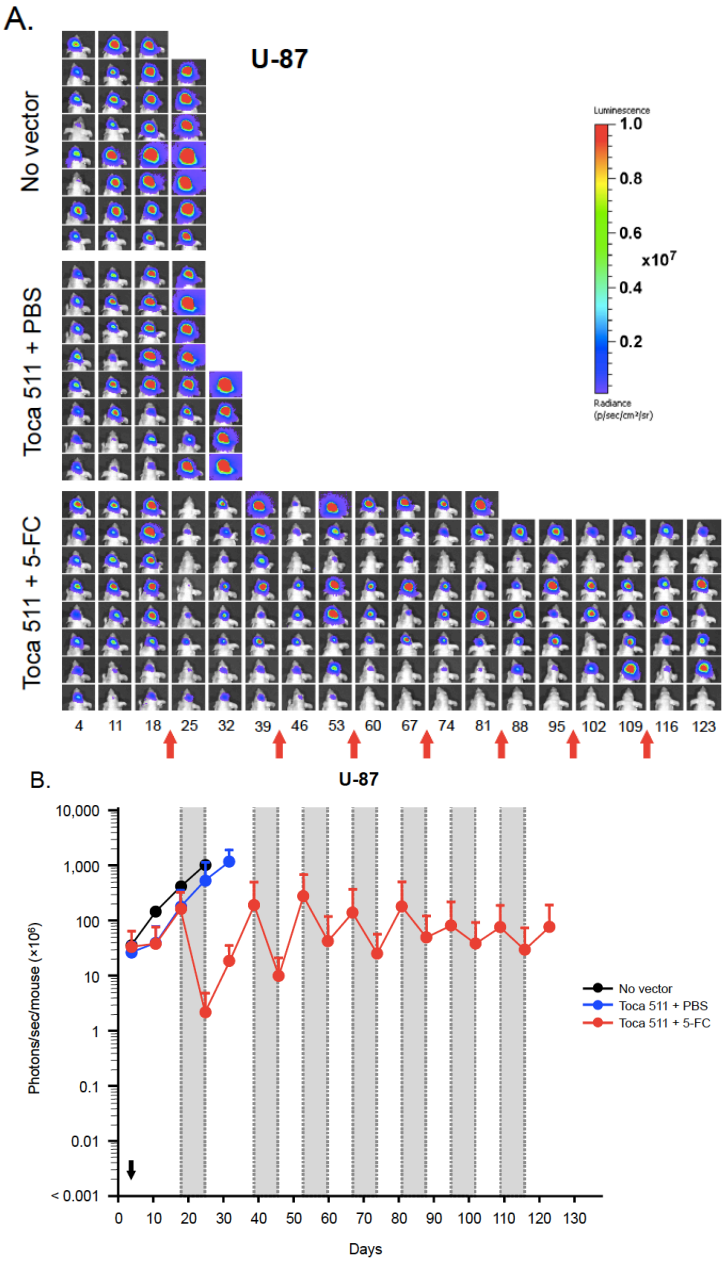

Figure 1-8. Bioluminescence imaging of glioma tumors in vivo. (A) U-87 and **(C)** Tu-2449 sequential bioluminescence imaging of individual animals treated with: no vector; Toca 511+PBS; or Toca 511+5-FC. **(B)** U-87 and **(D)** Tu-2449 average signal intensity for each group: black curves, no vector; blue curves, Toca 511+PBS; red curves, Toca 511+5-FC; gray area, daily 5-FC treatment. In both tumor models, the group treated with Toca 511+5-FC showed significant inhibition of average tumor growth compared with the control groups after the initial cycle of 5-FC treatment in both U-87 ($p < 0.0001$) and Tu-2449 ($p < 0.0001$) tumor models.

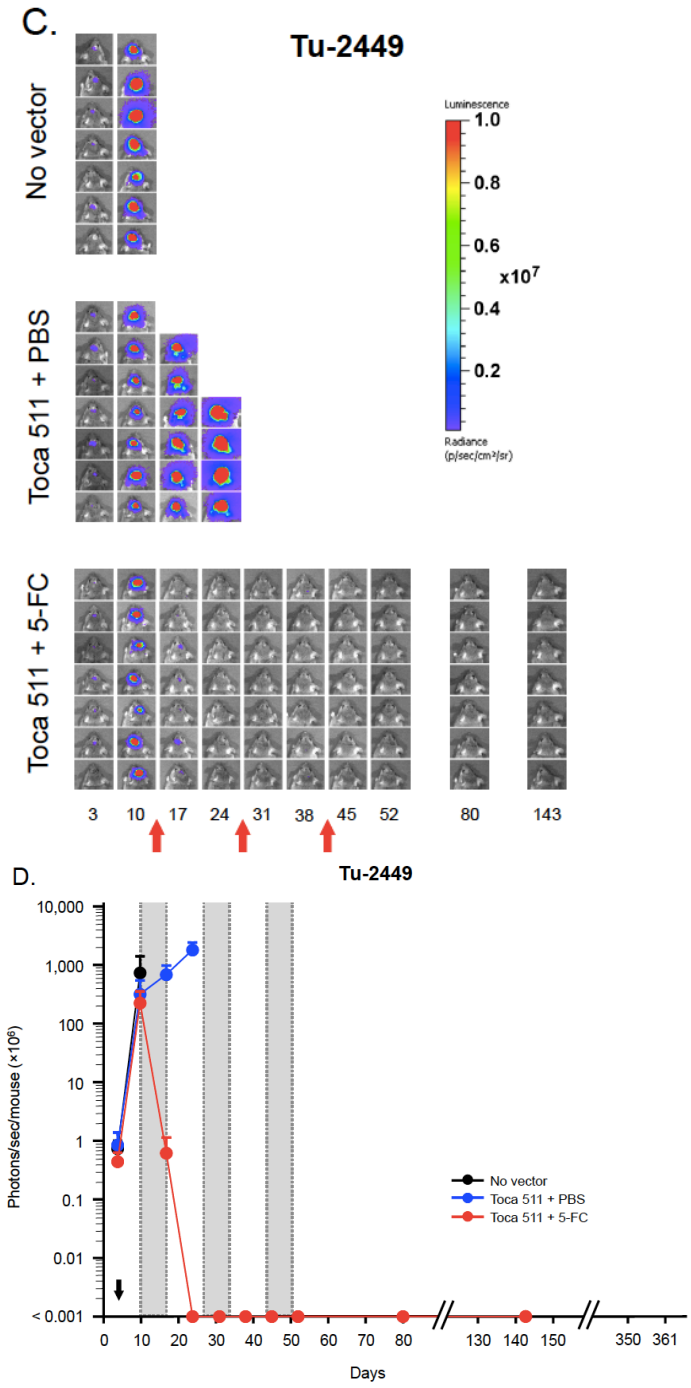

Figure 1-8, continued. Bioluminescence imaging of glioma tumors in vivo.

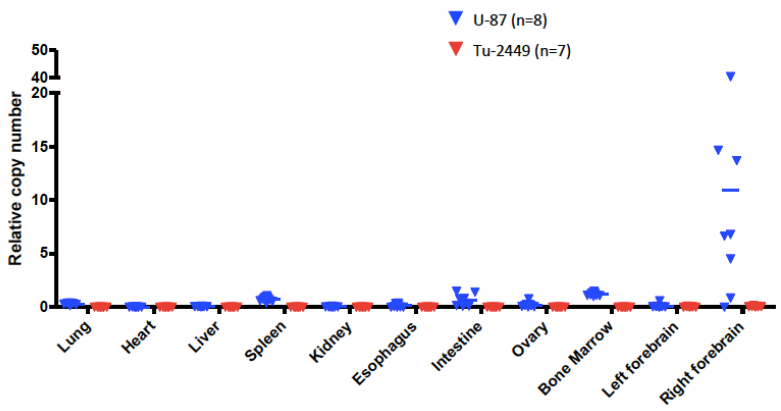

Figure 1-9. Systemic biodistribution from long-term survivors after Toca 511+5-FC treatment in intracranial tumor models. Tissues (lung, heart, liver, spleen, kidney, esophagus, intestine, ovary, bone marrow, left forebrain and right forebrain) from all of the survived mice at day 125 (U-87, Fig. 1-5A) or 361 (Tu-2449, Fig. 1-5D) after initial intracranial tumor establishment were harvested and genomic DNA analyzed by qPCR analysis using primers and probe sequences specific for the 4070A amphotropic envelope. Cell genome as measured by RNase P (human) or mouse beta-actin (mouse) copy number. In cured immunocompetent B6C3F1 mice, viral signal was below the detection limit in normal tissues other than a single animal each with trace signal in spleen and esophagus. Average copy number was 6,338 copies/ 1x10^5 cells in right forebrain, the site of tumor inoculation. In the immunodeficient U-87 mice, as expected based on previous studies, higher viral signals could be detected in all normal tissues. Average copy number was 1x10^6 copies/ 1x10^5 cells in right forebrain. The high residual signal in brain tissues from some U-87 animals supports the existence of a reservoir of infected tumor cells.

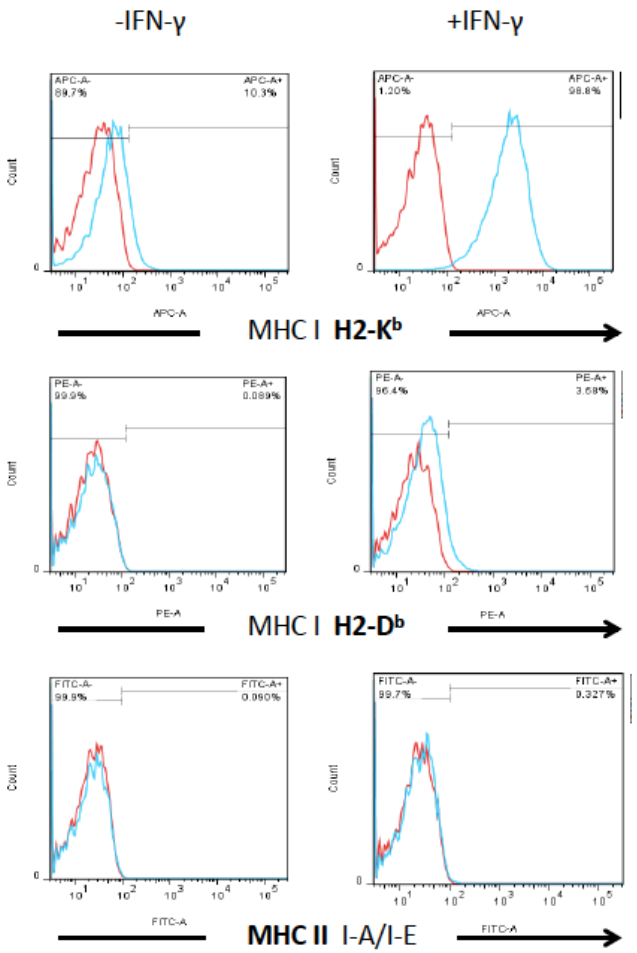

Figure 1-10. Analysis of MHC cell surface expression levels on Tu-2449 cells. Cells were cultured in the absence or presence of murine IFN-γ (10ng/mL) for 24 hr, and after non-enzymatic dissociation, cell surface expression levels of H-2Kb and H-2Db Class I MHC and I-A/I-E Class II MHC were evaluated by flow cytometry. Isotype control curves are indicated in red, MHC-specific staining in blue.

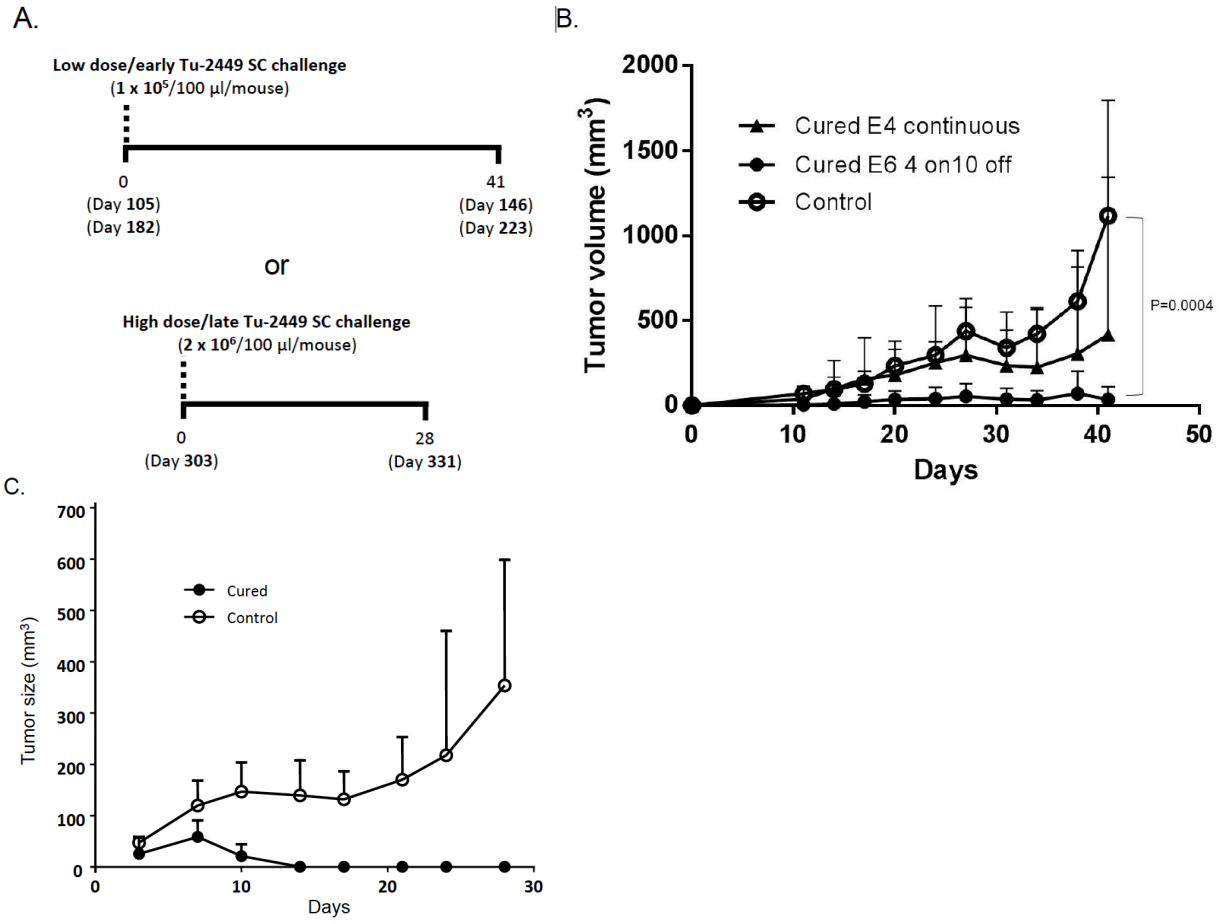

Fig. 1-11. Tumor re-challenge assays. (A) Timeline of re-challenge experiment. Cured mice from Tu-2449 intracranial tumor long-term survival studies (Fig. 1-5B-D) were subcutaneously challenged with uninfected parental Tu-2449SC cells on day 0 (days 105, 182, and 303 after initial tumor establishment, respectively) at low (1x10^5) or high (2x10^6) cell doses. As a control, Tu-2449 cells were implanted into naïve B6C3F1/J mice. **(B)** Tu-2449SC cells (1x10^5 cells) were implanted in cured mice (Fig. 1-5B, C) at early time points (day 105 or day 182) after continuous 5-FC or 4-day cyclic 5-FC regimens, respectively. Open circles: naïve controls. Closed triangles: cured mice from Fig. 1-5B. Closed circles: cured mice from Fig. 1-5C. Tumor growth was significantly reduced in mice cured of brain tumor with high dose Toca 511 and cyclic 5-FC compared to naïve controls (=0.0004). **(C)** Tu-2449SC cells (2x10^6 cells) were implanted in cured mice (Fig. 1-5D) at late time point (day 303) after 7-day cyclic 5-FC regimen. Tumor growth was spontaneously reduced in cured mice. Open circles: naïve controls. Closed circles: cured mice from Fig. 1-5D.

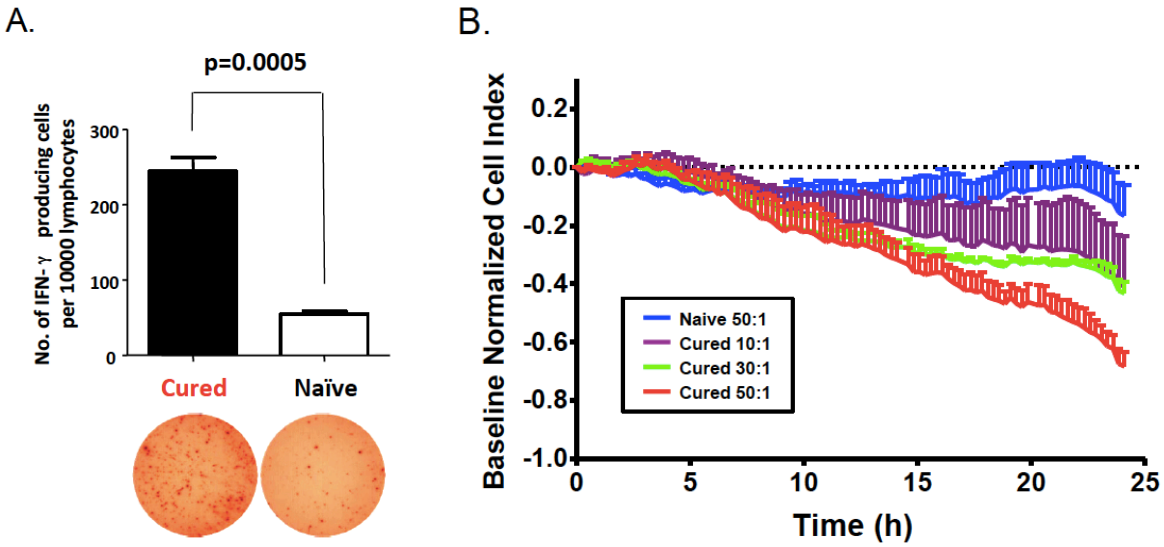

Fig. 1-12. Cured animals have a robust T cell mediated antitumor response. (A) ELISPOT assay to quantitate IFN-γ-producing cells in splenocytes from cured mice from Fig. 1-5D vs. naïve controls. The number of spots per 10^4 splenocytes, representing the number of IFN-γ-producing cells, was counted using an ELISPOT plate reader. **(B)** xCELLigence real-time cell impedance analysis showed antitumor response of splenocytes from immune-boosted cured mice against Tu-2449SC cells (effector : target ratio=50:1). Baseline: target cells only.

A.

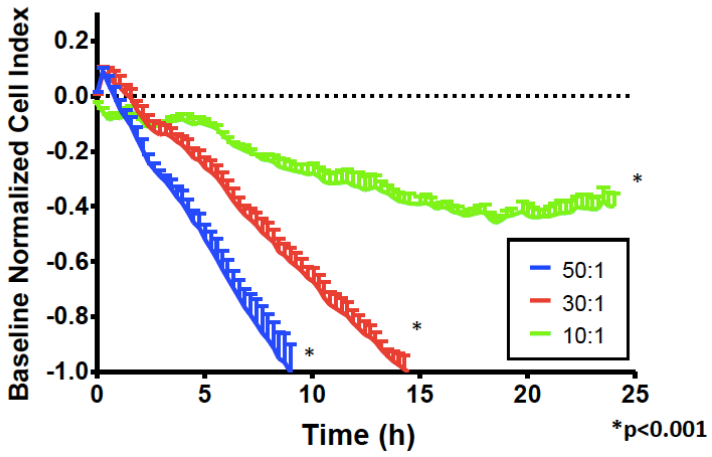

B.

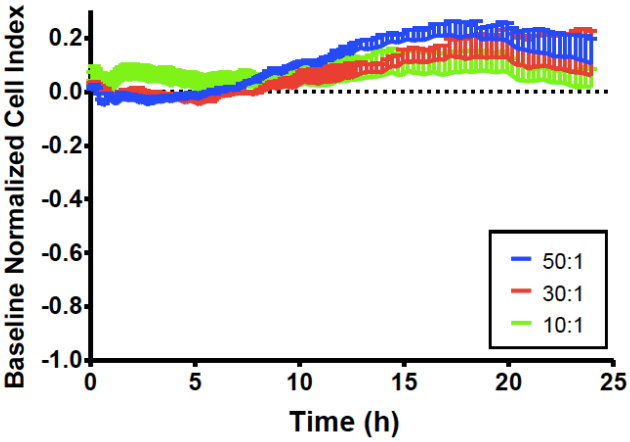

Figure 1-13. xCELLigence analysis of cytotoxic T cell activity against parental Tu-2449 glioma cells. Cellular immunity by splenocytes from naïve mice was evaluated by xCELLigence real-time cell analysis monitoring electrical impedance of Tu-2449SC target cell monolayers after overlaying stimulated **(A)** or non-stimulated **(B)** splenocytes over time. Splenocytes from naïve mice activated against Tu-2449SC cells exhibit effector:target cell ratio-dependent killing. Values are normalized to baseline values at each time point from wells seeded with target cells only.

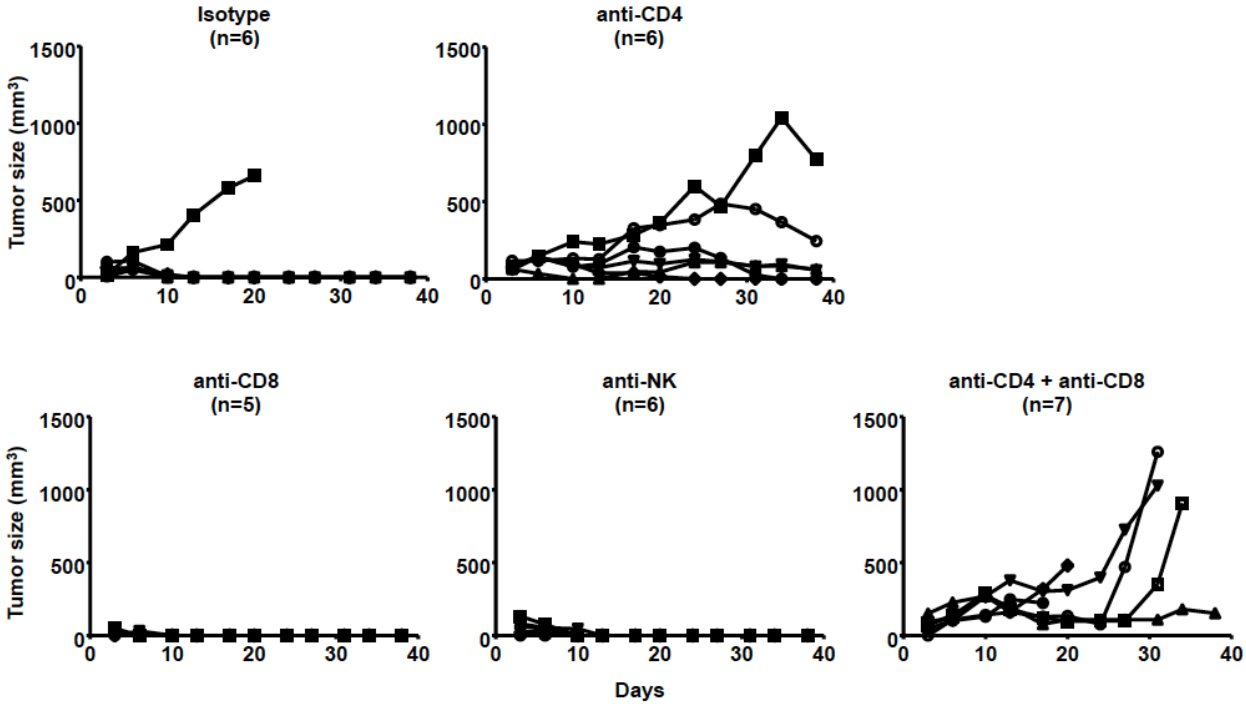

Fig. 1-14. CD4+ or CD4+/CD8+ T cell depletion completely prevented tumor rejection in previously cured animals. Immune cell depletion assays: anti-CD4 (50 µg), anti-CD8 (50 µg) or anti-NK (25 µg) antibodies were injected into cured mice as described in Materials and Methods prior to s.c. challenge with parental naïve Tu-2449SC cells. Tumor measurements were performed twice a week.

Chapter Two: RRV Gene Therapy Combined With Adoptive T Cell Therapy Using Alloreactive CTL for Treatment of Gliomas

Introduction

Gliomas are the most common primary malignant brain tumors in adults. According to the American Cancer Society, 16,500 cases of malignant glioma are diagnosed annually in the U.S., and account for 13,000 deaths/year (2.5% of adult cancer deaths) [1]. In addition to focal solid tumor growth, glioma cells extensively infiltrate surrounding normal brain tissue making their complete removal by surgery extremely unlikely. While improvements to conventional radiotherapy and chemotherapy have been made, the tumors still do not respond well to the therapies. Glioblastoma patients have a median survival that does not exceed 15 months [47].

CNS metastases of systemic cancers are equally incurable, and this patient population is more than 10 times larger, and NIH has designated brain metastasis as an orphan disease of emerging importance. In the U.S., annually there are >200,000 cases of cancer metastasis to the brain, over 20% of all cancer deaths each year. In particular, breast cancer metastasizes to the brain in ~15-20% of women with metastatic disease, and the incidence of CNS-metastatic breast cancer is increasing, even as systemic treatments improve[48]. It is generally thought that the blood-brain barrier (BBB) significantly hinders CNS penetration of most treatment agents, including not only antibodies but also most chemotherapeutics. Thus, the brain is a site offering sanctuary to breast cancer cells that escape systemically administered therapies. Despite current treatment options, including steroids, surgical resection of solitary metastases, stereotactic radiosurgery for small lesions, and whole brain irradiation, the prognosis remains dismal. The median survival time of a patient with breast cancer metastatic to the brain is 4 - 6 months following diagnosis; as few as 20% of patients survive 1 year, and only about 2% survive 2 years after CNS involvement [48].

In primary brain tumors such as glioblastoma, surgery can effectively eliminate bulk tumor in accessible sites, but it is rarely possible to resect adequate margins, and adjuvant therapies must eliminate the infiltrating cells that have migrated from the main tumor mass. Moreover, secondary brain tumors such as CNS-metastatic breast cancer frequently present with multiple foci, making complete surgical resection difficult or impossible. Experimental cellular and gene therapies have been investigated as adjuvant therapies for gliomas [49], and there is precedent for administering adjuvant immunotherapies early on to newly diagnosed glioblastoma patients [50]. T lymphocytes in particular are able to move through tissue as part of their immunosurveillance function. Activated cytotoxic T lymphocytes (CTL) can traffic to and make direct contact with tumor cells to effect their lysis, or come within close proximity while producing cytokines that induce tumor cell apoptosis [27, 51]. Adoptive transfer of CTL may also result in the induction of endogenous immune cell activation.

Rejection responses due to recognition of allogeneic histocompatibility antigens are among the most potent of immunological reactions. Alloreactive CTL (alloCTL), sensitized to the human leukocyte antigens (HLA) of the tumor-bearing host, have demonstrated *in vitro* and *in vivo* success in preclinical glioma model studies [51, 52, 53, 54]. This cellular therapy approach was based upon the observations that HLA expression, especially class I, is absent on normal brain cells, i.e., neurons, oligodendrocytes, and astrocytes [27, 28, 29], but is present on brain tumor cells [27, 30, 31]. Thus, intratumorally-administered alloCTL should largely exert their effector function to tumor cells displaying HLA. This target cell specificity would hold true not only for primary brain tumors such as glioma, but also for secondary brain tumors arising from systemic cancers metastasizing to the brain, as many such cancers would normally express HLA, while the normal brain milieu does not. While alloCTL potentially can inflict collateral damage to endothelial cells, microglia and reactive astrocytes [55], these cells are capable of repopulating in the brain. Encouraging clinical results were documented in recurrent glioma patients receiving intratumoral infusions of alloCTL derived from multiple donors [56, 57].

However, it is postulated that tumor cells use a number of mechanisms to escape immune effector T cells, including downregulation of HLA or co-stimulators, upregulation of dominant-negative HLA-G or inhibitory co-stimulators and inhibitory immunocytokines such as TGF-β, and induction of regulatory T cells [58, 59, 60, 61, 62]. Hence, combining this cellular therapy approach with chemotherapy or prodrug-activator gene therapy may be appropriate for circumventing such tactics, and could lead to tumor mass reduction as well as destruction of the immunosuppressive stromal microenvironment [61, 63]. However, with regard to prodrug activator gene therapy *per se*, despite promising initial results *in vitro* and in animal studies employing replication-defective retroviral (RDR) vectors [12, 64, 65, 66, 67], this approach ultimately failed in Phase III clinical trials because these vectors could not achieve therapeutically adequate transduction levels *in vivo* [68, 69].

More recently, uniquely designed retroviral replicating vectors (RRV) have been shown to achieve highly efficient gene transfer in a variety of solid tumors [13, 14, 15, 16, 70, 71, 72, 73], including gliomas [17, 18, 19, 20, 21, 22, 24, 25, 74]. Notably, animals bearing intracranial gliomas demonstrated significantly prolonged survival when tumors were stereotactically injected with a single dose of RRV coding for yeast cytosine deaminase (CD) followed by systemic administration of prodrug. Furthermore, demonstration of the lack of detectable RRV spread to normal tissues provided a key element of safety for this approach. Following encouraging results from phase I/II studies, this therapy is now in phase II/III clinical trials for patients with recurrent glioblastoma.

Here, we first conducted an in vivo pilot study examining individual and combined immune and gene therapies in an intracranial model of CNS-metastatic human breast cancer MDA-MB-231BR. Administering RRV-CD and unmodified alloCTL together as two individual treatments showed significantly greater efficacy than either alone, as indicated by improved survival until prodrug was discontinued.

We next postulated that alloCTL that have been transduced with RRV, and thereby converted into vector producer cells (alloCTL/RRV), would be equally or more efficacious, and could represent a

translationally feasible strategy. The use of alloCTL/RRV would represent a single combined modality, which utilizes alloCTL, not only as an immunotherapeutic agent for direct killing of HLA-mismatched cancer cells in the context of the HLA-non-expressing brain, but also as a migratory cellular carrier that will provide enhanced tissue penetration and improved intratumoral distribution of RRV.

To this end, the feasibility of engineering human alloCTL to serve as RRV producer cells was first investigated. AlloCTL were transduced with RRV encoding the green fluorescent protein (GFP) marker gene, and tested to determine whether they not only retain target-directed homing motility and anti-tumor cytotoxicity functions, but also whether they could facilitate transfer of RRV to glioma cells *in vitro* and *in vivo*. Based on these results, we further tested the ability of RRV-transduced alloCTL preparations to transmit RRV with an encoded CD gene to glioma cells *in vitro* and *in vivo*, and thereby achieve prodrug-activated cell killing in addition to immunological cytotoxicity. These results of these preclinical studies support clinical translation of this novel multi-modal approach combining intratumoral adoptive transfer of alloCTL administered in parallel or as a combined modality with RRV-mediated prodrug activator gene therapy.

Materials and Methods

Cell culture and HLA characterization.

Human glioma cells

Human glioma cell line U-87MG (ATCC, Manassas, VA) was grown in Dulbecco's modified Eagles medium (DMEM) with 10% fetal bovine serum (FBS; Gemini-Bioproducts, Woodland, CA). The 13-06-MG glioma cell line was derived from a left temporal lobe surgical specimen (collected under Institutional Review Board approved practices) obtained from a glioblastoma patient at initial diagnosis [75]; the cells were established in culture and characterized [27, 58, 76, 77, 78]. The 13-06-MG cells were maintained in RPMI 1640 (Mediatech, Herndon, VA) containing 10% FBS in a 37ºC humidified chamber with 5% CO_2.

Human breast cancer cells

The human breast tumor cell line MDA-MB-231 (ATCC, Manassas, VA) was grown in L15 medium supplemented with 10% FBS (Aleken). The brain-seeking 231 subline 231BR (provided by Dr Toshiyuki Yoneda, University of Texas, San Antonio) was maintained in DMEM supplemented with 10% FBS, sodium pyruvate, and penicillin/streptomycin (Sigma). For some studies, 231BR cells were transduced with RRV expressing the GFP reporter gene (231BR-GFP) or the CD prodrug activator gene (231BR-CD).

Murine glioma cells

Murine glioma cell line Tu2449 was grown in DMEM with 10% FBS.

Characterization of HLA

Class I HLA was examined by flow cytometric analysis using RPE-conjugated mouse anti-human antibodies to HLA-ABC; RPE-conjugated mouse IgG served as the isotype control. The percentage of positive cells and the relative antigen density indicated by mean fluorescence intensity (MFI) were

determined [27]. The specific HLA-AB types determined by serological HLA typing for U-87MG were: HLA-A2, B44, and for 13-06-MG were: HLA-A1,2 and B44,57 . For MDA-MB-231 and MDA-MB-231BR, the serological HLA typing results were: HLA-A2, B40, B41 [77, 78].

Generation of alloCTL

AlloCTL against 13-06 and U-87MG

Whole blood was collected in heparinized tubes from normal donors under an Institutional Review Board (IRB)-approved protocol, and peripheral blood mononuclear cells (PBMC) were isolated by density gradient centrifugation on Ficoll-Hypaque and washed twice with Hank's balanced salt solution (HBSS) as described [79]. Prior to performing the one-way MLTR, the glioma cells underwent 48 hr incubation in culture medium supplemented with 500 IU/ml of recombinant human interferon-γ (IFN-γ, RD Systems Inc, Minneapolis, MN) to upregulate their HLA expression [27]. The stimulator (S) glioma cell monolayers were then washed with phosphate buffered saline (PBS), inactivated by their treatment with mitomycin C (MMC, 25 μg/ml) in culture medium for 1 hr, then washed twice more before combining them with responder (R) PBMC at a R:S ratio of 10:1. The cell mixtures were placed into RPMI-1640 containing 10% FBS and 60 IU interleukin-2 (IL-2)/ml (Proleukin, Novartis, San Carlos, CA). Growth was monitored daily by taking measurements of lactic acid concentration. Plots of the rate of lactate production were extrapolated to determine medium feedings by keeping them optimally at a lactate concentration between 0.5-0.7 gm/liter [79]. At day 12 post-MLTR and every week thereafter, alloCTL cultures were either restimulated with MMC-inactivated relevant or partially-relevant glioma cells. In some cases, the stimulator glioma cells were 100% transduced with RRV-GFP. The optimized R:S ratio of 3:1 was used unless otherwise specified in individual experiments.

AlloCTL against 231-BR

To generate alloCTL against 231-BR brain-adapted human breast cancer cells, PBMC were collected as described above. Before one-way mixed lymphocyte tumor reaction (MLTR), 231-BR cells underwent 48-hour incubation in culture medium with 500 IU/mL recombinant human IFN-ɣ (RD Systems Inc.) to upregulate their HLA expression. The stimulator (S) 231-BR-cell monolayers were then washed with PBS and detached with 2 mmol/L EDTA containing 1% bovine serum albumin, washed and inactivated with 7000 rad (X-ray Irradiator, Gulmay Medical, Inc.). Responder (R) PBMC were mixed with inactivated S cells at a R:S ratio of 10:1. The cell mixtures were placed into Aim-V medium (Life Technologies, Inc.) containing 5% heat-inactivated autologous plasma and 60 IU of IL-2/mL (Proleukin; Novartis). Lactate production, a measure of cell culture expansion, was measured daily and maintained between 500-700 mg/L throughout the culture period by adding fresh medium, as previously described. AlloCTL preparations were used in assays between 12 and 14 days post-MLTR.

Murine alloCTL

Murine alloCTL were generated by lymphocyte-dendritic cell reaction (LDCR). Dendritic cells were made by flushing the bone marrow of B6/C3F1 mice, then culturing with 400ng/mL Flt-3L in complete IMDM (10% FBS, 1% penicillin/streptomycin, 50uM beta-mercaptoethanol). On day 3, 5ng/mL GM-CSF was added to the culture. The next day, stimulator dendritic cells were mixed with red blood cell-lysed responder splenocytes from Balb/c mice at a R:S ratio of 10:1. The culture was maintained at 2-3x10e6 c/mL concentration of responder cells and 100IU/mL IL-2 in complete X-VIVO 15 (2% FBS, 1% P/S, 50uM beta-mercaptoethanol).

Virus vector production.

Viral vector stocks were generated by transient transfection of the human embryonic kidney-derived

293T cell line (ATCC, Manassus, VA) using FuGENE6 (Roche Molecular Biochemicals, Mannheim, Germany) as a transfection agent per manufacturer protocol [20]. The cells were grown in DMEM containing 10% FBS. The conditioned medium (viral supernatant) was collected 48 hr after transfection with the pACE-GFP, pAC3-GFP, or pACE-CD plasmids (**Figure 2-1**). These vector constructs have been described previously. For titer determination of the viral stock, 50 μM of 3'-azido-deoxythymidine (AZT, Sigma Aldrich, St. Louis, MO) was added to U-87MG cells 48 hr post-transduction to prevent further virus replication [80]; the virus titer was then determined as described and expressed as transducing units (TU)/ml [19].

Transduction of alloCTL by RRV using conventional and nonconventional transduction techniques and conditions.

Transduction with cell-free virus supernatant

ACE-GFP or AC3-GFP RRV viral stocks were used to infect alloCTL at a multiplicity of infection (MOI) of 10 or 7, respectively, using conventional techniques involving spinoculation, polybrene, or retronectin-coated plates. For spinoculation, 6-well plates containing the alloCTL and viral stock were centrifuged at 200 x g for 60 min. Alternatively, polybrene (8 μg/ml, Sigma, St. Louis, MO) was added to the virus stock before their incubation with alloCTL in suspension [74], or the alloCTL and virus stock were added to Retronectin coated plates (20 μg/ml fibronectin fragment CH-296, Takara Pharmaceutical, Mountain View, CA) with transduction following manufacturer protocol [81]. All the transductions were performed 1 to 3 times. The alloCTL were analyzed for GFP expression by flow cytometric analysis using a Coulter EPICS (Beckman Coulter, Fullerton, CA) or a LSR II (BD Biosciences, San Jose, CA).

Transduction by producer cell coculture

In initial experiments alloCTL that were initially sensitized with 13-06-MG cells were restimulated at

day 12 post-MLTR, with either MMC-inactivated adherent cultures of 13-06-MG cells to which they were initially sensitized, or with MMC-inactivated U-87MG glioma cells bearing partial HLA allelic identity with 13-06-MG, at multiple R:S ratios of 10:1, 3:1, 1:1, 1:10, and 1:50. For later experiments, since the effector function of alloCTL was quite potent, the alloCTL restimulations were performed with adherent cultures of MMC-inactivated, 100% ACE-GFP RRV transduced U-87MG glioma cells (i.e., U-87MG/ACE-GFP) at a R:S ratio of 3:1. Transduction efficiencies were determined by flow cytometry at various times after restimulation.

Cell Growth Assays for Assessment of Anti-Tumor Activity

Human gliomas

The CellTiter 96 Non-Radioactive Cell Proliferation Assay (Promega, Madison, WI) was used to determine the metabolic activity of U-87MG glioma cells after their exposure to alloCTL, or to alloCTL/RRV-CD preparations exposed to prodrug. This kit employs the soluble tetrazolium salt, MTS [3-(4,5-dimethylthiazol-2-yl)-5-(3-carboxymethoxy-phenyl)-2-(4-sulfophenyl)-2H-tetrazolium], which is reduced by metabolically active cells into formazan that is measured at an optical density of 490 nm [65]. Reference control groups are as described in the individual experiments presented.

In one set of experiments, anti-13-06 alloCTL at day 12 post-MLTR were coincubated with U-87MG glioma target cells bearing partial HLA in common to 13-06-MG. Wells were seeded with 10^3 target cells/well and alloCTL were added at E:T of 1:1, 1:10, and 1:100. Control wells contained only U-87MG cells (i.e., E:T = 0:1). After removing nonadherent cells and washing the adherent U-87MG cells three times the growth was assessed by MTS assay at days 2, 5 and 8 following incubation. Absorbance at 490 nm was measured from pentaplicate wells. Cell growth data were plotted over time, expressed as mean metabolic activity units ± SEM.

In another set of experiments, alloCTL/RRV-GFP or alloCTL/RRV-CD preparations were cocultured with U-87MG cells in six well plates at 1:10 for 7 days. The nonadherent cells were removed and the U-87MG adherent cells were washed before performing the MTS assay (day 0), or the cultures received medium supplemented with 2 mM 5-FC. The cultures were continued for 2, 5 or 8 days before performing MTS assays for cell growth on pentaplicate wells. Metabolic activities derived from the optical densities were plotted over time and displayed as cell growth rate ± SEM.

In a separate experiment**,** U-87MG cells were collected after their coculture with an alloCTL/RRV-CD preparation at a ratio of 1:10 for 4, 7, or 10 days. The U-87MG cells were then seeded into 96-well plates at 2.5 x 10^3 cells/well and wells in pentaplicate were exposed to the prodrug 5-FC (2 mM) for either 2, 4, or 6 days before determining cell viabilities by the MTS assay. Nontransduced U-87MG cells exposed to 5-FC were used as the reference control and 100% transduced U-87MG/RRV-CD cells were used as a positive control. The data were expressed as percentages ± SEM of the metabolic activity values obtained for nontransduced U-87MG control wells and compared with reference to the 100% transduced U-87MG wells.

Murine glioma

Electrical impedance was continuously monitored using the xCELLigence system (ACEA Biosciences) in E-plate 96 (ACEA). The background was measured in wells containing 50µL of T cell culture medium without cells for 60s. Tu2449 cells were detached from the flasks by a brief treatment with trypsin/EDTA, re-suspended in T cell culture medium and adjusted to 8x10^3 cells in 100µL. These cell suspensions were added to wells containing 50µL of culture medium. Three wells were seeded for each effector to target ratio (E:T). The E-plates were incubated at room temperature for 30 min and placed on the plate reader in the incubator for continuous impedance recording. Cell index (CI) data were recorded every 15 min for 24 h, then effector cells were added. 24 h later, effector alloCTLs (one day post LDCR) suspended in T cell culture medium were added at E:T of 10:1, 1:1, or 0.1:1 in appropriate wells, with IL-2 (100 IU/mL). 0.1% Triton-X was added for maximal kill wells. All procedures were

performed in laminar flow cabinet. The cells were real-time monitored at 37°C in humidified 5% CO_2 atm. CI data were recorded every 2 min for 13.3 h, then every 15 min for 25 h. Wells containing only effector cells were used as negative control for impedance baseline measurement. In all the experiments, the final volume in the microwells was 160µL. Data was acquired through the RTCA software, and CI were normalized at a time point immediately post effector cell addition.

Cytotoxicity Assays for Assessment of Anti-Tumor Activity

Lytic activity of alloCTL/RRV preparations were assessed at various effector to target ratios (E:T) by ^{51}Chromium release cytotoxicity assays at day 14 post-MLTR [56]. Briefly, 5 x 10^6 tumor target cells, suspended in 0.1 ml of their growth medium, were labeled with 100 mCi $Na_2{}^{51}CrO4$ (Amersham, Park Ridge, IL) for 60 min at 37°C. Cells were washed twice with HBSS and suspended in AIM-V growth medium. In a final volume of 0.2 ml, 10^4 cells were placed into 96-well round-bottom microtitration plate wells that contained different concentrations of alloCTL/RRV. In blocking assays, neat conditioned medium from the W6/32 hybridoma making anti-HLA-ABC was also placed into wells containing the effectors and targets. The plates were centrifuged at 200 x g for 5 min and then incubated for 4 hr at 37°C, in a humidified, 5% CO_2 atmosphere. Following centrifugation at 200 x g for 10 min, 50% of the well volume was harvested and counted. Maximal release was produced by incubation of the targets with 0.1 M HCl. Spontaneous release was the radioactivity as cpm of targets in assay medium alone. The percentage specific release was calculated by the formula: $[(^{51}Cr_{experimental} - {}^{51}Cr_{spontaneous}) / (^{51}Cr_{maximal} - {}^{51}Cr_{spontaneous})] \times 100\%$. Data are given as the mean specific release of triplicate wells, provided that the standard error did not exceed 10% and the specific release was greater than 10%.

Cytokine Production for Assessment of Anti-Tumor Activity

Human IFN-γ concentrations were measured in clarified supernates 48 hr after coincubation of alloCTL/RRV-GFP, at day 14 post-MLTR, with relevant or partially relevant tumor target cells (E:T of 10:1). Aliquots of the anti-13-06 alloCTL either were or were not restimulated at day 12 post-MLTR with MMC-inactivated U-87MG/RRV-GFP at a R:S of 3:1. Manufacturer instructions were followed for a Quantikine ELISA kit specific for human IFN-γ (R&D Systems, Minneapolis, MN) with a sensitivity of 2 pg/ml [82]. Various dilutions of the supernates were analyzed so that we could evaluate the samples in the linear range.

AlloCTL Migration on Glioma Cell Monolayers

The procedure for assessing the radial migration of alloCTL over a monolayer of glioma cells has been described. Briefly, a stainless steel manifold and 10-well Teflon slide was used to focally deposit non-adherent T cells into wells prepared with confluent tumor cell monolayers. Multi-channel fluorescence microscopy was used to track the movement and behavior of the effector cells over time. Fluorescent dyes and/or viral vectors that code for fluorescent transgenes were used to differentially label the cell types for imaging.

Kinetics of glioma cell transduction by alloCTL/RRV-GFP preparations *in vitro*.

AlloCTL/RRV-GFP preparations were placed onto monolayers of glioma cells in six well plates at a ratio of 1:10 and the kinetics of transduction were monitored between 12-20 days. We generally discontinued the monitoring when the transduction exceeded 90% or more in culture. In parallel for the human alloCTL/RRV, we also collected similar data by light and fluorescence microscopy, where assessments of GFP positive U-87MG cells were made at days 0, 5, 7, 10, 13, and 17 after being placed into chamber slides with alloCTL/RRV-GFP (Nalge Nunc International, Rochester, NY).

Genomic PCR analysis

To demonstrate the spread of RRV-CD vector within U-87MG cells, PCR analysis was performed to monitor stable integration of the CD transgene sequence in the genomic DNA from U-87MG cells cocultured with alloCTL/RRV-CD at a ratio of 1:10 for 4 days. The adherent glioma cell monolayers were washed three times to remove the alloCTL/RRV-CD and trypsinized. An aliquot was removed for genomic DNA extraction and the remaining cells were replated and cultured for a total of 7 or 10 days before harvest and extraction. Genomic DNA was extracted using DNeasy Tissue Kit (Qiagen, Valencia, CA) from U-87MG cells prior to coculture and then at serial time points after coculture, and used as templates for PCR amplification. PCR to detect the CD sequence was performed with the upstream primer (5'-GATTTCGGCGTGAAGAAAAT-3') and downstream primer (5'-ACTCTTTATCGCCCAGCAGA-3') and visualized by ethidium bromide staining of agarose gels for the 431-bp CD PCR product. Briefly, each genomic DNA sample (600 ng) was used in a 50 µl PCR reaction with High-Fidelity PCR Master Mix (NEB Inc., Ipswich, MA) and the above primers hybridizing to the CD gene. Products were amplified by 25 cycles of successive incubation at 98ºC for 10 s, 60º C for 30 s, and 72º C for 30 s. Reaction product (8 µl) was resolved on a 1.0% agarose gel and visualized by ethidium bromide staining. The U-87MG cells fully transduced with CD (i.e., U-87MG/RRV-CD) and the pACE-CD template were used as a positive controls. A 610-bp fragment of the human β-actin gene was used as an internal control and also amplified using the primers (5'-CTAGAAGCATTTGCGGTGGACGATGGAGGG-3', 5'-TGACGGGGTCACCCACACTGTGCCCATCTA-3'). Densitometric analysis was performed on the gel and the values obtained for each experimental lane were analyzed relative to the 100% transduced U-87MG/RRV-CD lane and converted to a percentage of that control.

In vivo therapeutic efficacy studies with human 231-BR intracranial xenografts in immunodeficient mice.

All animal experiments were performed according to institutional guidelines under UCLA Animal Research Committee (ARC)-approved protocols. $Rag2^{-/-}gc^{-/-}$ mice (Taconic Farms) underwent surgery for placement of intracranial cannulas (Plastics One) that were inserted through a burr hole in the right side of the skull at stereotactic coordinates 1 mm anterior to bregma, 1.5 mm lateral to midline, 2.8 mm deep. The cannulas extended 3 mm into the brain and were affixed to the skull with resin. Six days later, tumor cells ($2x10^5$ total cells in 3 uL), consisting of either 100% 231BR, or 98% 231BR cells + 2% 231BR-GFP or 2% 231BR-CD cells, were infused through the cannulas and the animals were placed into various treatment groups. AlloCTL or unstimulated PBMC ($2x10^6$/3 uL) or PBS were infused through the cannulas into the tumor on days 9 and 16 posttumor instillation. All groups of mice (n = 9–10) were treated with 3 cycles of 5 daily i.p. 5-FC (500 mg/kg) injections (per cycle) beginning on days 12, 26, and 47 posttumor instillation. Mice were monitored for signs of morbidity and weighed every 3 to 4 days for the duration of the experiment.

***In vivo* therapeutic efficacy studies with subcutaneous human U-87MG xenograft tumors in immunodeficient mice.**

AlloCTL treatment

As above, all animal experiments were performed according to institutional guidelines under UCLA ARC-approved protocols. One experiment involved a Winn-type assay (preventative) performed with two groups (n=12/group). Either the nude mice received a subcutaneous injection of U-87MG cells (10^6) or a mixture of U-87MG with alloCTL that were initially sensitized to the HLA of 13-06-MG and restimulated with MMC-inactivated U-87MG at day 12. The glioma cells were mixed with post-MLTR day 14 alloCTL immediately before injection and growth was monitored by caliper measurements for 35

days.

AlloCTL, AlloCTL/RRV, and RRV treatments

In another set of experiments, U-87MG cells (10^6) were injected subcutaneously into 6-week old female nude mice. After allowing tumor to establish for 7 days, each mouse was assigned randomly to a treatment group (n=12). Treatment on day 7 was given to groups that involved either a single intratumoral injection (0.1 ml) of: 1) PBS followed with daily ip administration of 5-FC prodrug (500mg/kg) between days 35 to 42, 2) viral RRV-CD stock ($5x10^4$ TU/ml), 3) viral RRV-CD stock ($5x10^4$ TU/ml) followed with ip administration of 5-FC prodrug between days 35 to 42, 4) anti-13-06 alloCTL at day 14 post-MLTR (restimulated with $5x10^4$ U-87MG cells at day 12 post-MLTR), and 5) anti-13-06 alloCTL/RRV-CD at day 14 post MLTR (restimulated with $5x10^4$ cells U-87MG/RRV-CD at day 12 post-MLTR) followed with ip administration of 5-FC prodrug between days 35 to 42. Assessments for tumor growth, made by caliper of tumor width and length, were performed every several days over a period of 42 days. Tumor volumes were calculated for the individual animals using the formula: Volume = $(4/3)\pi(\text{width}/2)^2(\text{length}/2)$. The mean tumor volumes for each treatment group ± SEM were plotted over time.

Quantitative PCR analysis for RRV biodistribution *in vivo*.

Genomic DNA was extracted from the harvested tissues (lung, liver, spleen, kidney, bone marrow, and tumor) of mice 42 days after treatment with RRV vector using the DNeasy tissue kit (Qiagen, Valencia, CA). To detect integrated RRV sequences, quantitative real-time PCR was performed in a 25 μL reaction mixture containing genomic DNA and TaqMan Universal PCR Master Mix (PE Applied Biosystems, Foster City, CA). Amplifications were carried out in duplicate using an ABI Prism 7700 sequence detector. The primers and probe were designed to target the 4070A amphotropic env gene (4070A-F, 5'-GCGGACCCGGACTTTTGA-3'; 4070A-R, 5'-ACCCCGACTTTACGGTATGC-3';

probe, FAM-CAGGGCACACGTAAAA-NFQ).

Statistical analyses.

Statistical analyses were performed using GraphPad Prism software (version 4, GraphPad Software, San Diego, CA). The average metabolic activities determined from viable cells were determined by MTS assays and displayed ± SEM. The tumor volumes obtained for treated vs nontreated groups were compared either using an unpaired Student t test or a two-way ANOVA; p values of ≤ 0.05 were considered significant. Median survival times (MST) from the Kaplan– Meier curves were analyzed by nonparametric log-rank tests.

Results

Generation of breast cancer-targeted alloCTL

The standard technique used to generate alloCTL is by one-way mixed lymphocyte reactions (MLR) where inactivated stimulator PBMC from the tumor patient are combined with responder PBMC from normal donors unrelated to the patient [79]. Restimulation of the cells is usually required with relevant, inactivated target cells within a couple of weeks and then on a routine basis thereafter to maintain growth. MLRs could not be used in these studies because PBMC were no longer available from the patients from whom the tumor cells were obtained. Therefore, cancer cell lines were incubated in the presence of IFN-γ to increase their surface HLA expression before their inactivation and use as stimulators in one-way mixed lymphocyte-target cell reactions (MLTR).

Adherent MDA-MB-231 cells were irradiated and used as stimulator cells in a one-way mixed lymphocyte-tumor reaction (MLTR) with responder PBMC from donors who were HLA-mismatched with MDA-MB-231 (**Table 2-1**), and lactate production was monitored daily as a measure of cell culture expansion. PBMC from donor D10-18 emerged as the highest producer of lactate, indicating that cell growth in this culture was more robust after stimulation with irradiated MDA-MB-231 cells as compared to PBMC from the other donors, and this was confirmed by counting viable cells after restimulation with OKT3 (data not shown). Based on these results, donor D10-18-derived alloCTL were used in subsequent studies.

Immune and/or prodrug activator gene therapies demonstrate therapeutic benefit to intracranial 231-BR xenografts *in vivo*

Initial studies to examine therapeutic efficacy of alloCTL adoptive immunotherapy and RRV suicide gene therapy, individually and in combination, were performed in secondary brain tumor models using MDA-MB-231BR, a brain-tropic subline of the metastatic triple-negative human breast cancer cell line

MDA-MB-231, isolated by repeated cycles of intra-cardiac injection and recovery of brain metastases. Flow cytometric analysis with anti-HLA antibodies confirmed cell surface HLA expression on MDA-MB-231BR cells was comparable to the parental cell line MDA-MB-231. Indwelling intracranial cannulas were used to establish intracerebral 231BR tumors in 7 groups (n = 9–10) of immunodeficient $Rag2^{-/-}gc^{-/-}$ mice, consisting of either 100% 231BR or 98% 231BR mixed with either 2% 231BR-GFP or 2% 231BR-CD cells (**Figure 2-2**). Control groups of mice were injected with non-therapeutic 231BR-GFP tumor cells instead of 231BR-CD, or were infused with PBS or unstimulated PBMC in place of alloCTL. On days 9 and 16 post-tumor instillation, effector alloCTL, or control PBMC or PBS was infused into the established tumor bed through the cannula. All mice were treated with 5-day cycles of 5-FC (500 mg/kg, i.p.); up to 3 cycles were possible, spaced 2 or 3 weeks apart beginning on day 12 post-tumor instillation (**Figure 2-2**). Kaplan–Meier survival plots and median survival time (MST) for the control and experimental groups are shown in **Figure 2-2B**. The MST of the untreated control group (no RRV, no alloCTL effector cells, group 1) was 31.5 days, whereas the MST of the sham-treated control group given nontherapeutic 231BR-GFP vector producing cells with the tumor inoculum and unstimulated PBMC was 40 days (group 3). The MSTs for mice treated with individual experimental modalities ranged from 50 to 83 days. The MSTs of the 2 groups receiving alloCTL therapy alone (with RRV-GFP infection or no RRV infection) were 65 and 83 days respectively (groups 4 and 2), whereas the MSTs of the 2 groups receiving prodrug activator gene therapy alone (with PBMC or PBS, instead of alloCTL) and up to 3 prodrug cycles were 50 and 57 days, respectively (groups 6 and 5). Statistical significance was reached ($P < 0.05$) for all of the individual immune or gene therapy–treated groups compared to each of the control groups. The MST of the group receiving the combined intratumoral effector alloCTL and RRV prodrug activator gene therapies (group 7) was 97.5 days, thus exhibiting a highly statistically significant survival benefit compared to each of the control groups. Furthermore, the group receiving combined immune and gene therapies showed a statistically significant addi- tional survival advantage compared to those groups receiving gene therapy alone ($P < 0.0001$ and 0.0123, groups 7 vs. 6 and 5, respectively). The combination treatment also showed a trend toward statistical

significance compared to the groups receiving alloCTL cellular therapy alone ($P < 0.0511$ and 0.6380, groups 7 vs. 4 and 2, respectively).

Glioma-targeted alloCTL generated by one-way MLTR also exhibit anti-tumor function *in vitro* and *in vivo*

Activated T cells possess immunosurveillance function and therefore have an innate ability to migrate through brain parenchyma to reach infiltrating tumor cells. We then postulated that if alloCTL and RRV were combined into a single modality by converting alloCTL themselves into RRV producer cells (alloCTL/RRV), this capability would be particularly advantageous for dissemination of RRV to diffusely infiltrating cancer cells in the brain, as seen in glioblastoma. Accordingly, for these studies, we generated glioma-targeted human alloCTL for subsequent transduction with RRV.

Human alloCTL targeting mismatched HLA on U-87MG and 13-06-MG human glioma cells were first generated from donor PBMC by MLTR, as above. Class I HLA expression of U-87MG target cells was 93.9% positive with an MFI of 200 pre-exposure to IFN-γ, and after incubation with 500 U IFN-γ/ml for 48 hr became 99% positive with an MFI of 308. Also, as previously reported, 100% of the 13-06-MG cells already expressed Class I HLA at baseline, but the MFI increased from 346 to 617 upon incubation with IFN-γ [27]. Thus, alloCTL were generated after Class I HLA was upregulated by IFN-γ on these glioma stimulator cells.

To determine if the glioma-stimulated alloCTL made by MLTR had anti-tumor function *in vitro,* we performed MTS assays starting at day 12 following the MLTR. The alloCTL effectors were mixed with U-87MG target cells at low ratios of 1:1, 1:10, and 1:100 and placed into culture over a period of 8 days. At days 2, 5 and 8 the metabolic activity ± SEM of the adherent U-87MG cells was determined and compared to U-87MG control cells that were not exposed to alloCTL (**Figure 2-3A**). The MTS assay

demonstrated marked *in vitro* growth inhibition of the U-87MG glioma cell targets exposed to alloCTL at ratios of 1:1 and 1:10.

Next, we examined whether the anti-13-06 alloCTL displayed anti-tumor activity toward partially relevant U-87MG cells when placed *in vivo*. In a Winn-type assay, the alloCTL were mixed with U-87MG cells (1:10) immediately before subcutaneous implantation into nude mice. The tumor volumes of U-87MG were monitored over time. **Figure 2-3B** shows the average tumor volumes at day 35 post-implantation of U-87MG versus the U-87MG when premixed with the alloCTL. Tumor growth was measurable in 12 out of 12 mice in the group given only U-87MG cells, but only in 1 out of 12 mice given the mixture of U-87MG and alloCTL. The *in vivo* data are consistent with the *in vitro* data showing that alloCTL inhibit tumor cell growth at a 1:10 ratio.

Transduction of alloCTL with RRV

The transduction efficiency and replicative spread of the RRV-GFP vector (**Figure 2-1**) into anti-13-06 alloCTL was monitored at various times after inoculation with ACE-GFP RRV virus stock at a multiplicity of infection of 10. Using conventional methods employing spinoculation, polybrene, or Retronectin-treated plates the flow cytometric analysis of alloCTL for GFP positivity peaked at 17-18% by day 4, but by day 8 the GFP-positive cells and viability of the alloCTL/RRV preparations plummeted. Since the conventional transduction methods were unsatisfactory, we tried nonconventional methods to determine if the transduction of viable alloCTL could be improved. At the time of restimulation (day 12 or later post-MLTR), the alloCTL were placed onto monolayer cultures of MMC-inactivated 13-06-MG or U-87MG cells that were 100% transduced and producing ACE-GFP virus (i.e., 13-06-MG/RRV-GFP or U-87MG/RRV-GFP). For experiments that involved restimulation with U-87MG/RRV-GFP glioma cells we confirmed that they maintained their Class I expression levels and thus could serve as effective stimulators (data not shown).

Transduction was assessed one week or later after restimulation of the anti-13-06 alloCTL with either inactivated U-87MG/RRV-GFP or 13-06-MG/RRV-GFP cells. It was best to perform the restimulation with U-87MG glioma cells bearing a partial HLA commonality to that of the stimulator 13-06-MG glioma cells, and at low responder to stimulator ratios (i.e., R:S of 3:1), since the U-87MG cells were not lysed as quickly as the 13-06-MG stimulator cells. However, only low levels of transduction occurred using this nonconventional method. At one week following transduction, the viable cell population within the alloCTL/RRV preparations contained between 2 to 7% GFP-positive cells (mean = 5%).

In an effort to investigate the combination of alloCTL and RRV in a syngeneic model, we characterized murine alloCTL/RRV as well. Murine alloCTL were generated by lymphocyte-dendritic cell reaction (LDCR). Using the spinoculation method, alloCTL were transduced by AC3-GFP at an MOI of 7 three days post LDCR. This method achieved 1.5% transduction by day 2, then 2.79% by day 5 post transduction of alloCTL (**Figure 2-4**).

Preparations of alloCTL/RRV-GFP with low level transduction of RRV-GFP exhibit anti-tumor functionality

To determine if the cytolytic effector function of the alloCTL/RRV-GFP preparations was maintained *in vitro* we performed 4 hr ^{51}Cr-release cytotoxicity assays at day 14 post-MLTR. The alloCTL/RRV-GFP were coincubated with 13-06-MG glioma target cells that display all the HLA-AB antigens to which the alloCTL were sensitized (i.e., HLA-A1,2 and B44,57) or coincubated with U-87MG target cells that display half of the HLA-AB alleles common to 13-06-MG cells (i.e., HLA-A2, B44). The anti-13-06 alloCTL that were restimulated at day 12 with 13-06-MG cells lysed the majority of the relevant 13-06-MG target cells (80-100% at 5:1, 10:1, 20:1 E:T), whereas half that number of U-87MG target cells (40-50%) were lysed at the same 3 E:T ratios tested (**Figure 2-5A**). Furthermore, to confirm that the alloCTL/RRV preparations made by MLTR contained CTL that were alloresponsive we placed

conditioned medium from the W6/32 hybridoma that produces anti-HLA-ABC at one E:T ratio for both targets. The lysis was inhibited by 50-60% (data not shown). The cytotoxicity data are demonstrative of the specificity of the alloCTL/RRV for relevant target antigens. One implication of these findings is that the temporal exposure of alloCTL at restimulation with inactivated 13-06-MG target cells displaying the full complement of HLA target antigens would be very brief compared to that of inactivated U-87MG cells with half that complement.

Similarly, to assess the retention of alloCTL/RRV's cytotoxic function, we measured target cell viability using the xCELLigence electrical impedance assay. AlloCTL or alloCTL/AC3-GFP preparations were added to plated target cells at an E:T of 10:1, 1:1, and 0.1:1. Cell viability index was normalized to the time immediately post effector cell addition, and to target cells. At 4 hours post alloCTL/RRV addition, titrated killing was observed by both non-transduced and transduced alloCTL (**Figure 2-5B**). Furthermore, by hour 10, AlloCTL/RRV 10:1 wells had no attached target cells, demonstrating strong killing capabilities comparable to its non-transduced counterpart.

Cytokine production by the alloCTL/RRV-GFP preparations at day 14 post-MLTR was analyzed from supernates collected 48 hr following their coincubation with 13-06-MG or with U-87MG target cells (**Table 2-2**). Similar to the cytotoxicity data, alloCTL/RRV-GFP that were initially sensitized to the HLA of 13-06-MG cells during the MLTR responded upon coincubation with relevant 13-06-MG cells by producing more than twice the amount of IFN-γ than alloCTL/RRV-GFP coincubated with U-87MG cells with partial HLA allelic display. The production of IFN-γ by alloCTL/RRV-GFP not exposed to target antigen was lower at 40 pg/ml. The alloCTL that did not undergo the restimulation/transduction step at day 12, but instead were exposed to relevant target 13-06-MG cells for the first time since the MLTR had been started showed evidence of robust proinflammatory T helper 1 response by producing nearly 600 pg/ml IFN-γ.

Preparations of alloCTL/RRV-GFP exhibiting low level transduction with RRV-GFP effectively transduce glioma cell monolayers *in vitro*

To examine whether alloCTL/RRV-GFP preparations could produce vector and transduce glioma cells in culture, we placed them onto viable U-87MG cell monolayers at a ratio of 1:10 and monitored the kinetics of vector spread over periods of 15 to 20 days.

The spread of GFP positive cells from a transduced alloCTL/RRV-GFP preparation to adherent U-87MG monolayers in slide chamber cultures was followed visually by light and fluorescence microscopy. At low power we show representative light microscopic (left column), fluorescent (middle column), then merged views (right column) at various time points between 0 and 17 days (**Figure 2-6A**). At days 0 and 5 only occasional small, bright focal fluorescent GFP+ alloCTL were seen to attach to the surfaces of large adherent glioma cells. The inset shown on the merge at day 5 best shows this at higher power magnification (**Figure 2-6B**), where multiple nontransduced alloCTL and a single, bright GFP+ alloCTL from the transduced alloCTL/RRV-GFP preparation are shown in contact with attached glioma cells. Increasingly greater numbers of GFP-positive U-87MG adherent cells displaying astrocytic-like morphology are seen at days 7, 10 and 13, indicating extensive spread of the RRV such that greater than 92% of the adherent cells are positive by day 17. **Figure 2-6C** shows flow cytometric data that were obtained in parallel with the microscopic data. The viably-gated cell histograms indicate the percentages of GFP-positive cells from the total. The results indicate that low numbers of alloCTL/RRV-GFP placed onto glioma cell targets can facilitate low level transfer of vector into glioma cells that later impart a highly accelerated replicative spread *in vitro*. **Figure 2-6D** shows the rate of glioma cell transduction where the percentages of GFP-positive U-87MG cells ± SEM are plotted over time. The U-87MG cells were only 8% GFP positive by day 5, when the nonadherent alloCTL/RRV-GFP cells were removed by washing, but between days 7 and 17 the culture went from 29.7% to 92.4% GFP positive.

In order to assess whether murine alloCTL/RRV is able to produce RRV, murine alloCTLs from 2 days post AC3-GFP transduction were incubated with monolayer Tu2449 cells at E:T = 1:10. Tu2449

cells were passaged and sampled every few days for flow cytometric analysis of GFP positive cells. By 10 days post the start of co-culture, over 90% of the adherent cells were positive for GFP (**Figure 2-6E**). This suggests that murine alloCTL/RRV are also able to produce functional virus that can subsequently infect glioma cells.

Migration of alloCTL/RRV preparations across glioma monolayers

T lymphocytes inherently have the ability to migrate, and it is this capability that is key to delivering RRV to infiltrating areas of the tumor *in vivo*. Therefore, we examined the ability of murine alloCTL/RRV to migrate across glioma monolayers *in vitro*. Fluorescently labeled alloCTL/AC3-GFP were deposited in the center of monolayer Tu2449 cells transduced with the mStrawberry gene. The well was monitored over time using multichannel fluorescence microscopy. By 48 hours, many cells from the alloCTL/RRV preparation had migrated out toward the edge of the well (**Figure 2-7**). However, as the transduction rate was low as previously mentioned, we were not able to see GFP positive alloCTL in the captured images and we can only surmise that the transduction procedure does not affect the migration of alloCTL/RRV any differently from alloCTL. In a separate experiment with human alloCTL transduced with GALV-pseudotyped RRV, we showed migration of bright green RRV-transduced alloCTL over a 72 hour time period (data not shown).

Integration of RRV-CD into U-87MG cell monolayers using alloCTL/RRV-CD

After validating the restimulation/transduction protocol with the RRV-GFP, we performed alloCTL transduction with RRV-CD (**Figure 2-1**) in preparation for later *in vivo* studies. Using methods similar to that with alloCTL/RRV-GFP, alloCTL/RRV-CD were overlaid onto plated U-87MG cells at a ratio of 1:10. At day 4, the glioma cell monolayers were washed to remove nonadherent alloCTL/RRV-CD, then

passaged. A glioma cell aliquot was taken for extraction of genomic DNA before replating the cells. Additional cells were harvested for extraction on days 7 and 10. Integration of RRV-CD vector into the glioma cell monolayers harvested at different times after their exposure to RRV-CD was demonstrated (**Figure 2-8A**). PCR with CD primers was performed on the DNAs of these cell extracts, on extracts of U-87MG cells not exposed to alloCTL/RRV-CD (negative control), and with extracts from 100% transduced U-87MG/RRV-CD (positive control). An extract from the plasmid ACE-CD served as a second positive control. The ethidium bromide stained agarose gel indicates increasing CD signal going from days 4 to 10, with no signal from the negative control, and equivalent signal from the day 10 cell extract as from the 100% transduced U-87MG cells. Based upon the 100% transduced U-87MG/RRV-CD reference control, the densitometric values indicate 100% spread of viral vector from alloCTL/RRV-CD to U-87MG cells at day 10; the spread was 55% at day 7 and 26% at day 4 (**Figure 2-8B**).

alloCTL/RRV-CD preparations are cytolytic and CD is a functional prodrug activator gene within alloCTL/RRV or U-87MG cells in the presence of prodrug 5-FC.

U-87MG cells were either cultured with alloCTL or alloCTL/RRV-CD for one week. If E:T ratios greater than 1:1 were used, U-87MG cells did not survive, indicating both RRV transduced and nontransduced alloCTL preparations retain potent cytolytic function. When the E:T ratios were adjusted to 1:1 or lower, a portion of the U-87MG cells survived and grew (data not shown).

In one experiment, prodrug 5-FC was added to the culture medium (2 mM) of U-87MG cells that had previously been incubated at an E:T of 1:10 with either alloCTL/RRV-GFP or with alloCTL/RRV-CD for one week. The MTS assay for cell growth was performed on pentaplicate wells at day 0 or those continued in culture for 2, 5 or 8 days. Only the U-87MG cells that were previously incubated with alloCTL/RRV-CD failed to thrive (**Figure 2-9**), indicating the CD gene was functionally active in the presence of prodrug and that a significant portion of the U-87MG cells were transduced and therefore

receptive to 5-FC treatment.

In another set of experiments, we placed U-87MG cells that we had previously cocultured with transduced alloCTL/RRV-CD for periods of 4, 7, or 10 days, before washing the alloCTL/RRV-CD from the U-87MG monolayers. We continued the culture of alloCTL/RRV-transduced U-87MG cells in medium containing 5-FC (2 mM) to obtain a sense of the levels of transduction and susceptibility to prodrug treatment over time. The metabolic activities were assessed by MTS assay after 2, 4, and 6 days and expressed as a percentage of the metabolic activity measured from the reference nontransduced 5-FC-treated U-87MG control cells (**Figure 2-10**). For comparison, we used 100% transduced U-87MG/RRV-CD cells that were cultured in medium containing 5-FC prodrug for the same periods. The U-87MG cells that were initially exposed to alloCTL/RRV-CD for increasingly longer times were progressively more sensitive to 5-FC-induced killing. The metabolic activities also decreased as a time-dependent function of 5-FC exposure. By day 6 following addition of 5-FC, nearly all of the cells that had been exposed to alloCTL/RRV-CD for the initial 7-day coincubation or longer were non-viable, equivalent to 100% transduced U-87MG/RRV-CD cells, indicative that a significant portion of the naive U-87MG cells had been transduced with RRV-CD vector and thereby killed upon 5-FC treatment.

Immune and/or prodrug activator gene therapies demonstrate therapeutic benefit to subcutaneous U-87MG xenografts *in vivo.*

The tumor volumes of nude mice bearing one-week established U-87MG tumors (initial inoculum of 10^6) were calculated from caliper measurements of width and length obtained over time, out to day 42. Different control groups were either sham-treated by intratumoral injections with PBS or with RRV-CD vector only, with subsequent prodrug. Experimental treatment groups were treated by intratumoral prodrug activator gene therapy i.e, RRV-CD vector plus 5-FC (500 mg/kg ip on days 35-42) alone, or cellular immunotherapy, i.e., alloCTL (10^5) alone. A combination immune and gene therapy treated group

(n=12) similarly received the same number alloCTL/RRV-CD and 5-FC injections. The control groups showed uninhibited progressive tumor growth *in vivo*, while growth inhibition was observed in all of the experimental treatment groups. Notably, however, the temporal patterns of tumor growth inhibition were characteristic of each type of treatment. As expected, the group treated with RRV-CD vector supernatant showed tumor growth kinetics comparable to those of the control group until administration of the prodrug, whereupon significant tumor regression was seen. In contrast, the group treated with alloCTL showed inhibition from the outset, but tumor growth was only delayed and tumor progression still continued. Notably, the greatest benefit was demonstrated by the combined therapy group, which exhibited both early tumor growth inhibition as well as additional regression upon prodrug administration (**Figure 2-11**).

RRV vector spread is limited to tumor tissues

Tissues from the treated animal groups given RRV-CD with or without 5-FC and that given alloCTL/RRV-CD with 5-FC were collected to monitor the spread of RRV-CD by quantitative PCR (qPCR) to other normal organs. Genomic DNA was extracted from tumor, lung, liver, spleen, kidney, brain, and bone marrow, then qPCR was performed using primers and probe sequences specific for the 4070A amphotropic envelope. Except for the recovered tumor tissue, no detectable RRV *env* signals by qPCR were obtained from the animal tissues regardless of whether they were or were not treated with 5-FC. Similar data were obtained with animals given alloCTL/RRV-GFP. Therefore, similar to findings of other experiments [13], RRV vector replication was confined to the tumors.

Discussion

AlloCTL are normally made by one-way MLR [79]. The alloCTL made in this study was by a one-way MLTR; therefore, the generated culture contains CTL directed to minor tumor associated antigens (TAA) as well as those to major histocompatibility complex antigens (aka HLA). Since the precursor frequency within PBMC is much higher to major antigens than to minor antigens [83, 84, 85] and since the tumor cells used for stimulation were preincubated with IFN-γ to upregulate their surface HLA, production of alloresponsive CTL should be enriched [27]. We confirmed the presence of alloreactive CTL in the MLTR-generated alloCTL preparations by demonstrating an inhibition in lysis when anti-class I antibody was titrated into effector/target cell mixtures in cytotoxicity assays (data not shown). We also verified that the MLTR-generated alloCTL preparations and those manipulated for RRV transduction retain their antitumor function (**Figures 2-3 & 2-5**).

Thus, MLTR-generated alloCTL should directly reduce tumor mass, and reduce the immunosuppressive stromal microenvironment. In addition, we hypothesized that a second, independent tumoricidal modality may further enhance the efficacy of alloCTL if used in combination. Indeed, in an intracranial brain tumor model, adoptive immunotherapy with MLTR-generated alloCTL improved survival as an individual treatment, as did RRV-CD mediated suicide gene therapy, but the best improvement in median survival time was observed when these individual treatments were combined together. These results thus provided proof-of-concept and feasibility for strategies to combine alloCTL immunotherapy and RRV gene therapy for brain tumors. Notably, however, the survival curve subsequently collapsed and the overall percentage of survival in the combined treatment group ended up being almost identical to that with alloCTL alone, indicating the need to further optimize this combination treatment strategy.

Subsequent studies therefore focused on developing a unique immuno/virogene therapy approach that utilizes adoptive transfer of alloCTL/RRV as a single combined modality, not only for direct alloreactive immunocytotoxicity to target cells at high E:T ratios, but also to improve the delivery of suicide genes to

diffusely infiltrating tumor cells characteristic of high grade gliomas. Our hypothesis was that this approach would (a) provide better tissue penetration and tumor homing capability for RRV through alloCTL-mediated delivery, and (b) greater potency to alloCTL at lower E:T ratios through additional suicide gene-mediated killing of tumor cells. The use of alloCTL/RRV should represent a tumor-restricted and acceptably safe delivery method, as previous studies showed that alloCTL egress out of the immunoprivileged environment of the brain over time, and are then eliminated by the host immune system.

To successfully implement this strategy, alloCTL must first be converted to RRV producer cells, but T cells are notoriously difficult to transduce with retroviral vectors [86, 87]. PBMCs characteristically do not support viral replication, possibly the result of low expression levels of the PiT-2 receptor to which amphotropic envelope glycoprotein binds for viral entry, and perhaps by their high expression levels of anti-viral proteins, such as APOBEC3G [18, 24, 75, 76]. Proinflammatory cytokines produced by alloCTL may also upregulate innate antiviral mechanisms to reduce transduction efficiency [88, 89]. We have investigated the level of APOBEC3G in PBMCs, PHA-activated PBMCs, OKT-3 activated PBMCs, and alloCTL, and found that OKT-3 activated PBMCs had the lowest level of APOBEC3G RNA compared to others (data not shown). Therefore, we tested transducing PBMCs post OKT-3 activation then co-culturing with irradiated target cells. This led to comparable transduction levels, but lower cytotoxicity against target cells (data not shown). The reason for this decrease in cytotoxicity may be a result of expanding many non-specific T cells with OKT-3. Of note, it has been reported that after activation of T cells, low molecular mass forms of APOBEC3G are recruited into high-molecular-mass APOBEC3G RNA–protein complexes that do not exhibit enzymatic activity [90]. Therefore, differentiating low versus high molecular mass forms of APOBEC3G in the various activated PBMCs may shed light on the most optimal method to produce alloCTL/RRV.

Nonetheless, even alloCTL/ACE-GFP preparations exhibiting very low percentages of transduction were still able to efficiently transmit RRV to tumor cells *in vitro* (**Figure 2-6A-D**). This is consistent

with previous studies demonstrating highly efficient replication and rapidly progressive spread of RRV transduction in tumor cells after inoculation of cell-free virus supernatant at an initial multiplicity of infection (MOI) as low as 0.01 [16, 19, 20, 74]. It is also possible that adsorption of virus particles to the surface of T cells may have contributed to tumor cell transduction via a "hitch-hiking" mechanism without involving actual infection of alloCTL [91].

Furthermore, the CD prodrug activator gene transmitted by RRV produced from alloCTL was functional when exposed to the prodrug 5-FC *in vitro* and *in vivo* (**Figures 2-9, 2-10, 2-11**). In a subcutaneous xenograft tumor model, we found that injection of an alloCTL/RRV-CD preparation followed by 5-FC administration mediated a significant reduction of tumor growth (**Figure 2-11**). Finally, the vector was confined to tumor tissue *in vivo*, demonstrating the safety of RRV-CD vectors when delivered via alloCTL, as was also demonstrated for RRV infused into locoregional circulation.

In an effort to investigate the combination of alloCTL and RRV in a syngeneic model, we have started to characterize murine alloCTL/RRV as well. Murine alloCTL were generated through LDCR rather than MLR or MLTR. For reasons that are not clear, MLR and MLTR cultures tend to die out quickly, which is a problem taking into account the need for extended culture for transduction and functionality assays. Dendritic cells are antigen presenting cells and have yielded robust alloCTL cultures that will reliably last for at least 5-7 days. However, we must also take into consideration that peptides presented through dendritic cells may be different from the peptide on tumors, which may, to a certain extent lead to an expansion of non-tumor specific T cells. Therefore, optimization of murine alloCTL whether it be MLR, MLTR, or LDCR warrants further research. Here, we showed that the spinoculation method achieved about 1-2% transduction of alloCTL (**Figure 2-4**). The alloCTL/RRV preparations were then tested for cytotoxicity as well as migratory capabilities on monolayer target cells. Cytotoxicity was comparable between non-transduced alloCTL and alloCTL/RRV preparations (**Figure 2-5B**). We demonstrated through radial migration assay that cells from the alloCTL/RRV preparation had migrated to the edge of the wells (**Figure 2-7**). In separate studies utilizing a GALV-pseudotyped RRV-GFP, we

were able to achieve over 80% transduction of alloCTL, which were used for the radial migration assay. Green fluorescent cells were seen migrating across target monolayer as well as transmitting RRV to target cells. Henceforth, we can assume that the transduction procedure is innocuous to alloCTL in terms of its migratory ability. These results demonstrated the ability of alloCTL to retain cytotoxicity and migratory abilities post transduction procedures. Next, we again asked whether alloCTL/RRV is able to produce functional virus that can subsequently transduce target glioma cells was addressed, especially because the transduction rate was low. Therefore, we co-cultured RRV-GFP-transduced murine alloCTL with murine glioma cells at E:T ratio of 1:10 and monitored the percentage of GFP positive glioma population over time. Over 90% of glioma cells were transduced with RRV by day 10, indicating efficient horizontal transmission of RRV from alloCTL to glioma cells (**Figure 2-6E**).

Taken together, murine alloCTL data are consistent with human alloCTL. Whether murine alloCTL/RRV can achieve therapeutic efficacy in a syngeneic model is yet to be investigated, particularly in an intracranial glioma model in immunocompetent mice. It may be difficult, however, to "de-optimize" RRV prodrug activator gene therapy so as to determine the additive or synergistic effectiveness of the combination therapy, if any. To this end, a multifocal approach may be useful, wherein alloCTL/RRV are injected intratumorally on just one side. On a different note, although the xenograft model used in the study did not allow a determination of the degree of inflammation induced by the viral vector interacting with endogenous immune cells in the brain, prior studies in syngeneic animal models indicate that this is not likely to present a problem [7, 17].

Overall, our results confirm that alloCTL/RRV preparations not only have effector function, but also efficiently promote vector spread in gliomas and impart them with susceptibility to prodrug activator gene therapy. Hence, these data support the feasibility of combining adoptive immunotherapy with viroreplicative gene therapy for CNS malignancies. To date, the clinical feasibility and safety of intratumoral alloCTL for adoptive immunotherapy for gliomas has already been confirmed in a small pilot study [56, 57] and was investigated in a Phase I dose escalation study at UCLA (NCT01144247). In

addition, as noted above, the clinical feasibility of RRV coding for prodrug activator gene administered with prodrug is also currently being tested in a registrational Phase II/III study (NCT02414165). Clinical testing of these individual therapies should accelerate translation of this unique combined cellular and gene therapy strategy.

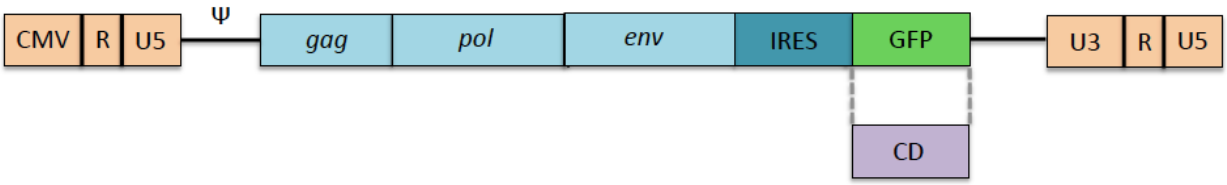

Figure 2-1. Diagrammatic representation of the RRV construct. CMV: cytomegalovirus promoter. U3, R, U5: sequences in retrovirus long terminal repeat (LTR). ψ: retrovirus packaging signal. *gag, pol, env*: retrovirus coding sequences. IRES: internal ribosome entry site. GFP: green fluorescent protein, marker gene. CD: yeast cytosine deaminase, prodrug activator gene. ACE-GFP and ACE-CD are prototype vectors, and AC3-GFP and AC3-CD are the 2nd generation vectors with optimized codons.

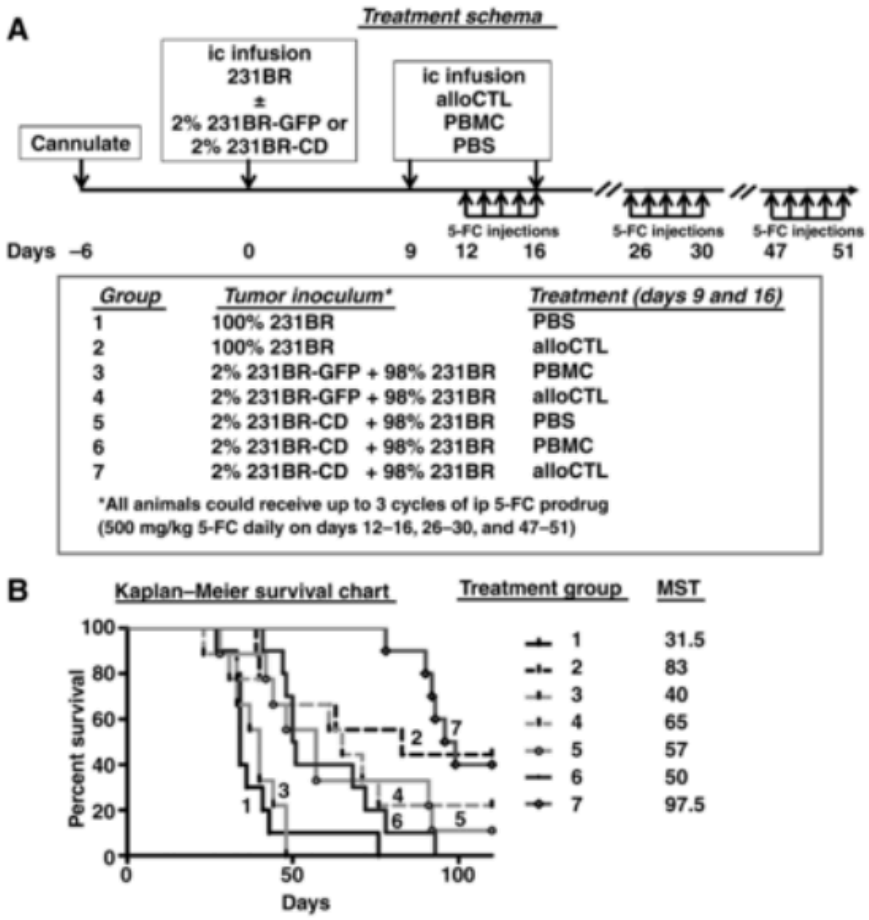

Figure 2-2. Immunogene treatment schema, control, and experimental treatment groups, Kaplan–Meier survival plots with mean survival times.

(A) the treatment schema along with the 7 control or experimental groups are detailed. Mice were first surgically implanted with cannulas. Six days later they were intracranially infused with either nontransduced 231BR cells or 2%/98% mixtures of RRV-transduced/ nontransduced 231BR cells. The transduced 231BR cells had RRV coding for either nontherapeutic GFP marker gene (control) or therapeutic CD gene. AlloCTL (therapeutic cells) or PBMC (unstimulated control cells) were infused into the tumor site on days 9 and 16 posttumor infusion. All animals received the nontoxic prodrug, 5-FC, which was intraperitoneally injected daily for 5 days (one cycle; up to 3 cycles were possible spaced 2–3 weeks apart). Groups 1 and 3 were controls for the suicide gene therapy and cellular therapy treated groups. The experimental groups testing cellular therapy with alloCTL were groups 2 and 4. The experimental groups testing suicide gene therapy were group 5 and 6. The combination immunogene therapy was group 7. **(B)** The Kaplan –Meier survival plots along with the MST are shown for all 7 control or experimental groups (n= 9–10/group) as observed to day 112 posttumor injection. Long-term survivors were obtained for all individual or combined cellular and gene therapeutic groups. The P values of significance ($P < 0.05$) calculated by nonparametric log-rank (Mantel–Cox) tests were as follows from this singular experiment:Three separate survival experiments were conducted; 2 pilot studies with n = 4 to 6/group gave similar findings.

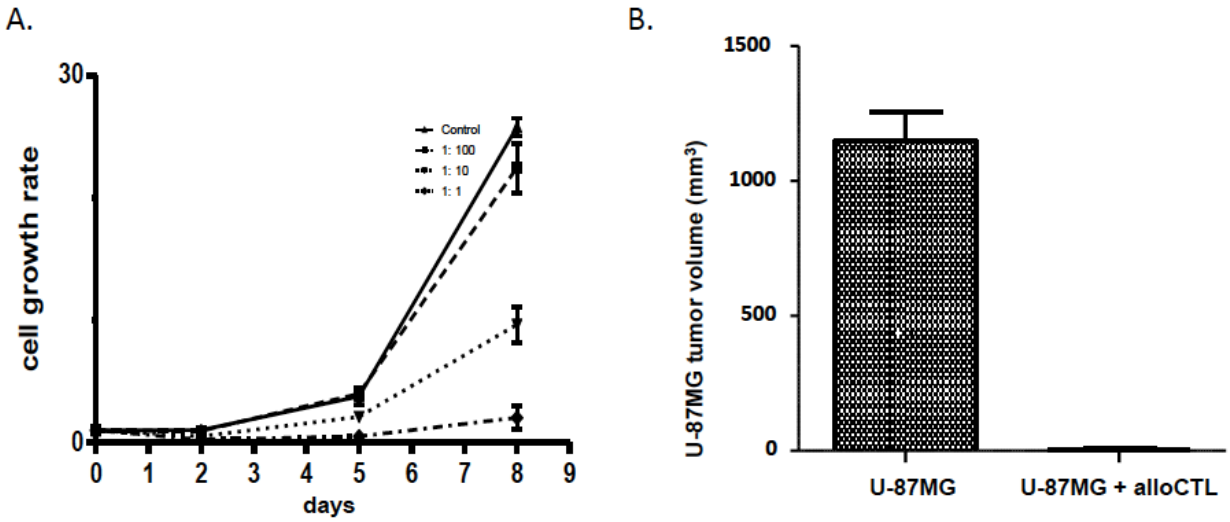

Figure 2-3. ***In vitro*** **and** ***in vivo*** **anti-glioma effects of alloCTL generated by MLTR.** **(A)** MTS assays performed to determine *in vitro* cell growth of U-87MG at 0, 2, 5, and 8 days after their incubation with anti-13-06 alloCTL at day 12 post-MLTR. The alloCTL to U-87MG glioma cell E:T ratios were 0:1 (control), 1:1, 1:10, and 1:100. Cell growths are indicated as average metabolic activities ± SEM determined from wells in pentaplicate. **(B)** Subcutaneous U-87MG tumor volumes at day 35 post-implantation into the hind flank of nude mice. The first and second columns show the average tumor volumes ± SEM of U-87MG cells injected alone (10^6 cells) or when U-87MG cells (10^6) were mixed immediately before implantation with alloCTL (10^5), respectively (n=12/group). The difference between the two groups was highly significant at $p \leq 0.005$ by unpaired Student *t* test.

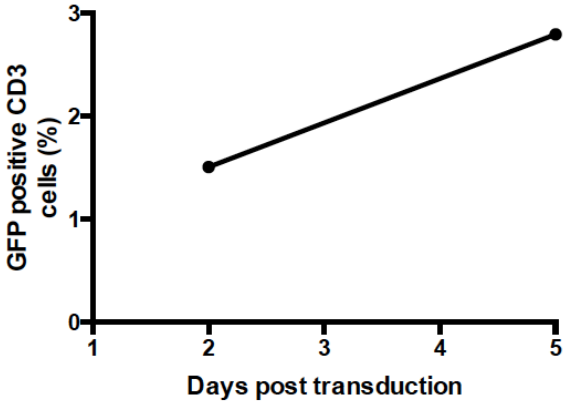

Figure 2-4. Transduction of murine alloCTL.
Murine alloCTL were generated by LDCR. Three days post LDCR, alloCTL were transduced by AC3-GFP at an MOI of 7 by spinoculation on rectronectin coated plates. On days 2 and 5 post transduction, alloCTL were stained for CD3e, and cells were analyzed for the percentage of CD3 positive, GFP positive populations.

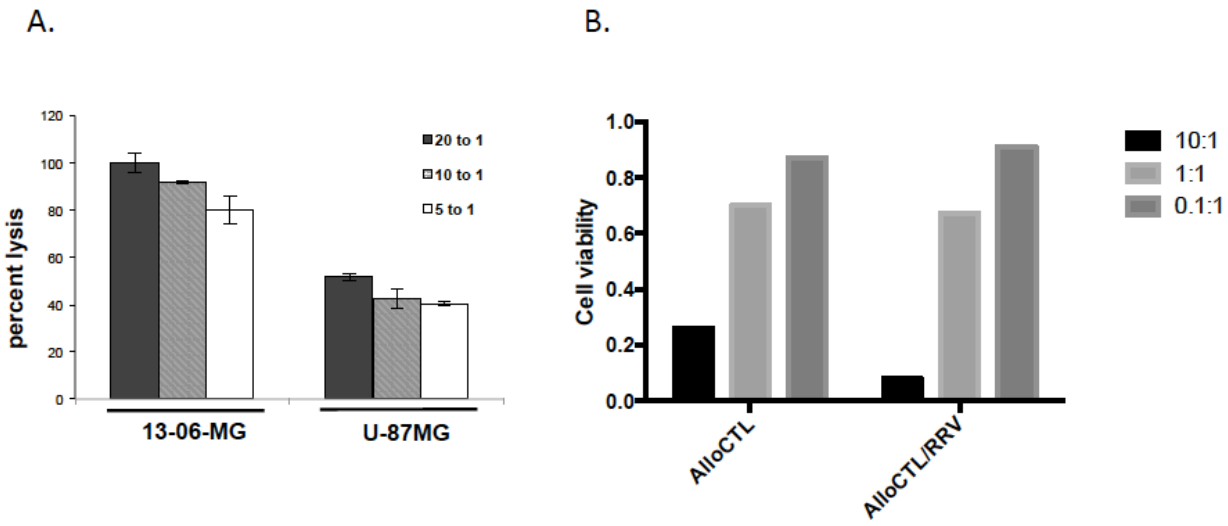

Figure 2-5. *In vitro* anti-glioma effects of alloCTL/RRV-GFP shown by cytotoxicity assay. **(A)** Anti-13-06 alloCTL were restimulated with U-87MG/RRV-GFP at day 12 post-MLTR. The cytotoxicity of the alloCTL/RRV-GFP preparations to 13-06-MG or U-87MG target cells was determined 2 days later by 4 hr ^{51}Cr-release assay. The percentage lysis ± SEM at E:T ratios of 20:1, 10:1, and 5:1, as shown, was calculated from wells in triplicate. **(B)** Cell viability was continuously monitored over time by the xCELLigence electrical impedance assay. Tu2449 murine glioma cells were plated on gold 96 well plate on day 1. Murine alloCTL against B6/C3F1 cells both non-transduced and RRV-transduced were added to the target Tu2449 cells on day 2 and co-cultured until data collection 24 hours later. 4th hour data points were normalized to time post effector cell addition and to target cell viability.

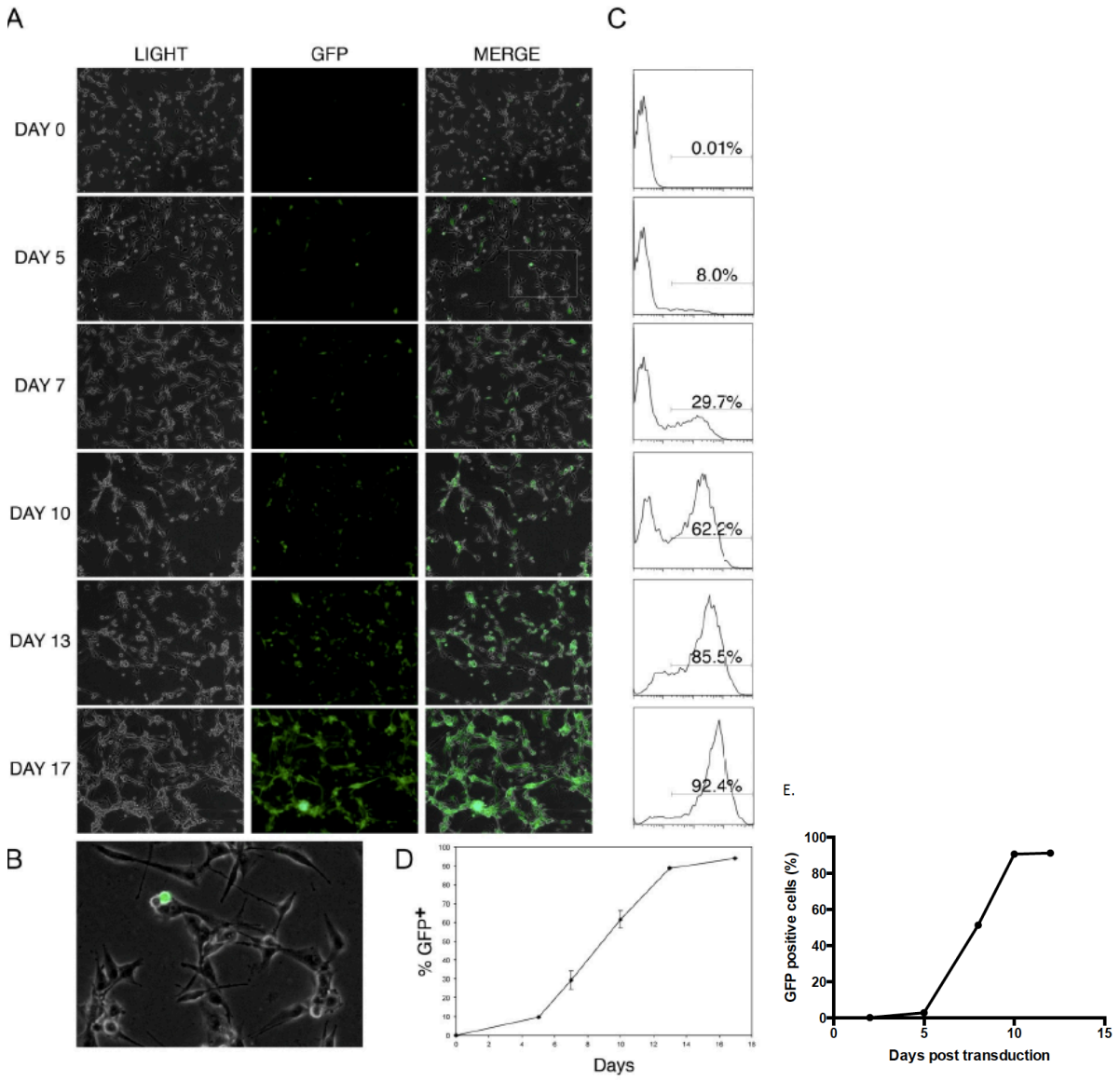

Figure 2-6. Kinetics of RRV-GFP vector spread from alloCTL/RRV *in vitro*. AlloCTL/RRV-GFP preparations were placed onto monolayers of naïve U-87MG glioma cells at an E:T ratio of 1:10, and monitored by light and fluorescent microscopy, as well as flow cytometry, over 15 to 20 day intervals. **(A)** Representative light, fluorescent and merged photomicrographs of the same field at serial time points visually demonstrate the increase in GFP-positive U-87MG cells observed over time. **(B)** Higher magnification view (inset from day 5 merge) clearly shows nontransduced and a single GFP-positive alloCTL from the transduced alloCTL/RRV-GFP preparation in contact with an adherent U-87MG cells. **(C)** Flow cytometric histograms displaying the percentages of GFP-positive cells at matched time points. **(D)** Line graph demonstrating the rate of transduction of U-87MG cells. The percentage transduction ± SEM at each time point was determined by flow cytometric analysis. **(E)** 1.5% AC3-GFP transduced murine alloCTL were co-cultured with target Tu2449 cells at an E:T of 1:10. The percentage of GFP positive cells was measured by flow cytometry and plotted over time.

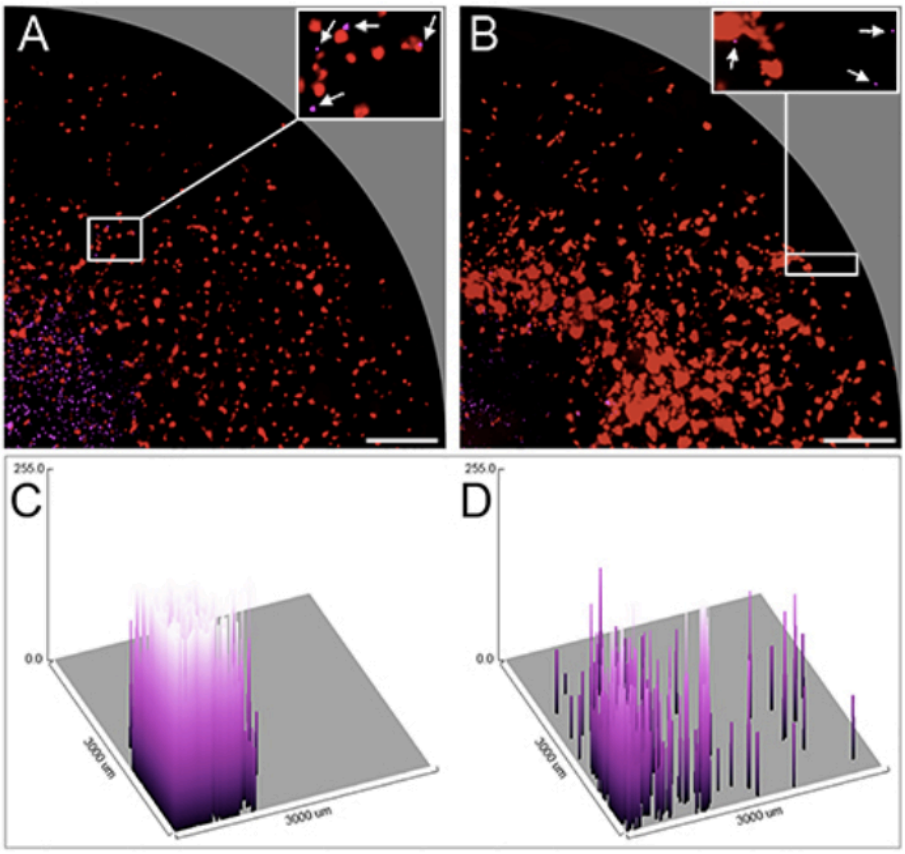

Figure 2-7. Radial migration of murine alloCTL stained with eFluor 670 on mStrawberry-labeled glioma cells shown at 1 and 48 hr. Fluorescent photomicrographs of one quadrant of the same well at **(A)** 1 hr and **(B)** 48 hr after sedimentation of fluorescently-labeled non-adherent alloCTL onto a monolayer of TU-2449 glioma cells. The low power photomicrographs reflect the area contained within one quadrant of the CSM well (radius 3 mm). At high power (A and B, insets) alloCTL (white arrows) are shown in proximity to or associated with individual tumor cells; one has a disintegrated appearance with fragmented nuclei and is apoptotic. **(C and D**) respective surface intensity fluorescence maps obtained using ImageJ software showing pixel values of the digitized purple fluorescent images in three-dimensional graphic form and placed on a grid representing the well radius of 3 mm. Bar = 500 µm.

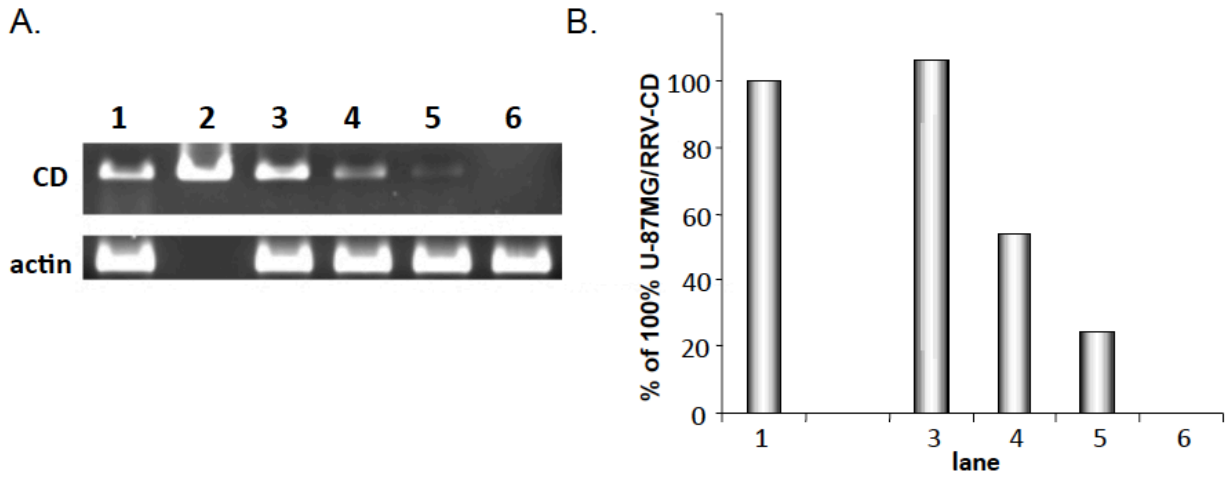

Figure 2-8. Integration of the CD gene into U-87MG glioma cells after coculture with alloCTL/RRV-CD. (A) alloCTL/RRV-CD and U-87MG cells at a 1:10 ratio were cocultured for 4 days. The adherent glioma cells were washed, trypsinized and an aliquot taken for extraction (lane 5). The glioma cells were replated and continued in culture to days 7 (lane 4) and 10 (lane 3). PCR with primers for the CD gene was performed on genomic DNA extracts of the cells. The negative control was nontransduced U-87MG cells (lane 6). Positive controls were 100% transduced U-87MG/RRV-CD (lane 1) and the plasmid ACE-CD (lane 2). Actin primers were run in parallel to confirm equal loading of the ethidium bromide stained agarose gels. **(B)** Densitometric values obtained for each experimental lane were compared to the reference control 100% U-87MG/RRV-CD in lane 1. The values were converted to a percentage of the control.

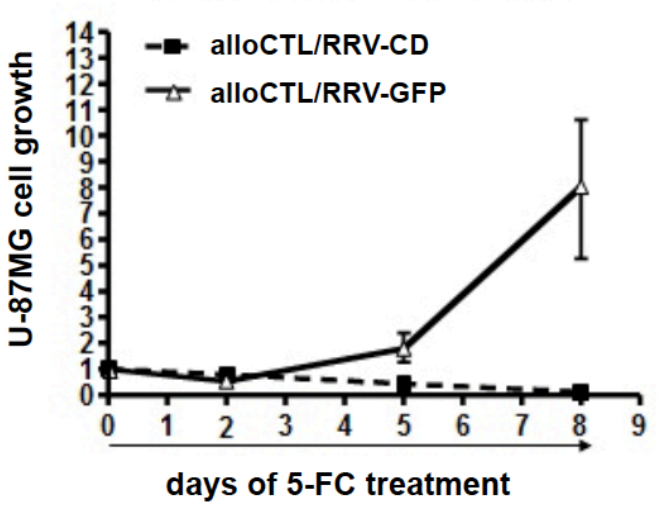

Figure 2-9. U-87MG glioma cell growth cultured in the presence of prodrug 5-FC for 8 days, after first coincubating them with alloCTL/RRV-CD or alloCTL/RRV-GFP controls for one week. The U-87MG cells underwent coincubation with the two alloCTL/RRV preparations at an E:T of 1:10 for 7 days. After washing alloCTL/RRV from the cultures, the adherent U-87MG cells were continued in culture after adding 2 mM 5-FC to the medium. MTS assays were performed on U-87MG cells at days 0, 2, 5, and 8. Cell growths are plotted at the indicated times as average metabolic activities ± SEM determined from wells in pentaplicate, normalized to the average value of the control cells on day 0.

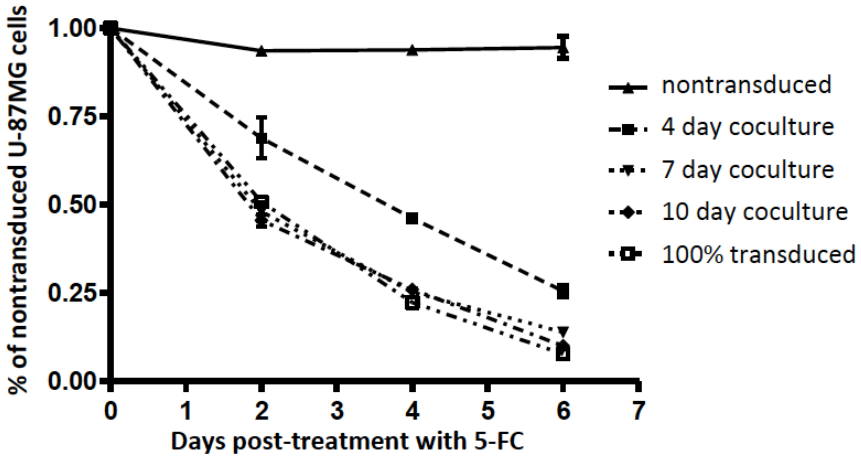

Figure 2-10. U-87MG cell viabilities after initial incubation with alloCTL/RRV-CD for various time intervals, followed by 5-FC treatment. U-87MG cells were cultured with alloCTL/RRV-CD for 4, 7 or 10 days at a ratio of 1:10 (alloCTL/RRV:U-87MG). The alloCTL/RRV-CD were washed from the monolayers and the U-87 cells were continued in culture with medium containing 2 mM 5-FC for 2, 4 or 6 days. MTS assays were performed and the metabolic activities were expressed as a percentage of the nontransduced, 5-FC-treated cells ± SEM. The metabolic activities obtained with 100% transduced U-87MG/RRV-CD cells cultured in 5-FC-containing medium for the indicated times were obtained for comparison.

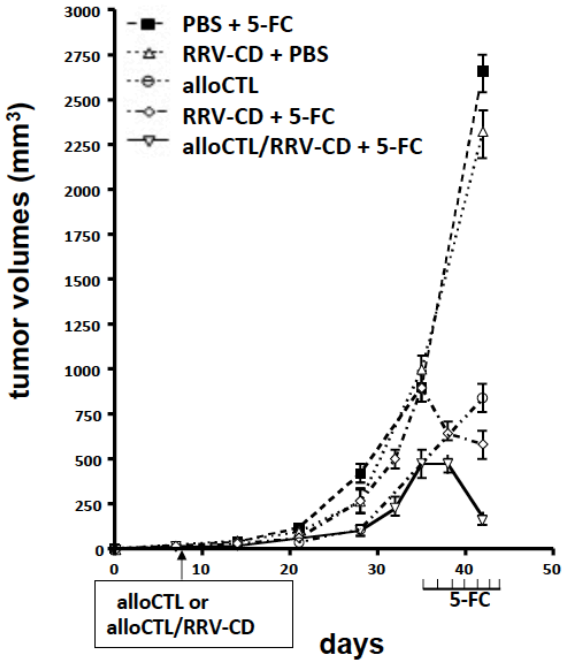

Figure 2-11. Subcutaneous U-87MG tumors treated with individual or combined gene and immune therapy modalities. U-87MG glioma cells (10^6) were implanted into the hind flanks of nude mice and allowed one week to establish their growth. From day 7, the animals (n=12) were divided into the following treatment groups: PBS + 5-FC (control group receiving intratumoral PBS followed by systemic 5-FC prodrug only), RRV-CD + PBS (control group receiving 5 x 10^4 TU/ml intratumoral RRV-CD followed by systemic PBS instead of prodrug), alloCTL (treatment group receiving immunotherapy alone with 10^5 alloCTL by intratumoral injection), RRV-CD + 5-FC (treatment group receiving 5 x 10^4 TU/ml intratumoral RRV-CD followed by systemic 5-FC prodrug), or alloCTL/RRV-CD + 5-FC (treatment group receiving 10^5 alloCTL/RRV-CD followed by systemic 5-FC prodrug). Animals receiving 5-FC were given 7 daily ip injections at 500 mg/kg starting at day 35. At day 42 the differences between the control groups and the experimental groups were highly significant ($p \leq 0.001$) by two-way ANOVA.

Tumor*	HLA A	HLA B	HLA C
231 tumor	A*02	B*41,*40	C*17,*02
D10-18	A*24,*34	B*15,*38	C*07
D13-06	A*01	B*08,*57	C*06,*07
D03-18	A*02,*68	B*35,*40	C*04,*08
D13-08	A*01,*02	B*08,*44	C*05,*07

Table 2-1. HLA Class I typing of MDA-MB-231 and donors

Serological HLA typing was performed on the triple negative human breast cancer cell line MDA-MB-231, and PBMC from four donors (D10-18, D13-06, D03-18, D13-08), as shown. Flow cytometric analysis with anti-HLA-ABC (W6/32) antibody confirmed cell surface HLA expression on the brain-tropic variant MDA-MB-231BR cells was comparable to the parental cell line MDA-MB-231.

Restimulation**	Target	IFN-γ produced (pg/mL ± SEM)**
U-87MG/RRV-GFP	13-06-MG	174.0 ± 3.1
U-87MG/RRV-GFP	U-87MG	73.9 ± 3.4
U-87MG/RRV-GFP	none	40.0 ± 0.7
none	13-06-MG	599.5 ± 18.1

Table 2-2. **IFN-γ produced by an alloCTL/RRV-GFP preparation exposed to glioma target cells expressing the full or partial complement of HLA alleles to which they were initially sensitized.**

*The initial sensitization of the alloCTL during MLTR was to 13-06-MG cells (HLA-A1,2 & B44,57). Restimulation at day 12 post-MLTR was with inactivated U-87MG/RRV-GFP cells (HLA-A2, B44) at a R:S of 3:1.

**IFN-γ concentration in supernates collected 48 hr after target tumor cells were coincubated with alloCTL/RRV-GFP at day 14 post-MLTR (E:T 10:1). Tumor target cells produced background levels of IFN-γ at $\leq 0.7 \pm 1.1$ pg/mL.

Chapter Three: Retroviral Replicating Vector-Mediated Delivery of an Immunodominant Neo-antigen Epitope Target for Viro-Immunotherapy in Experimental Glioma

Introduction

Patients with malignant glioblastoma have a dismal prognosis, with a median survival of only 12-15 months despite advances in surgery, radiation therapy and chemotherapy [1, 92, 93]. The infiltrating nature of the tumor makes complete resection extremely difficult. FDA approved treatments for glioblastoma are temozolomide, lomustine, carmustine, and bevacizumab. However, most patients experience recurrent disease for which there is no standard of care, and the lack of effective therapies represents an unmet medical need.

The use of RRV represents a novel gene delivery platform technology that achieves a significant enhancement in transduction efficiency and therapeutic efficacy of gene therapy for cancer. The feasibility of engineering RRV to achieve highly efficient gene delivery has already been established, and due to the intrinsic inability of the virus to infect post-mitotic normal cells, as well as innate and adaptive immunity which are intact in normal tissues but suppressed in tumors, RRV spread after direct intratumoral injection is highly restricted to the tumor tissue itself in immunocompetent hosts [7]. Furthermore, RRV achieve persistent infection of solid tumors in vivo, thereby allowing the virus to track tumor cells even as they migrate and form invading tumor foci.

Since retroviruses are not inherently cytolytic, RRV can be engineered to deliver a pro-drug activator ("suicide") gene, which is stably seeded throughout the tumor as the virus replicates, and simultaneous killing of infected cancer cells is triggered by administration of the prodrug. This results in significant tumor destruction and extension of survival as long as prodrug treatment is continued.

Through studies spanning the past decade, we and others have established that after intratumoral or intravenous injection of RRV at realistic levels, significant *in vitro* efficacy and long-term survival benefit

in intracranial cancer models was possible, while maintaining tumor selectivity and safety [7, 16, 17, 19, 21, 22, 74]. In murine syngeneic intracranial glioma models, we have shown that RRV-mediated prodrug activator gene therapy can further induce immune responses leading to tumor clearance (Chapter 1).

There has also been a long-standing interest in inducing anti-tumor immune responses by applying immunotherapeutic approaches to brain tumors. Significant efforts have been made in this field but have yielded modest results in prolonging overall survival in patients. Part of the difficulty has been the lack of well-defined, highly immunogenic tumor-rejection antigens in gliomas as well as tumor heterogeneity and antigen loss [94, 95]. In a study evaluating an autologous dendritic cell vaccine pulsed with Class I peptides from tumor-associated antigens (TAA) expressed on gliomas and overexpressed in their cancer stem cell population, overall survival (OS) did not reach statistical significance for the intent-to-treat population in this study. However, expression of targeted antigens in the pre-vaccine tumors correlated with prolonged OS and progression free survival in newly diagnosed glioblastoma patients [96]. Furthermore, a case study revealed that a prototypic viral antigen (CMV pp65) expressed by one glioblastoma patient's tumor lysate was shown to effectively prime a tumor-viral T cell response when such lysate was used to pulse dendritic cells, highlighting the importance of immunogenic antigens for effective immunotherapy [32].

We hypothesize that the highly efficient spread of RRV throughout the tumor can be utilized to induce stable expression and robust presentation of viral antigens that may represent useful immunotherapeutic targets, in effect "xenogenizing" the tumor. Thus, the use of RRV to deliver highly immunogenic viral antigens to glioma could help set the stage for more effective immunotherapy for this disease, by negating the reliance on endogenous TAA expression and overcoming the heterogeneity of tumors.

Accordingly, here we investigated the use of RRV to introduce a major histocompatibility complex I

(MHC I)-restricted lymphocytic choriomeningitis virus (LCMV) glycoprotein gp33-43 (gp33) sequence, an immunodominant epitope, into glioma cells for subsequent targeting by adoptive T cell transfer.

Materials and Methods

Animals and cell lines

C57BL/6 and B6/C3F1 mice were obtained from The Jackson Laboratory. P14 transgenic T cell receptor mice were kindly provided by Dr. D. Brooks (University of Toronto, Toronto, Canada). The Tu2449, GL26, and GL261 murine glioma cell lines were maintained in DMEM with 10% FBS, penicillin/streptomycin.

RRV vectors

Details of parental RRV design and modification have been previously described [33]. pgAC3-GFP was constructed by modifying the original construct, pAC3-GFP, to contain an envelope sequence with 99 bp of 5' ecotrophic envelope, followed by the gp33-43 epitope, then amphotrophic envelope. This construct (provided by Dr. David Klatzmann and Dr. Charlotte Dalba, Universite Pierre et Marie Curie / Hôpital Pitié-Salpêtrière, Paris, France) was excised at 2 kb using 5' Xba I and 3' Cla I sites. Corresponding sites were used to insert the epitope tagged envelope into the original pAC3-GFP construct. The RRV containing the yCD2 transgene was cloned by cutting at the 5' Psi I and 3' Not I sites, excising the original emd transgene, and replacing it with the yCD2 sequence. To produce all RRV, 293T cells were transiently transfected with vector plasmid as previously described. Supernatants were harvested and filtered 48 hours later, and stored at −80 °C. For titer determination, after incubation of each cell line with virus for 24 h, 50μM AZT (Sigma) was added to prevent ongoing virus replication, and cells were analyzed for GFP expression by using flow cytometry on a FACS LSR II apparatus (Becton-Dickinson, Franklin Lakes, NJ, USA). Viral titer was represented as transducing units/ml (TU/mL).

PCR spanning gp33 and *env*

For the PCR assay, genomic DNA was prepared from approximately $5x10^5$ cells each. PCR was used to detect gp33 insertion in Tu2449/AC3-GFP, Tu2449/gAC3-GFP, GL26/AC3-GFP, and GL26/gAC3-GFP using the following primers: forward primer, 5'-gp33-TCG CCA CCT GTG GGA TAT TA; reverse primer, 3'-env-AGG GTC AAT GAT ACT GGC TCT CTT, with the PCR performed in a Bio-Rad iCycler Thermal Cycler. AC3-GFP and gAC3-GFP plasmids were used as negative and positive controls, respectively.

In vitro sensitivity to prodrug 5-FC

To determine the toxicity of 5-FC (Sigma) in vitro,uninfected, AC3-yCD2-transduced, or gAC3-yCD2-transduced Tu2449 cells were seeded in replicate 96-well plates (2000 cells/well), cultured overnight, and exposed to 5-FC at 0.1mM. Cell viability was determined on day 3, 5, and 7 by MTS assay using the CellTiter Aqueous One Solution Cell Proliferation Assay kit (Promega, Madison, WI, USA). All time points for each cell line and each concentration were performed in triplicate and the average calculated and plotted to give 5-FC killing profiles.

Serial passage stability studies

Approximately 10^5 naive U87 cells were initially infected with the viral vectors at a MOI of 0.1 and grown for 1 week to complete a single cycle of infection. 15 µl of the 1 ml of supernatant was then repassaged onto uninfected cells and the cycle repeated. Genomic stability of the yCD2 and gp33-41 sequences were assessed by PCR amplification of the integrated provirus from the infected cells using MLV-specific primers flanking the transgene insertion site. DNA was prepared from each set of infected cells as for the qPCR titer assay. PCR was performed using the following primers: 5′-CTGATCTTACTCTTTGGACCTTG-3′; 5′-CCCCTTTTTCTGGAGACTAAATAA-3′ which amplify a

fragment that span the CD transgene, and 5'- TCGCCACCTGTGGGATATTA-3'; 5'-AGGGTCAATGATACTGGCTCTCTT-3' which amplify a fragment that span the gp33-43 epitope insert. PCR products were visualized by running the reaction products on a 1% agarose gel. The appearance of bands other than the full-length amplicon, could either be primer-dimers or an indicator of vector instability.

RRV transduction of glioma cells

Viral replication was monitored by GFP expression. *In vitro,* Tu2449, GL26, and GL261 cells were infected with gAC3-GFP at a multiplicity of infection (MOI) of 0.1 or 5 and percentage of GFP-positive populations were measured by flow cytometry over time. For comparison of gAC3-GFP spread in vivo, 2% RRV-transduced cells were injected subcutaneously. GL26 and Tu2449sc3 (a subcutaenous model for Tu2449) were used for less immunogenicity and enhanced tumor take. $2x10^6$ Tu2449sc3 and $1x10^6$ GL26 cells were injected into the right flanks of B6/C3F1 and C57BL/6, respectively. Tu2449sc3 and GL26 tumors were excised for analysis on day 10, and GL26 tumors on day 17. Tumors were finely dissected with razor blades, and then digested overnight in collagenase at 37°C, 5% CO_2. 18 hours later, tumor cells were washed with PBS, then cultured in DMEM with 50μM AZT at 37°C, 5% CO_2. 24 hours later, adhered cells were analyzed for percentage of GFP-positive populations by flow cytometry on an LSR II. Viral replication kinetics were determined by plotting the percentage of GFP-positive cells over time.

Major Histocompatibility Complex (MHC) levels

MHC levels of Tu2449 and GL26 cells were measured using flow cytometry. Prior to analyses, Tu2449 and GL26 cells were cultured for 24hr with or without murine IFN-γ (10ng/mL). Cells were then dissociated with 10mM EDTA, washed, and stained for MHC class I H-$2D^b$ (BD Pharmingen) and H-$2K^b$

(eBioscience) and respective isotype controls, and analyzed on flow cytometry. MHC positive populations were gated based on isotype controls. Percentage of positive cells and median fluorescence intensity (MFI) were calculated using the FlowJo software.

P14 cell culture

For the adoptive transfer of P14 TCR transgenic CD8 cells, spleens and lymph nodes were aseptically obtained from P14 mice. A single cell suspension was prepared in PBS by filtering through a mesh cell strainer. Red blood cells were lysed with PharmLyse (BD Pharmingen), cells were washed, resuspended in RPMI, and counted. The cells were resuspended at $5x10^5$ cells/mL in X VIVO-15 (Lonza) supplemented with 2% FBS and 50μM β-mercaptoethanol (complete X VIVO) with 1 ng/mL LCMV gp33-41 (AnaSpec) and 50 IU/mL IL-2 and cultured for 3 days at 37°C and 5% CO_2. On the 3rd day, cells were washed, counted, then resuspended at $1x10^5$ cells/mL in complete X VIVO with 50 IU/mL IL-2. Cells were used for CTL assays or for adoptive transfer on day 5.

ELISA for IFN-γ

IFN-γ production was measured by EILSA post P14 cell and tumor cell co-culture at effector to target ratio (E:T) of 1:1. GL26 and Tu2449 murine glioma cells transduced with the epitope display vector gAC3-GFP were either pre-incubated with IFN-γ for 24hr or not pre-incubated. Naïve GL26 cells and Tu2449 cells transduced with AC3-GFP underwent the same treatment for control. $1x10^6$ glioma cells were then co-cultured with $1x10^6$ P14 cells in T cell culture medium with 100 IU/mL IL-2 for 18 hours. Supernatants were used to detect murine IFN-γ with ELISA. Briefly, capture antigen was incubated overnight, then serum samples were added and incubated before goat anti-mouse horseradish peroxidase

(HRP)-conjugated antibody was added for detection. Plates were read at 450 nm with an ELISA reader (SpectraMax 190; Beckman Coulter, Brea, CA).

Cytotoxicity and selectivity of P14 cells

Electrical impedance was continuously monitored using the xCELLigence system (ACEA Biosciences) in E-plate 96 (ACEA). The background was measured in wells containing 50µL of T cell culture medium without cells for 60 s. Tu2449/AC3-GFP, Tu2449/gAC3-GFP, GL26/AC3-GFP, and GL26 /gAC3-GFP cells were detached from the flasks by a brief treatment with trypsin/EDTA, re-suspended in T cell culture medium and adjusted to $8x10^3$ or $1x10^4$ cells in 100µL, respectively (per cell line). These cell suspensions were added to wells containing 50µL of culture medium. Three wells were seeded for each effector to target ratio (E:T). The E-plates were incubated at room temperature for 30 min and placed on the plate reader in the incubator for continuous impedance recording. Cell index (CI) data were recorded every 15 min for 24 h, then effector cells were added. 24 h later, effector P14 cells suspended in T cell culture medium were added at E:T of 10:1, 1:1, 0.1:1, or 0.01:1 in appropriate wells, with IL-2 (100 IU/mL). 0.1% Triton-X was added for maximal kill wells. All procedures were performed in laminar flow cabinet. The cells were real-time monitored at 37°C in humidified 5% CO_2 atm. CI data were recorded every 2 min for 13.3 h, then every 15 min for 25 h. Wells containing only effector cells were used as negative control for impedance baseline measurement. In all the experiments, the final volume in the microwells was 160µL. Data was acquired through the RTCA software, and CI were normalized at a time point immediately post effector cell addition, and to target only wells by cell line.

Intracranial tumor challenge in mice

Before tumor challenge, Tu2449 or GL26 cells were grown in supplemented DMEM, harvested,

washed, and resuspended in PBS. For the intracranial implantation of murine glioma cells, animals were first anesthetized with ketamine/xylazine. The head was shaved and the skull exposed. Thereafter, the animal was positioned into a stereotactic frame (David Kopf Instruments). A burr hole was made using a Dremel drill 1.5 mm lateral and 1 mm posterior from the intersection of the coronal and sagittal sutures (bregma). A total of $1x10^4$ Tu2449 cells or $1.5x10^4$ GL26 cells were injected using a Hamilton syringe at a depth of 3 mm in a volume of 2µl.

P14 cell migration in spleens and brains

P14 cell migration to spleen and tumor bearing hemisphere of the brain was assessed using flow cytometry. $1.5x10^4$ GL26 cells 100% transduced with AC3-GFP or gAC3-GFP were implanted into the right hemisphere of the brains of C57BL/6 mice. Four days later, mice were lymphodepleted with 2.4mg cyclophosphamide (CTX) and subsequently received $5x10^6$ P14 cells via i.p. on day 5. P14 cell expansion and proliferation was supplemented with 100,000 IU IL-2 for 3 consecutive days starting on day 5. Three days post adoptive cell transfer, spleens were crushed to isolate splenocytes. The right hemispheres of the brains were dissected and digested in Collagenase V (Advanced Biofactures Corp.) for 4 hours at 37°C, 5% CO_2. Similarly, $1x10^4$ Tu2449 cells 100% transduced with RRV or RRV-gp33 were implanted in B6/C3F1 mice. 9 days later, mice were lymphodepleted with 2.4mg CTX and injected $5x10^6$ P14 cells via i.p. on day 10. Supplemental IL-2 (100,000 IU) was injected for 3 consecutive days starting on day 10, and spleens and brains were harvested three days post adoptive cell transfer. Tumor infiltrating lymphocytes (TIL) were isolated by percoll gradient. Red blood cells were lysed with PharmLyse (BD Pharmingen), and cells were washed, resuspended in Dulbecco's PBS, and counted. A total of $1x10^6$ splenocytes and TIL were then labeled with mAbs to CD3-FITC, CD8-APC, PerCP Cy5.5-CD4, APC-Cy-7-CD25, PE-Cy7-Thy1.1, and PE-Thy1.2 (BioLegend). Cells were labeled for 30 min at 4°C, in the dark. The cells were then washed twice and were collected on a BD LSR II machine and FACSDiva software. Cell populations were analyzed using FlowJo software. To calculate the number of P14 cells

reaching the tumor-bearing hemisphere, the percentage of P14 cells reaching the tumor bearing hemisphere or the spleen were derived from the FlowJo software and extrapolated to lymphocyte counts post rbc lysis.

GL26 survival study

GL26/AC3-GFP and GL26/gAC3-GFP were sorted for GFP positive cells on a BD FACSAriaIII Cell Sorter to derive RRV-GFP-transduced cell lines. GL26/gAC3-yCD2 were made by transducing at high MOI (>10) multiple times. Complete transduction was confirmed by adding AC3-GFP to cells, and the lack of GFP expressing GL26 cells due to superinfection resistance on subsequent days. For the study using 100% RRV-transduced GL26 cells, $1.5x10^4$ GL26/AC3-GFP, GL26/gAC3-GFP, or GL26/gAC3-yCD2 were implanted into the right hemisphere of the brains of C57BL/6 mice. 4 days later, mice were total body irradiated (500cGy) and subsequently received $1x10^6$ P14 adoptive cell transfer on day 5 via i.v. T cell proliferation and expansion was supplemented with 100,000 IU IL-2 injected via i.p. for three consecutive days starting on the day of adoptive cell transfer. 500mg/kg 5-FC was administered via i.p. daily for seven consecutive days starting day 12.

For a separate study, 2% GL26/gAC3-yCD2 + 98% GL26 cells ($1.5x10^4$ total) were implanted into the right hemisphere of the brains of C57BL/6 mice. 500mg/kg of 5-FC was administered via i.p. daily for seven consecutive days starting day 10. Mice were lymphodepleted with 2.4mg cyclophosphamide on day 16, then subsequently received $5x10^6$ P14 cells on day 17 via i.p. T cells were supplemented with 100,000 IU IL-2 injected via i.p. for three consecutive days starting on the day of adoptive cell transfer. For both studies, median survival time (MST) was compared for statistical differences.

CD3 analysis using immunohistochemical staining

Brains were harvested from morbid mice which received 2% GL26/gAC3-yCD2 + 98% GL26 cells where possible, and embedded in paraffin. 5 micron sections were stained with anti-mouse CD3 antibody (Pathology Core Laboratory at UCLA). The region of interest was hand drawn and outlined on Aperio software (Leica Biosystems), then CD3 positive and negative cells with nuclei were quantified using Definiens Tissue Studio (Definiens Inc.) from 3-8 sections per group.

Tu2449 survival study

Similarly, $1x10^4$ Tu2449 cells were implanted into the right hemisphere of the brains of B6/C3F1 mice. 4 days later, $2x10^3$ TU AC3-yCD2 or gAC3-yCD2 was injected into the same coordinates. 9 days later, mice were lymphodepleted with 2.4mg cyclophosphamide and subsequently received $5x10^6$ P14 cells on day 10 via i.p. T cells were supplemented with 100,000 IU IL-2 injected via i.p. for three consecutive days starting on the day of adoptive cell transfer.

For the combination treatment study, 2% Tu2449/AC3-yCD2 + 98% Tu2449 or 2% Tu2449/gAC3-yCD2 + 98% Tu2449 cells ($1x10^4$ total) were implanted into the right hemisphere of the brains of B6/C3F1 mice. Combination groups received 500mg/kg 5-FC starting day 10, then $5x10^6$ P14 cells on day 17 via i.p., with IL-2 supplement. Monotherapy groups received P14 cells on day 17 with IL-2 supplement. Naïve Tu2449 cells were implanted in mice as a control group. For both studies, median survival time (MST) was compared for statistical differences.

Subcutaneous tumor challenge

Uninfected Tu2449 (2×10^6 cells in 100 µl PBS) were subcutaneously injected into the right flanks of long-term surviving mice from the Tu2449 pre-transduced survival experiment. Tumor sizes were measured every few days, and tumor volumes were calculated by this formula: volume = length ×

width^2/2. Animals were sacrificed when the tumor diameter reached 15mm.

Statistical analysis

All error bars represent standard deviations (SD). Continuous variables were compared using a paired Student t test. The survival curves were determined using the Kaplan-Meier method. The log-rank test was used to compare curves between study and control groups. All statistical values were assessed by the Student t test or ANOVA using Prism statistical software (GraphPad Software, Inc.). Values of p were two-tailed, and $p<0.05$ was considered statistically significant.

Results

Modification of parental vectors by insertion of LCMV gp33-43 sequence at the N-terminus of *env* gene

The lymphocytic choriomeningitis virus (LCMV) glycoprotein sequence gp33-43 (hereafter referred to as "gp33") was inserted into the end of the N-terminus of the mature *env* gene, immediately downstream of the signal peptide cleavage site, in parental RRV constructs AC3-GFP and AC3-yCD2 (**Figure 3-1A**), resulting in the gp33 epitope display vectors gAC3-GFP and gAC3-yCD2, respectively (**Figure 3-1B**). Preparations of infectious vector particles were obtained by transient transfection. Insertion of the gp33 sequence did not affect the ability of either epitope-display RRV to replicate, which is consistent with a previous study that characterized the N terminus of murine leukemia virus envelope proteins [97]. Transduction of Tu2449 and GL26 murine glioma cells by gAC3-GFP was confirmed by PCR spanning gp33 and the *env* gene (**Figure 3-1C**).

Genome stability over multiple cycles of viral replication

To test genomic stability of the epitope-display therapeutic vector gAC3-yCD2, infectious virus was serially passaged on U87 human glioma cells as described in Materials and Methods for up to 10 serial passages. At the end of each passage, genomic DNA from the cells was isolated and stored, and at the completion of serial passaging, PCR was performed on all of the collected DNA samples using one set of primers spanning the transgene and another set of primers spanning the gp33 epitope insert in the provirus. The amplification products were run on a gel to assess the integrity of the transgene. The results for the newly constructed epitope-display therapeutic vector gAC3-yCD2 are shown in (**Figure 3-1D, E**). The transgene of gAC3-yCD2 is stable until about passage 6, which is similar to the prototypic vector shown to be therapeutic in a mouse xenograft model. As each passage consisted of 10-fold diluted virus (MOI 0.1) proceeding to replicate and fully transduce approximately 10^5 cells per passage, and each

passage could generate 10 more aliquots of 10-fold diluted virus, each of which could fully transduce another 10^5 cells, and so on, this indicates that if all of the aliquots from 6 serial passages were used, the full-length virus has the potential to remain intact as it replicates and transduces at least $1x10^5$ (1^{st} passage) + $10x10^5$ (2^{nd} passage) + 10^2x10^5 (3^{rd} passage) + 10^3x10^5 (4^{th} passage) + 10^4x10^5 (5^{th} passage) + 10^5x10^5 (6^{th} passage) cells, i.e., over 10^{10} total cells. The gp33 epitope sequence on the other hand, demonstrated higher stability, with visible full-length bands until passage 10.

Cell killing efficiency of infected cells by 5-FC

In order to confirm the susceptibility of glioma cells infected by gAC3-yCD2 to 5-FC, Tu2449 cells transduced with AC3-yCD2 or gAC3-yCD2 were exposed to 0.1mM 5-FC. Cell killing was detected using an MTS assay on days 3, 5, and 7 post 5-FC addition. This resulted in a near identical curve between the two vectors, thus no statistical difference in susceptibility to 5-FC was observed (**Figure 3-1F**).

Replication kinetics of epitope display vector RRV-gp33

From here on, the murine glioma models Tu2449 and GL261 / Gl26, which vary in permissivity to virus as well as in immunological sensitivity, were used in parallel to assess specificity and therapeutic efficacy of adoptive immunotherapy with gp33-specific cytotoxic T lymphocytes (CTL) (**Table 3-1**). First, in order to assess replication kinetics of the vectors, Tu2449, GL26, and GL261 cells were infected *in vitro* with gAC3-GFP at a multiplicity of infection (MOI) of 0.1 or 5, and the percentage of GFP positive cell population was measured overtime. Tu2449 cells were more permissive to gAC3-GFP replication than GL26 or GL261 cells, and RRV-gp33 exhibited similar replication kinetics as the parental vector in all cell lines (data not shown). To assess *in vivo* spread of gAC3-GFP, subcutaneous

tumors were established using Tu2449sc3, a subline of Tu2449 adapted for subcutaneous growth, and GL26, a subline of GL261 showing reduced immunogenicity and enhanced tumor take. Animals were subcutaneously injected with 2% RRV-transduced glioma cells mixed with 98% naïve glioma cells in mice, and then tumors were harvested on day 10 and 17 (all Tu2449sc3 animals were sacrificed before day 17 due to oversized tumors). The percentage of GFP positive cells was analyzed by flow cytometry after collagenase digestion. Correlative to *in vitro* results, replication was slower in GL26 tumors as compared to Tu2449sc3 tumors (**Figure 3-2C**).

Major histocompatibility complex levels

Major histocompatibility complexes (MHC) play vital roles in presenting processed antigens to activate the immune system. Expression levels of major histocompatibility complexes (MHC) were measured in order to assess immunological sensitivity. LCMV GP1 epitopes gp33-41/43 located in the signal sequence of LCMV have been shown to be the immunodominant epitopes recognized by CTL at the surface of the infected cells in the context of H-2D^b or H-2K^b restriction [98], while P14 transgenic T cell receptor CD8 cells recognize gp33-41 solely in the context of H-2D^b [99]. Tu2449 and GL26 cells were cultured without or with IFN-γ, which is known to modulate MHC I expression [100], then stained and analyzed for H-2D^b and H-2K^b expression. Incubation with IFN-γ increased H-2K^b and H-2D^b expression in both cell lines (**Table 3-2**). GL26 cells consistently expressed more H-2Db and H-2Kb cell surface molecules than Tu2449 cells, regardless of IFN-γ pre-incubation. This suggests that GL26 cells may be more immunologically sensitive than Tu2449 in H-2D^b and H-2K^b-mediated antigen recognition.

P14 cell specificity towards gp33-expressing glioma cells

In order to assess whether the P14 transgenic TCR CD8 cells can recognize the gp33-41 peptide

presented by glioma cells, P14 cells were co-incubated with gAC3-GFP-transduced Tu2449 and GL26 cells, AC3-GFP-transduced Tu2449, and naïve GL26 cells at 1:1 for 18 hours, then the supernatant was analyzed for secreted murine IFN-γ by ELISA. Secretion of IFN-γ was detectable only when P14 cells were co-cultured with glioma cells transduced with gAC3-GFP (**Figure 3-3A**). When co-cultured with GL26/gAC3-GFP target cells, P14 effector cells secreted IFN-γ into the supernatant regardless of whether or not the target glioma cells had been pre-incubated with IFN-γ for 24hr to induce MHC expression, followed by washout of the cytokine prior to co-culture. Tu2449 cells, on the other hand, required pre-incubation with IFN-γ to induce MHC in order for co-incubated P14 cells to produce detectable levels of IFN-γ during co-culture.

In a separate experiment, P14 effector cells and GL26 or Tu2449 target cells were co-cultured at various effector to target ratios (E:T) and cell viability was measured using the xCELLigence electrical impedance assay. Cell viability was continuously monitored for over 24 hours after P14 cell addition to adhered glioma cells. Titrated killing was observed in both glioma cell lines transduced with gAC3-GFP, while no cytotoxicity was detected against glioma cells transduced with parental RRV, aside from non-specific toxicity at 10:1 E:T ratio in GL26 cells (**Figure 3-3B-E**). In both cell lines transduced with gAC3-GFP, complete killing was achieved by about 3 hours post co-culture at 10:1 E:T, and co-culture at 1:1 also ultimately resulted in complete lysis. Interestingly, while P14 cells had little to no effect on Tu2449 cells transduced with gAC3-GFP at 0.1:1 E:T when the glioma cells were not pre-incubated with IFN-γ (**Figure 3-3F,G**), cytotoxicity was observed at 0.1:1 E:T when Tu2449 cells were pre-incubated for 24 hours with IFN-γ. GL26 cells did not require IFN-γ pre-incubation for lysis at 0.1:1 E:T.

P14 cell migration to intracranial tumors expressing gp33

To examine whether P14 cells home to tumors expressing gp33, syngeneic C57BL/6 mice were implanted with $1.5x10^4$ GL26 murine glioma cells transduced with AC3-GFP or gAC3-GFP in the right

hemisphere of the brain. On day 4, mice were given cyclophosphamide (CTX) to induce lymphodepletion. The next day, $5x10^6$ P14 cells were adoptively transferred via i.p. injection, and mice were further injected with IL-2 (100,000 IU) for 3 consecutive days. On day 8-post tumor implantation, tumor-bearing brain hemispheres were processed for tumor-infiltrating lymphocyte (TIL) analysis. P14 T cells are derived from a Thy1.1 congenic strain of C57BL/6 mice, whereas endogenous T cells are Thy1.2 positive, enabling differentiation of adoptively transferred T cell versus endogenous T cell infiltration by flow cytometry. As expected, P14 cells selectively homed to gp33-expressing tumors over non-gp33-expressing tumors (**Figure 3-4A**). The number of P14 cells in the spleen was similar between the two groups (**Figure 3-4B**).

Similarly, $1x10^4$ Tu2449 murine glioma cells transduced with AC3-GFP or gAC3-GFP were implanted in syngeneic B6/C3F1 mice. $5x10^6$ P14 cells were adoptively transferred on day 10-post tumor implant, one day post lymphodepletion by CTX. Supplemental IL-2 was administered for 3 consecutive days starting day 10, then as above, TIL and splenocytes were stained and analyzed by flow cytometry 3 days post adoptive cell transfer. TIL analysis suggested that P14 cells migrated selectively to RRV-gp33 expressing Tu2449 cells (**Figure 3-4C**). The number of P14 cells in the spleen was similar between RRV-gp33 and parental RRV tumor-bearing mice (**Figure 3-4D**).

Therapeutic efficacy of P14 adoptive cell transfer

Therapeutic efficacy of P14 adoptive cell transfer and prodrug activator gene therapy was assessed using the GL26 and Tu2449 syngeneic intracranial tumor models. First, orthotopic intracranial tumors were established in syngeneic C57BL/6 mice using $1.5x10^4$ GL26 cells, which had been 100% transduced with either parental RRV or epitope-display RRV-gp33, and these models were used to assess the therapeutic efficacy of gp33-specific P14 cells. Four days post intracranial tumor implantation, all mice underwent total body irradiation (TBI), then $1x10^6$ P14 cells were administered via i.v. on day 5, with 3

consecutive days of supplemental IL-2 (100,000 IU). Treatment with P14 cells increased the median survival time (MST) in mice implanted with gAC3-GFP expressing GL26 cells (**Figure 3-5A**, $p<0.002$).

For the Tu2449 intracranial tumor model, $1x10^4$ Tu2449 cells pre-marked with a replication-defective lentiviral vector expressing the firefly luciferase gene were implanted into the cerebrum in syngeneic B6/C3F1 mice. On day 4, $2x10^3$ transducing units (TU) of either the AC3-yCD2 parental vector or the gAC3-yCD2 epitope-display vector was intratumorally injected using the same stereotactic coordinates. Subsequently, $5x10^6$ P14 cells were administered via i.p. on day 10, one day post lymphodepletion with CTX. Treatment with P14 cells significantly increased the MST in mice that received gAC3-yCD2 (**Figure 3-5B**, $p=0.0008$).

Therapeutic efficacy of P14 adoptive cell transfer and prodrug activator gene therapy combination treatment

Again, GL26 cells that had been 100% pre-transduced with gAC3-yCD2 were used to assess the efficacy of the combination treatment in C57BL7 mice. As previously, 4 days post intracranial tumor implant, all mice were given total body irradiation (TBI), then $1x10^6$ P14 cells were administered iv on day 5, with 3 consecutive days of supplemental IL-2 (100,000 IU). Thereafter, the mice received 7 consecutive days of 5-FC a week post P14 cell injection. However, when compared with the control and monotherapy groups, the efficacy was not enhanced with the additional 5-FC prodrug administration (**Figure 3-5A**).

In a different study, mice were implanted with 2% pre-mixed GL26 cells that had been transduced with gAC3-yCD2. RRV was allowed to spread for 10 days, then 7 consecutive days of 5-FC was given in treatment groups. $5x10^6$ P14 cells were injected via i.p. one day after the last day of 5-FC, post lymphodepletion with cyclophosphamide (CTX). In this study, RRV-mediated suicide gene therapy achieved survival benefit in the intracranial GL26 glioma model, but was not enhanced by adoptive cell

therapy (**Figure 3-5C**). To investigate whether the early deaths in the combined treatment group were caused by an excessive intracerebral pro-inflammatory response associated with lymphocytic infiltration, brain sections of morbid animals were stained for CD3 and counted. CD3 immunohistochemical staining within GL26 tumors suggested enhanced immune infiltration in treatment groups (**Figure 3-5D-F**), although the difference between the monotherapy group and combined treatment group was unclear due to small sample size (**Figure 3-5G**).

In a final study, intracranial tumors in syngeneic B6/C3F1 mice were established with mixtures of 2% Tu2449 cells transduced with AC3-yCD2 or gAC3-yCD2 and 98% naïve Tu2449 cells. RRV was allowed to spread for 10 days, then 7 consecutive days of 5-FC was given in two of the treatment groups, receiving AC3-yCD2 or gAC3-yCD2 respectively. Subsequently, $5x10^6$ P14 cells were adoptively transferred via i.p. on day 17 without prior lymphodepletion in all treatment groups. In this model, P14 adoptive cell transfer alone in either the parental vector or gAC3-yCD2-transduced tumor group did not show any improvement in survival compared to controls, likely due to the lack of lymphodepletion conditioning. On the other hand, 5-FC prodrug treatment achieved long-term survival in both groups, but was not statistically enhanced by adoptive cell therapy (**Figure 3-5H**), although there was a trend for increased percentage of survival in the gAC3-yCD2 epitope-display RRV-transduced group as compared to the AC3-yCD2 parental RRV-transduced group. On day 150-post tumor implantation, long-term survivors as well as naïve mice from this study were re-challenged with $2x10^6$ Tu2449sc3 cells subcutaneously. Tumor growth was suppressed and/or delayed in all long-term survivors, while naïve animals were sacrificed at early time points due to uncontrolled tumor growth (**Figure 3-5I**). Subsequently, all long-term survivors from the parental RRV group eventually succumbed to tumor, but some mice from the gAC3-yCD2 group demonstrated complete tumor clearance, although without statistical difference between the two groups ($p=0.2264$, data not shown).

Discussion

Advances in tumor immunotherapy may be of tremendous importance and relevance to primary brain tumors, particularly if immune effectors can track and destroy infiltrating tumor cells. However, the scarcity of well-characterized, highly immunogenic tumor-associated antigens with defined epitopes in glioblastoma has limited the implementation of targeted immune-based therapies. We demonstrated here that RRV-mediated tumor transduction stably conferred the gp33 epitope to glioma target cells, enabling P14 effector cells to migrate selectively to intracranial tumor. Furthermore, adoptive cell therapy was associated with a survival advantage in both models after RRV-mediated delivery of the highly immunogenic epitope. Thus, the RRV platform enables stable delivery of an exogenous targetable immunogenic antigen to tumor cells and these studies demonstrate the feasibility of this approach for viro-immunotherapy for brain tumors.

Two models, which vary in permissivity to virus as well as immunological sensitivity, were used to investigate the applicability of the technology. The non-permissivity of GL261 and GL26 cells for RRV replication may be due to multiple factors. There have been reports indicating high levels of 4070env glycoprotein detected on the surface of non-RRV-permissive cell lines, including GL26, suggesting that the phosphate transporter-retrovirus receptors Pit-2 may be saturated in these cells by a previous amphotropic virus infection. Multiple rounds of retroviral entry, or superinfection, are blocked in many retroviruses as a mechanism to avoid metabolic burden for the host cell through the process of viral interference [101, 102, 103]. This is further supported by the fact that GL26 and GL261 cells are more permissive to a 10A1-pseudotyped RRV, which uses both Pit-1 and Pit-2 receptors for entry [104] (**Figure 3-6**). The use of 10A1 pseudotyped RRV, which are able to utilize both Pit-1 and Pit-2 receptors, may be considered for future use in glioma cells such as GL26 that have low levels of Pit-2 receptors and/or higher levels of Pit-1 receptors.

Alternatively, MLVs do not possess a nuclear localization signal, but rather rely on the host cell's ability to divide for integration [105]. Others have shown correlation between the rate of cell proliferation

and efficient viral spread and productive infection [7]. Tu2449 cells have a faster doubling rate of 26 hours, whereas GL26 cells have a doubling rate of 36 hours [37, 106]. Although the rate of viral replication does not always correlate with cell proliferation, proliferation is necessary for virus replication and thus cannot be ruled out. Other possible causes include antiretroviral defense mechanisms such as APOBEC3 [107], which may cause inhibition of further replication after initial transduction.

While the *in vitro* assays indicated differences in immunological sensitivity between the two cell lines, with lower levels of MHC expressed in Tu2449 cells, we were able to induce a tumor suppressive response in the Tu2449 model nonetheless. Interestingly, Tu2449 cells increased their H-2D^b levels after passage in vivo, likely due to exposure to interferons, which may have contributed to the increased survival in RRV-gp33 implanted mice that received P14 adoptive cell transfer (data not shown). In fact, contrary to tumor types of differing origins in which immune evasion by MHC downregulation is common, upregulation of MHC I in human gliomas and feasibility of CTL therapy targeting MHC I have been reported [27] (Chapter Two). Therefore, it is further suggestive that engineering a dominant viral antigen to be presented through MHC I may be a rational combination.

One possible reason for the lack of efficacy in combined treatment groups in both GL26 and Tu2449 studies is that lymphodepletion prior to adoptive cell transfer may be eradicating immune cell populations necessary for sustained immune response against the tumor, as indicated in Chapter 1. Another plausible reason is that the combination treatment may be causing toxicities by creating an extremely pro-inflammatory environment. Although CD3 staining of brain sections from morbid mice showed increased infiltration of lymphocytes in the combination treatment, definitive conclusions could not be drawn due to small sample size and large variability in the monotherqpy group. Further studies are underway to investigate the therapeutic effect of combining RRV-mediated prodrug activator gene therapy and neo-antigen target delivery for adoptive immunotherapy. The two individual therapies are each potently cytoreductive by themselves, and the combination regimen is expected to achieve higher efficacy when

combined in an optimal manner. Nonetheless, carefully designed combinatorial regimens will likely be required to ensure maximal potent antitumor immune response.

By conferring a targetable neo-antigen epitope to tumor cells, we may potentially address some of the challenges currently faced in immunotherapeutic strategies for gliomas. It enables us to overcome the issue of low immunogenicity of the target cells as well as make the tumor a more homogenous entity. Furthermore, this novel approach may open doors to various combination treatments with existing immunotherapies for which the target epitope sequence is available to engineer the RRV (eg. CAR-T, dendritic cell vaccines, monoclonal antibodies, and antibody-drug conjugates). For example, collaborative efforts are being pursued to use the EGFRvIII epitope in lieu of gp33, so that RRV-transduced gliomas may be targeted with existing anti-EGFRvIII CAR-T cells currently in development. The combined use of checkpoint inhibitors may also be investigated to address immune evasion mechanisms that may dampen the immune response. If successful, this would represent a new paradigm for combining viro- and immunotherapy strategies, which can also be applied to other types of cancers that share a similarly poor prognosis and suffer from lack of targetable tumor associated antigens.

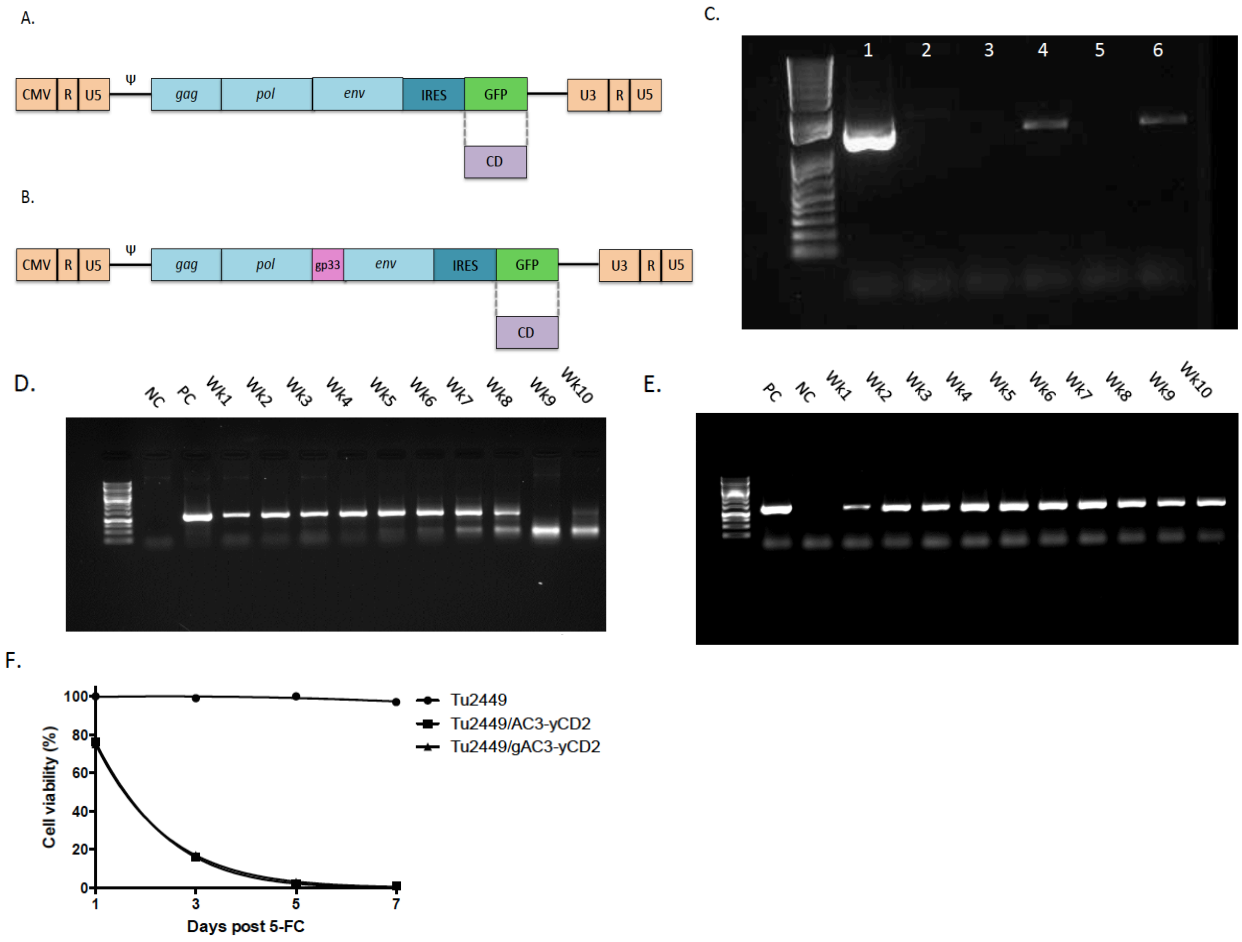

Figure 3-1. RRV constructs. (A) Replication competent murine leukemia virus (MLV) vector AC3-GFP and AC3-yCD2 showing the location of the IRES-GFP and cytosine deaminase (CD) insert between *env* and the 3' UTR. **(B)** The lymphocytic choriomeningitis virus (LCMV) peptide sequence gp33-43 was inserted into the extreme end of the N-terminus of the *env* gene in parental RRV plasmids to generate gAC3-GFP and gAC3-yCD2. **(C)** Gp33 insertion in Tu2449/gAC3-GFP and GL26/gAC3-GFP cells were confirmed by PCR spanning gp33 and the *env* gene (Lane 1: RRV-gp33 plasmid, lane 2: RRV plasmid, lane 3: Tu2449/RRV gDNA, lane 4: Tu2449/RRV-gp33 gDNA, lane 5: GL26/RRV gDNA, lane 6: GL26/RRV-gp33 gDNA). To assess stability of the epitope display vector, gAC3-yCD2 viral supernatant was passaged on U-87MG cells for 10 weeks. gDNA from cells from each infection were amplified using two sets of primers to assess the stability of **(D)** the transgene and **(E)** the gp33 epitope sequence and ran on an agarose gel. **(F)** Naïve Tu2449, Tu2449/AC3-yCD2, and Tu2449/gAC3-yCD2 were exposed to 0.1mM 5-FC. Cell viability was measured by MTS assay on days 1, 3, 5, and 7 post 5-FC addition.

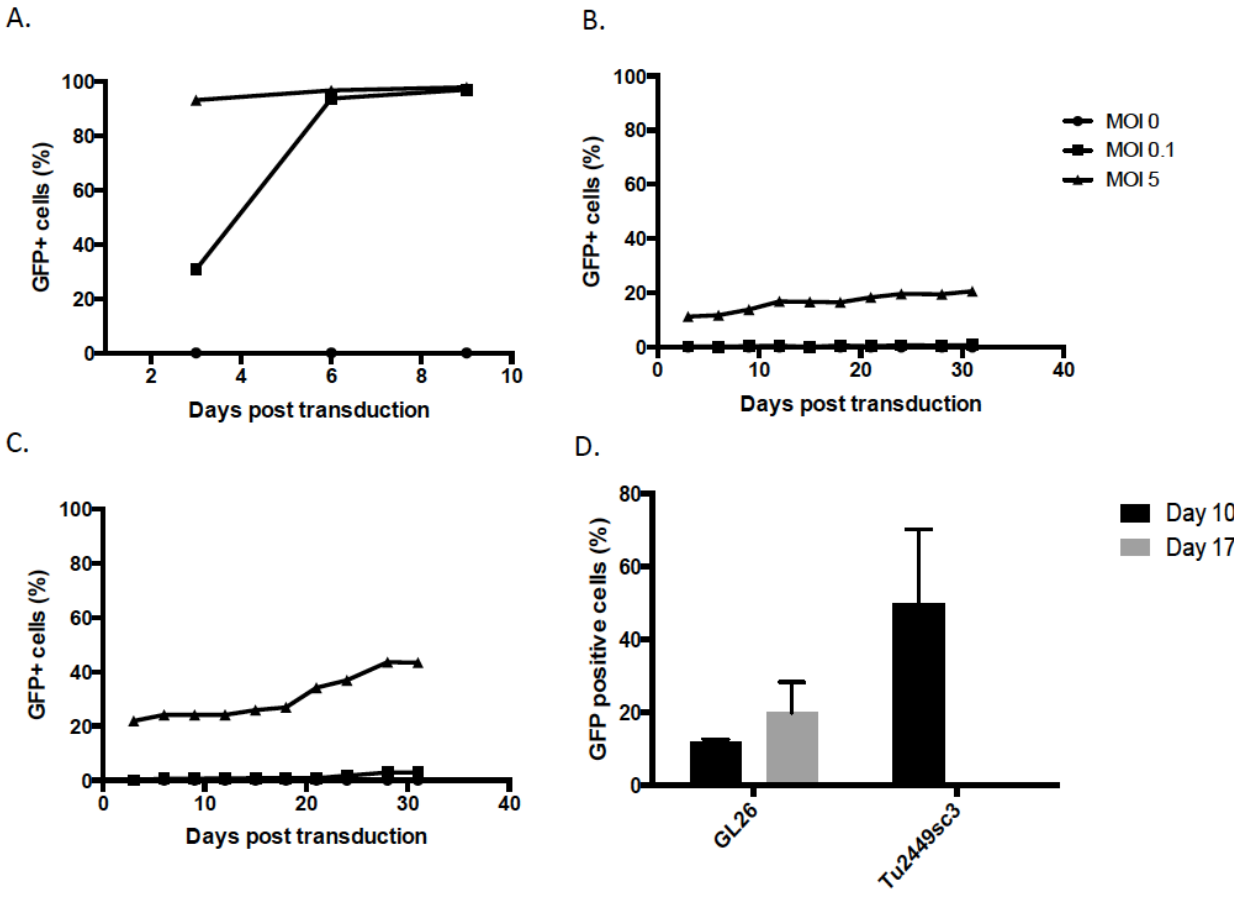

Figure 3-2. RRV-gp33 replication kinetics. gAC3-GFP viral replication kinetics was measured on **(A)** Tu2449, **(B)** GL26, and **(C)** GL261 cells. Cells were infected at MOI 0.1 and 5 and the percentage of GFP positive cells was monitored over time. **(D)** Viral replication was measured *in vivo*. GL26, a subline of GL261, and Tu2449sc3, a subcutaenous model for Tu2449, were used for less immunogenicity and enhanced tumor take. $2x10^6$ Tu2449sc3 and $1x10^6$ GL26 cells with 2% aAC3-GFP transduced cells were injected into the right flanks of B6/C3F1 and C57BL/6, respectively. Subcutaenous tumors were excised on day 10 and 17 where possible, dissected, and digested in collagenase overnight. Next day, tumor cells were placed in culture with 50µM AZT. 24hr later, percentage of GFP positive cells was measured by flow cytometry.

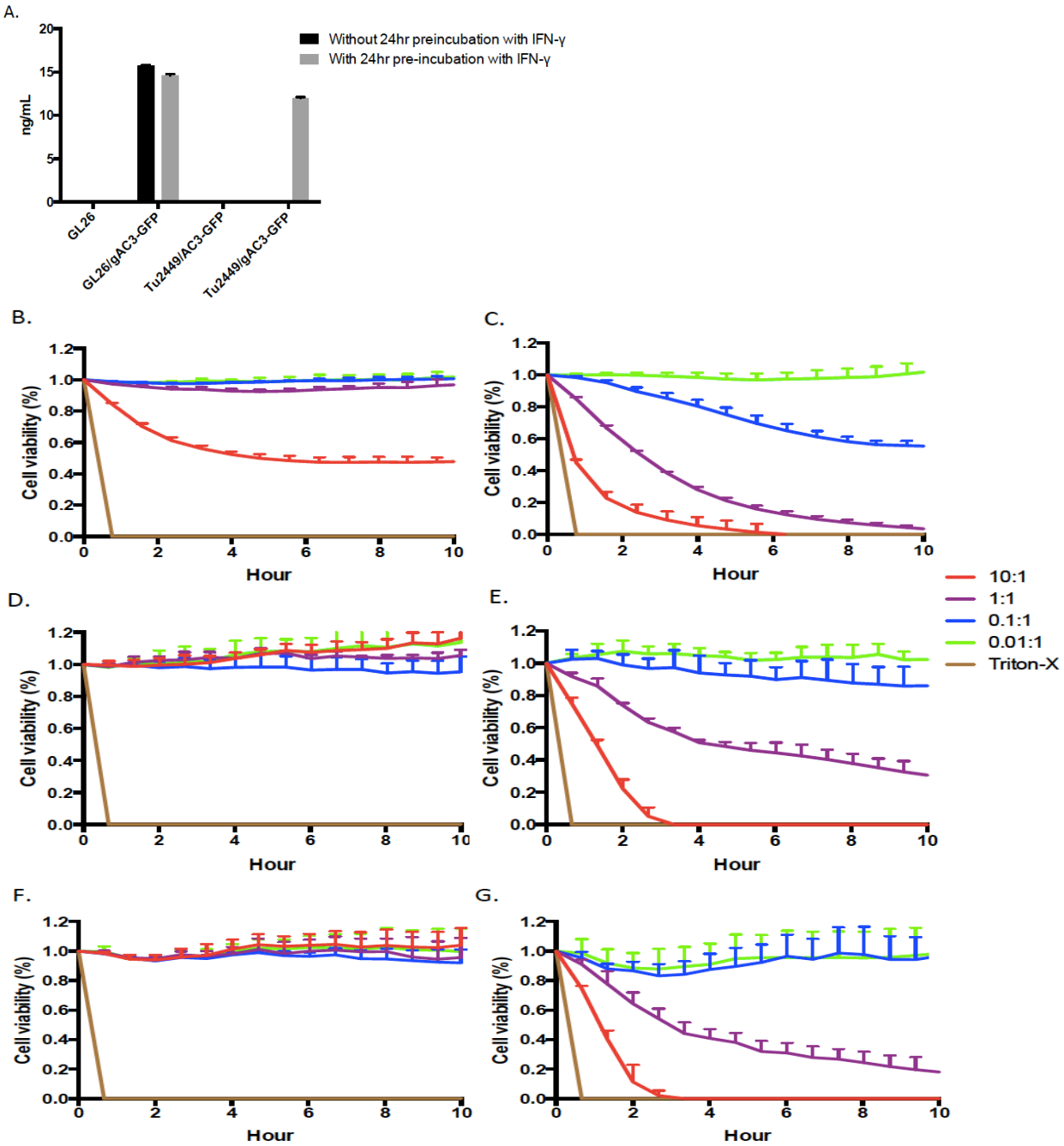

Figure 3-3. Specificity of P14 cells to gAC3-GFP transduced glioma cells. (A) IFN-γ production was measured post P14 and tumor cell co-culture at effector to target ratio (E:T) of 1:1., GL26, GL26/gAC3-GFP, Tu2449/AC3-GFP, or Tu2449/gAC3-GFP cells were either pre-incubated with IFN-γ for 24hr or not pre-incubated prior to co-culture. Supernatants after 18hr co-culture were measured for IFN-γ by ELISA. The specificity of P14 cells was assessed as a measurement of cytotoxicity to target cells. The xCelligence system was used, which enables continuous monitoring of cell viability by electrical impedance. **(B)** GL26/AC3-GFP, **(C)** GL26/gAC3-GFP, **(D)** Tu2449/AC3-GFP+ IFN-γ, **(E)** Tu2449/gAC3-GFP + IFN-γ, **(F)** Tu2449/AC3-GFP (-IFN-γ), and **(G)** Tu2449/gAC3-GFP (-IFN-γ) were co-cultured with P14 cells at various effector to target ratios of 10:1. 1:1, 0.1:1, and 0.01:1. In **(E)** and **(F)**, target cells were pre-incubated with 10ng/mL IFN-γ for 18 hours prior to plating on gold plates.

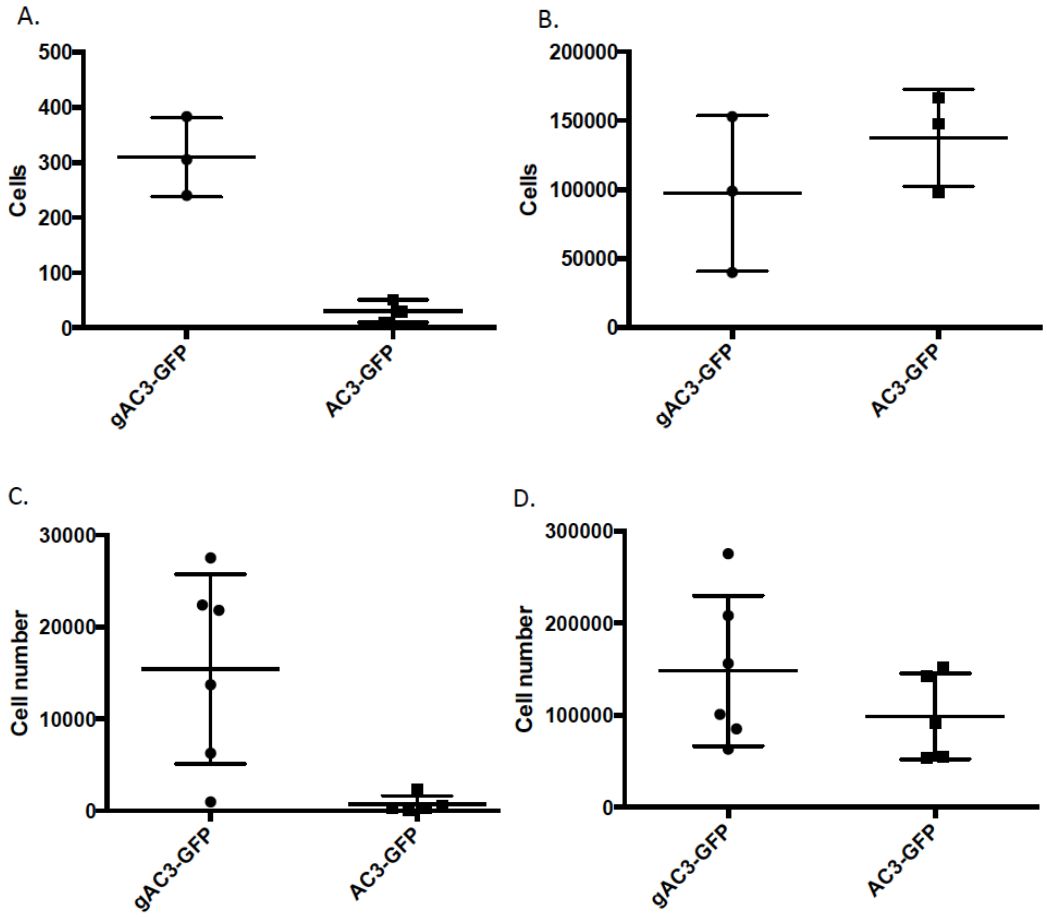

Figure 3-4. P14 migration to spleens and brains. P14 cell (CD3+ CD8+ Thy1.1+) migration to **(A)** tumor bearing hemisphere of the brain (p=0.0029) and **(B)** spleen (p=0.3529) was assessed using flow cytometry. $1.5x10^4$ GL26 cells 100% transduced with AC3-GFP or gAC3-GFP were implanted into the right hemisphere of the brains of C57BL/6 mice. 4 days later, mice were lymphodepleted with 2.4mg cyclophosphamide and subsequently received P14 adoptive cell transfer on day 5 with supplemental IL-2 (100,000 IU for 3 consecutive days). On day 8, spleens were crushed to isolate splenocytes. The right hemispheres of the brains were dissected and digested in collagenase for 6 hours at 37°C, 5% CO_2. Tumor infiltrating lymphocytes (TIL) were isolated by percoll gradient. Splenocytes and TIL were stained for CD3, CD4, CD8, CD25, Thy1.1, and Thy1.2, and the cells were acquired on an LSR II apparatus for analysis. Similarly, P14 cell migration to **(C)** tumor bearing hemisphere of the brain (p=0.0117) and **(D)** spleen (p=0.2640) was assessed in the Tu2449 model. $1x10^4$ Tu2449 cells 100% transduced with AC3-GFP or gAC3-GFP were implanted into the right hemisphere of the brains of B6/C3F1 mice. 9 days later, mice were lymphodepleted with 2.4mg cyclophosphamide and subsequently received P14 adoptive cell transfer on day 10 with supplemental IL-2 (100,000 IU for 3 consecutive days). On day 13, splenocytes and TIL were isolated by percoll gradient, stained, and the cells were acquired on an LSR II apparatus for analysis.

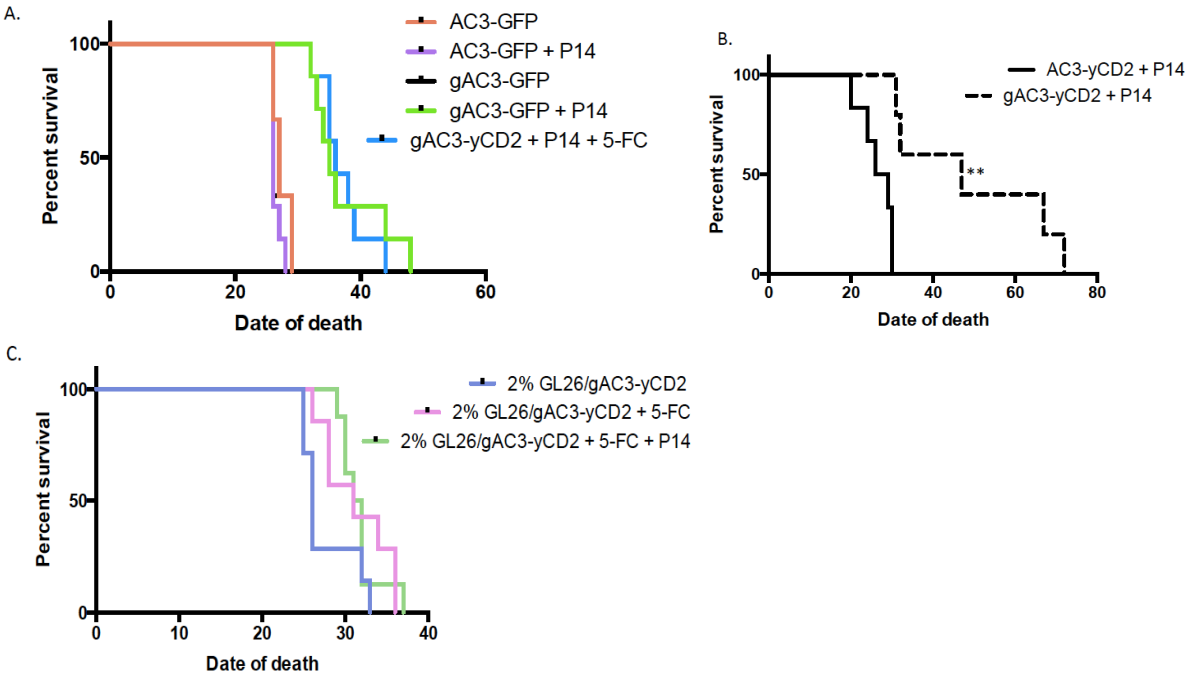

Figure 3-5. Therapeutic efficacy of immunotherapy and suicide gene therapy. (A) $1.5x10^4$ GL26 cells 100% transduced with AC3-GFP, gAC3-GFP, or gAC3-yCD2 were implanted into the right hemisphere of the brains of C57BL/6 mice. 4 days later, mice were total body irradiated (500cGy) and subsequently received $1x10^6$ P14 adoptive cell transfer on day 5 via i.v. P14 cells were supplemented with 100,000 IU IL-2 injected via i.p. for three consecutive days starting on the day of adoptive cell transfer. *p<0.002. **B)** $1x10^4$ Tu2449 cells were implanted into the right hemisphere of the brains of B6/C3F1 mice. 4 days later, $2x10^3$ TU AC3-yCD2 or gAC3-yCD2 were injected into the same coordinates. 9 days later, mice were lymphodepleted with 2.4mg cyclophosphamide and subsequently received $5x10^6$ P14 cells on day 10 via i.p. P14 cells were supplemented with 100,000 IU IL-2 injected via i.p. for three consecutive days starting on the day of adoptive cell transfer. **p=0.0008. **C)** 98% naïve GL26 cells premixed with 2% gAC3-yCD2-transduced GL26 cells were implanted intracranially in C57BL/6 mice. Monotherapy group received daily 5-FC injections starting day 10. Combination therapy group was lymphodepleted on the last day of the 5-FC treatment, and then administered $5x10^6$ P14 cells via i.p. on day 17 with 100,000 IU IL-2 supplement. While the monotherapy group had prolonged survival (p=0.0319), the combination group did not achieve statistical significance (p=0.0988).

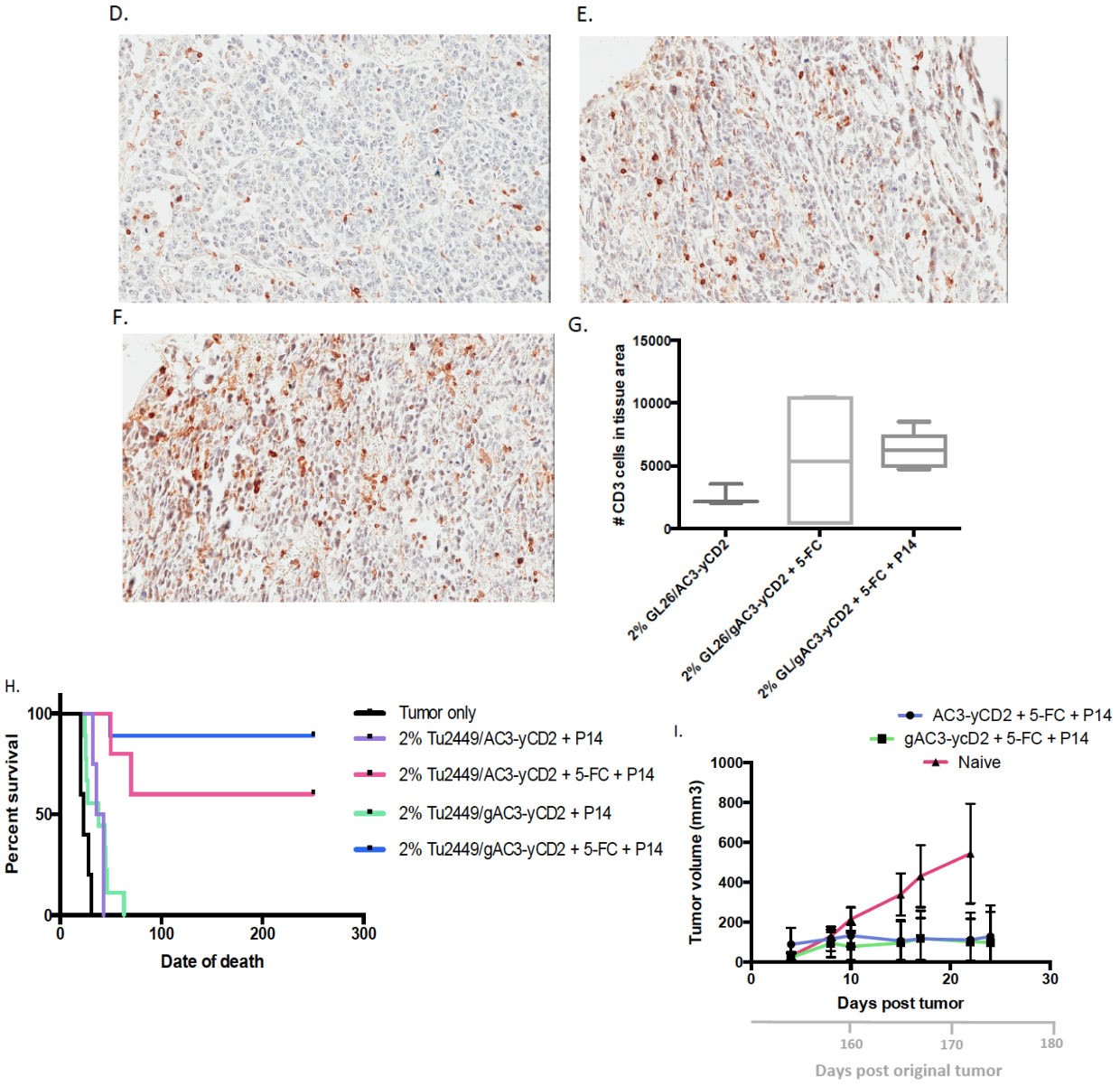

Figure 3-5, continued. CD3 cells were stained by IHC, then quantified using the Definiens software. Representative microfields from brain sections of **D)** 2% GL26/gAC3-yCD2, **E)** 2% GL26/gAC3-yCD2 + 5-FC, and **F)** 2% GL26/gAC3-yCD2 + 5-FC + P14 morbid mice show CD3 infiltration in tumor tissues. **G)** The number of CD3 cells in tumor tissue were plotted (+/-SD). Combination group showed increased infiltration of CD3 cells compared to the control group (p=0.0018). **(H)** Therapeutic efficacy of 5-FC monotherapy and combined therapy were assessed using 2% Tu2449/AC3-yCD2 or Tu2449/gAC3-yCD2 cells premixed with 98% naïve Tu2449 cells. Mice were injected daily with 5-FC starting on day 10 for seven consecutive days. On day 17, P14 cells with IL-2 supplement were adoptively transferred in combination groups. (I) Long-term survivors were re-challenged with subcutaneous Tu2449 cells, and tumor growth was monitored overtime. 2% AC3-yCD2 + 5-FC + P14 and 2% gAC3-yCD2 + 5-FC + P14 long term survivors were able to control tumor growth compared to naïve mice (p=0.0001, p=0.0004)

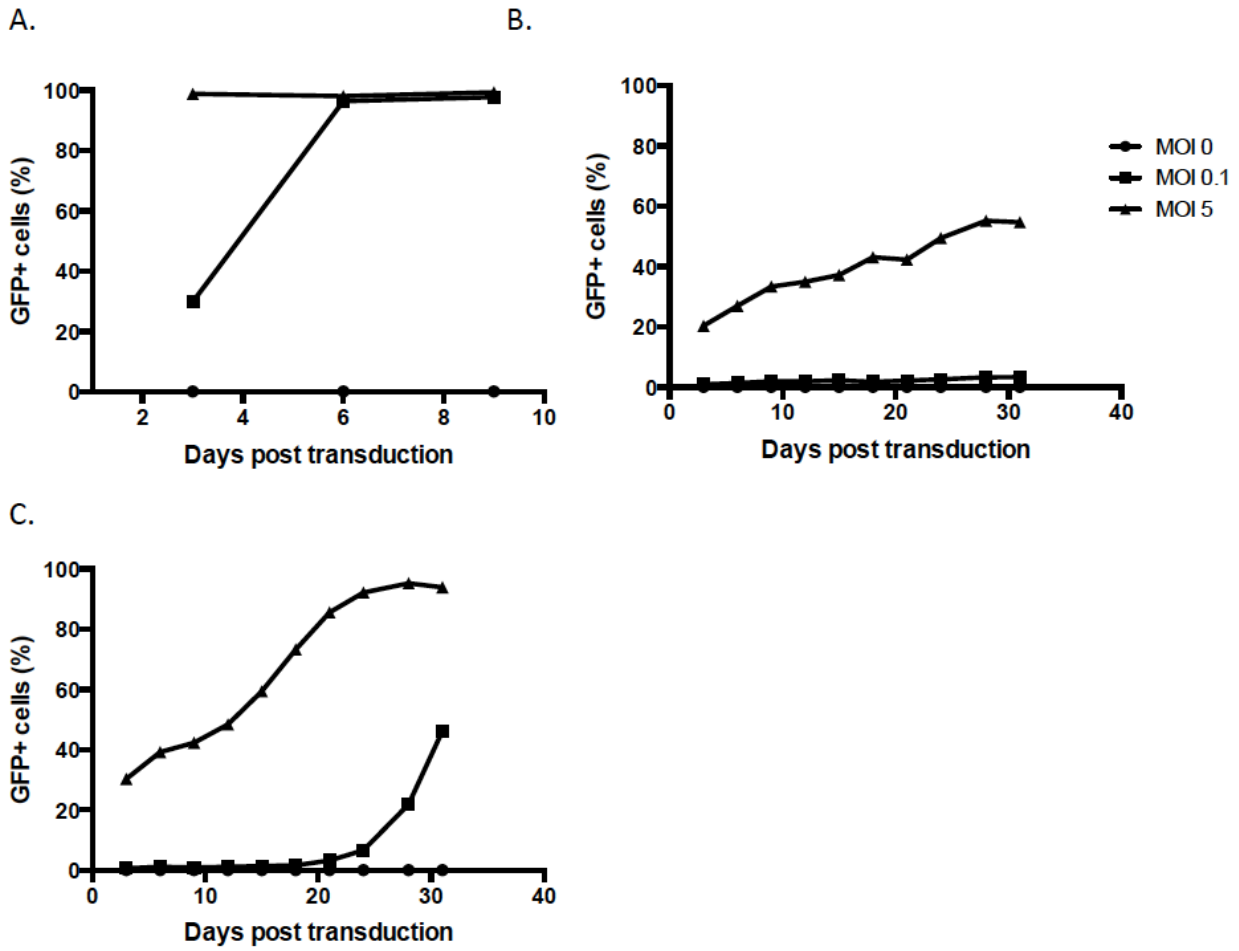

Figure 3-6. Replication kinetics of 10A1-pseudotyped RRV encoding GFP in murine glioma cells. Viral replication kinetics was measured on **(A)** Tu2449, **(B)** GL26, and **(C)** GL261 cells. Cells were infected at MOI 0.1 and 5 and the percentage of GFP positive cells was monitored over time.

Cell line	Strain derived : haplotype	Replication Virally Permissive	Major Histocompatibility Complex (MHC) levels
TU2449	B6/C3F1 : H-2K $^{b/k}$ H-2D $^{b/k}$	Fast replication Highly Permissive	Low MHC
GL26	C57BL/6 : H-2K^{b} H-2D^{b}	Slow replication Less permissive	High MHC

Table 3-1. Characterization of murine glioma models. Tu2449 cells were derived from B6/C3F1 mice, which have haplotype b/k. These cells are virally permissive, and have low MHC levels. GL26 cells were derived from C57BL/6 mice, which have haplotype b. These cells are resistant to viral spread, and have high MHC levels.

	H-2Db		H-2Kb	
	MFI	%	MFI	%
Tu2449	6	0.1	38	7.5
Tu2449 + IFN-γ	30	3.1	1532	94.5
GL26	20	3.4	561	74.2
GL26 + IFN-γ	313	55.5	8402	99.1

Table 3-2. Major Histocompatibility Complex (MHC) I levels. Tu2449 and GL26 cells +/- IFN-γ pre-incubation were stained for H-2D^b and H-2K^b and were analyzed on flow cytometry. Percentage of positive cells and median fluorescence intensity (MFI) were calculated using the FlowJo software.

Conclusions and Future Directions

In previous studies and the experiments presented here, we have shown that the RRV prodrug activator gene therapy is effective for the treatment of brain tumors. Chapter One presents strong evidence that the immune system plays a vital role in durable response, providing rationale for combining RRV therapy with immunotherapy. However, the dynamic nature of the immune system ensures that optimal timing and administration of treatments is paramount to achieving maximal efficacy.

In Chapter Two, we showed that both human and murine alloCTL could be transduced with RRV using spinoculation, to generate alloCTL/RRV. Most importantly, we were able to demonstrate that alloCTL/RRV served as motile cells that produce functional RRV, which can then subsequently infect target glioma cells. In both therapeutic efficacy studies presented here, the combination treatment groups survived the longest. The breast cancer xenograft model where alloCTL and RRV treatments were used as separate products confirmed the feasibility of combining these modalities. However, it is important to note that the benefit derived from the RRV modality may have been limited due to the use of 2% RRV-infected glioma cells, and by restricting prodrug treatment to 3 cycles in an immunodeficient model. Also, it is important to assess whether lower E:T ratios of alloCTL will still confer survival advantage, as would be the situation in patients with larger tumors in the clinical setting. Next, the subcutaneous glioma xenograft model provided the proof-of-concept for combining these two modalities into one product. AlloCTL successfully debulked tumor initially, when the E:T ratio was high, and further suppression of tumor growth was observed with subsequent prodrug administration. However, the need for testing in an intracranial model is apparent, as the tumor microenvironment can vastly differ in a subcutaneous versus intracranial setting. Furthermore, the combination of alloCTL and RRV needs to be investigated in a syngeneic model, to dissect its interaction with the endogenous immune system. We have not witnessed extreme proinflammatory events such as a cytokine storm when each modality is administered by itself in immunocompetent models, but immune responses may be heightened when combined. Taken together, the optimal timing of administration warrants further investigation.

Another potential means of combining alloCTL and RRV is to use a phenomenon called viral "hitchhiking" [97]. Viral particles can adsorb onto the surface of T cells, and act as passengers until it reaches a target with the necessary receptors for infection. We have tested this method and confirmed that after alloCTL incubation with high dose RRV, wash steps, and co-culture with glioma cells at E:T ratio of 1 to 10, RRV transduced glioma cells reach more than 90% by day 7 (data not shown). This may be an alternative way for RRV to navigate through infiltrating tumor cells, overcoming the need for a transduction step which often leads to lower viable cell yields. Especially since the variability of viable cell counts per batch has been one of the hurdles for the alloCTL treatment in the clinical setting, this method may provide an important technical advantage.

In Chapter Three, we successfully utilized RRV to confer a dominant viral antigen to target glioma cells, which was then recognized by antigen-specific T cells. To this date, we believe this is the first study of its kind to xenogenize a tumor using replicating retroviruses. Importantly, significant survival advantage was achieved in both Tu2449 and GL26 intracranial glioma models with a single dose of adoptive T cell transfer. Although we did not test multiple injections of T cells, it may be worthwhile to see whether this further prolongs survival or achieves tumor eradication. Interestingly, however, combination with the RRV prodrug activator gene therapy failed to enhance survival in animals. There are several plausible explanations for this phenomenon.

Both therapies are contingent on the tumor cells being transduced by RRV, which means that if one therapy successfully eradicates all RRV-transduced glioma cells, there would be no more glioma cells to target with the subsequent therapy. However, it is unlikely that one cycle of prodrug or a single injection of T cells would eradicate all cells transduced with RRV, since theoretically it only takes one cancer cell to survive and act as an RRV producer cell to continue intratumoral virus propagation. This is also corroborated by the fact that multiple cycles of 5-FC after a single RRV injection continue to suppress tumor growth in an immunodeficient model (Chapter One). It is possible, however, that more time is

necessary in between treatments to establish enough newly RRV-infected cells to derive therapeutic benefit from the second therapy, and optimization of this scheduling interval is worth exploring.

Another possible reason for rapid lethality seen after combination treatment is the induction of an extreme proinflammatory environment in the brain. Furthermore, tumor lysis syndrome could develop after simultaneous killing of RRV-transduced cancer cells upon 5-FC administation, and cytokine storms are not uncommon with immunotherapy, especially where it is difficult to control proliferation and expansion of immune cells after administration. Therefore, it is possible that combination regimens, which may be more potent, could also be associated with increased morbidity or mortality if the timing of administration is not optimized. Unfortunately, anti-CD3 staining of brain sections of morbid mice was inconclusive and requires further investigation. Further experiments should look at immune cell infiltration or cytokine secretion in the brain immediately post combination treatment. If an extreme proinflammatory environment is confirmed in the combined treatment groups, increasing the time interval between treatments or administering lower doses may be beneficial.

Alternatively, the opposite scenario can also be considered, where the lymphodepletion step is wiping out necessary immune cells for durable and sustained anti-tumor response. This view is supported by the fact that the only instance we did not observe any rapid deaths of the combination treatment mice was when we did not perform lymphodepletion in the Tu2449 model (**Figure 3-5H**). Although adoptive T cell therapy itself did not prolong survival in animals with the epitope-display RRV-transduced tumors in this particular experiment, this may be because the timing of administration was late, or from the lack of lymphodepletion necessary for T cell expansion. Further experiments may need to be conducted with "de-optimization" of the RRV prodrug activator gene therapy, and assess whether the added immunotherapy can be beneficial without lymphodepletion. There is substantial evidence indicating that anti-tumor immunological memory develops post RRV prodrug activator gene therapy (Chapter One), and it would be more advantageous to utilize this endogenous immune response instead of depleting these cells. It may

also be worthwhile to explore combinations with immunotherapies that do not require lymphodepletion, such as dendritic cell vaccines, monoclonal antibodies, or antibody-drug conjugates.

In conclusion, further experiments are necessary to optimize therapeutic efficacy for both types of combined viro-immunotherapy. Optimization of timing and lymphodepletion regimens may be crucial in order to potentiate maximal efficacy while minimizing adverse complications. If these combinatorial approaches show therapeutic improvement, clinical translation should be rapid, as there are now ample preclinical and clinical data supporting the safety and efficacy of RRV-mediated prodrug activator gene therapy and adoptive cellular immunotherapy as individual modalities.

REFERENCES

1. Ostrom, Q.T. *et al.* CBTRUS Statistical Report: Primary Brain and Central Nervous System Tumors Diagnosed in the United States in 2008-2012. *Neuro-oncology* **17 Suppl 4**, iv1-iv62 (2015).

2. Naik, S. & Russell, S.J. Engineering oncolytic viruses to exploit tumor specific defects in innate immune signaling pathways. *Expert opinion on biological therapy* **9**, 1163-1176 (2009).

3. Arens, R. Rational design of vaccines: learning from immune evasion mechanisms of persistent viruses and tumors. *Advances in immunology* **114**, 217-243 (2012).

4. Butt, A.Q. & Mills, K.H. Immunosuppressive networks and checkpoints controlling antitumor immunity and their blockade in the development of cancer immunotherapeutics and vaccines. *Oncogene* **33**, 4623-4631 (2014).

5. Prestwich, R.J. *et al.* The case of oncolytic viruses versus the immune system: waiting on the judgment of Solomon. *Hum Gene Ther* **20**, 1119-1132 (2009).

6. Dalba, C., Klatzmann, D., Logg, C.R. & Kasahara, N. Beyond oncolytic virotherapy: replication-competent retrovirus vectors for selective and stable transduction of tumors. *Current gene therapy* **5**, 655-667 (2005).

7. Lin, A.H. *et al.* Blockade of type I interferon (IFN) production by retroviral replicating vectors and reduced tumor cell responses to IFN likely contribute to tumor selectivity. *Journal of virology* **88**, 10066-10077 (2014).

8. Logg, C.R., Robbins, J.M., Jolly, D.J., Gruber, H.E. & Kasahara, N. Retroviral replicating vectors in cancer. *Methods in enzymology* **507**, 199-228 (2012).

9. Ram, Z. *et al.* Toxicity studies of retroviral-mediated gene transfer for the treatment of brain tumors. *Journal of neurosurgery* **79**, 400-407 (1993).

10. Traister, R.S. & Lynch, W.P. Reexamination of amphotropic murine leukemia virus neurovirulence: neural stem cell-mediated microglial infection fails to induce acute neurodegeneration. *Virology* **293**, 262-272 (2002).

11. Miller, D.G., Adam, M.A. & Miller, A.D. Gene transfer by retrovirus vectors occurs only in cells that are actively replicating at the time of infection. *Mol Cell Biol* **10**, 4239-4242 (1990).

12. Culver, K.W. *et al.* In vivo gene transfer with retroviral vector-producer cells for treatment of experimental brain tumors. *Science* **256**, 1550-1552 (1992).

13. Hiraoka, K. *et al.* Therapeutic efficacy of replication-competent retrovirus vector-mediated suicide gene therapy in a multifocal colorectal cancer metastasis model. *Cancer research* **67**, 5345-5353 (2007).

14. Hiraoka, K., Kimura, T., Logg, C.R. & Kasahara, N. Tumor-selective gene expression in a hepatic metastasis model after locoregional delivery of a replication-competent retrovirus vector. *Clinical cancer research : an official journal of the American Association for Cancer Research* **12**, 7108-7116 (2006).

15. Kikuchi, E. *et al.* Highly efficient gene delivery for bladder cancers by intravesically administered replication-competent retroviral vectors. *Clinical cancer research : an official journal of the American Association for Cancer Research* **13**, 4511-4518 (2007).

16. Logg, C.R., Tai, C.K., Logg, A., Anderson, W.F. & Kasahara, N. A uniquely stable replication-competent retrovirus vector achieves efficient gene delivery in vitro and in solid tumors. *Human gene therapy* **12**, 921-932 (2001).

17. Ostertag, D. *et al.* Brain tumor eradication and prolonged survival from intratumoral conversion of 5-fluorocytosine to 5-fluorouracil using a nonlytic retroviral replicating vector. *Neuro-oncology* **14**, 145-159 (2012).

18. Tai, C.K. *et al.* Enhanced efficiency of prodrug activation therapy by tumor-selective replicating retrovirus vectors armed with the Escherichia coli purine nucleoside phosphorylase gene. *Cancer gene therapy* **17**, 614-623 (2010).

19. Tai, C.K., Wang, W.J., Chen, T.C. & Kasahara, N. Single-shot, multicycle suicide gene therapy by replication-competent retrovirus vectors achieves long-term survival

benefit in experimental glioma. *Molecular therapy : the journal of the American Society of Gene Therapy* **12**, 842-851 (2005).

20. Wang, W., Tai, C.K., Kasahara, N. & Chen, T.C. Highly efficient and tumor-restricted gene transfer to malignant gliomas by replication-competent retrovirus vectors. *Hum Gene Ther* **14**, 117-127 (2003).

21. Huang, T.T. *et al.* Toca 511 gene transfer and 5-fluorocytosine in combination with temozolomide demonstrates synergistic therapeutic efficacy in a temozolomide-sensitive glioblastoma model. *Cancer gene therapy* **20**, 544-551 (2013).

22. Huang, T.T. *et al.* Intravenous administration of retroviral replicating vector, Toca 511, demonstrates therapeutic efficacy in orthotopic immune-competent mouse glioma model. *Human gene therapy* **26**, 82-93 (2015).

23. Duerner, L.J., Schwantes, A., Schneider, I.C., Cichutek, K. & Buchholz, C.J. Cell entry targeting restricts biodistribution of replication-competent retroviruses to tumour tissue. *Gene Ther* **15**, 1500-1510 (2008).

24. Hlavaty, J. *et al.* Comparative evaluation of preclinical in vivo models for the assessment of replicating retroviral vectors for the treatment of glioblastoma. *J Neurooncol* **102**, 59-69 (2011).

25. Solly, S.K. *et al.* Replicative retroviral vectors for cancer gene therapy. *Cancer gene therapy* **10**, 30-39 (2003).

26. Trajcevski, S. *et al.* Characterization of a semi-replicative gene delivery system allowing propagation of complementary defective retroviral vectors. *The journal of gene medicine* **7**, 276-287 (2005).

27. Read, S.B. *et al.* Human alloreactive CTL interactions with gliomas and with those having upregulated HLA expression from exogenous IFN-gamma or IFN-gamma gene modification. *Journal of interferon & cytokine research : the official journal of the International Society for Interferon and Cytokine Research* **23**, 379-393 (2003).

28. Lampson, L.A. Interpreting MHC class I expression and class I/class II reciprocity in the CNS: reconciling divergent findings. *Microsc Res Tech* **32**, 267-285 (1995).

29. Lampson, L.A. & Hickey, W.F. Monoclonal antibody analysis of MHC expression in human brain biopsies: tissue ranging from "histologically normal" to that showing different levels of glial tumor involvement. *J Immunol* **136**, 4054-4062 (1986).

30. Bigner, D.D. *et al.* Heterogeneity of Genotypic and phenotypic characteristics of fifteen permanent cell lines derived from human gliomas. *J Neuropathol Exp Neurol* **40**, 201-229 (1981).

31. Kuppner, M.C., Hamou, M.F. & de Tribolet, N. Activation and adhesion molecule expression on lymphoid infiltrates in human glioblastomas. *J Neuroimmunol* **29**, 229-238 (1990).

32. Prins, R.M., Cloughesy, T.F. & Liau, L.M. Cytomegalovirus immunity after vaccination with autologous glioblastoma lysate. *The New England journal of medicine* **359**, 539-541 (2008).

33. Perez, O.D. *et al.* Design and selection of Toca 511 for clinical use: modified retroviral replicating vector with improved stability and gene expression. *Molecular therapy : the journal of the American Society of Gene Therapy* **20**, 1689-1698 (2012).

34. Cloughesy, T.F. *et al.* IT-05. Administration of Toca 511 to Subjects with Recurrent HGG Undergoing Repeat Resection. *Neuro Oncol* **16 (suppl 5)**, v110-v111 (2014).

35. Vogelbaum, M.A. *et al.* SURG-09: Results of a Dose Escalation Trial of Toca 511 with Toca Fc in Recurrent HGG Undergoing Repeat Resection. *Neuro Oncol* **17 (suppl 5)**, v216 (2015).

36. Smilowitz, H.M. *et al.* Orthotopic transplantation of v-src-expressing glioma cell lines into immunocompetent mice: establishment of a new transplantable in vivo model for malignant glioma. *Journal of neurosurgery* **106**, 652-659 (2007).

37. Pohl, U. *et al.* Characterization of Tu-2449, a glioma cell line derived from a spontaneous tumor in GFAP-v-src-transgenic mice: comparison with established murine glioma cell lines. *International journal of oncology* **15**, 829-834 (1999).

38. Hung, K. *et al.* The central role of CD4(+) T cells in the antitumor immune response. *J Exp Med* **188**, 2357-2368 (1998).

39. Hirschhorn-Cymerman, D. *et al.* Induction of tumoricidal function in CD4+ T cells is associated with concomitant memory and terminally differentiated phenotype. *J Exp Med* **209**, 2113-2126 (2012).

40. Mucida, D. *et al.* Transcriptional reprogramming of mature CD4(+) helper T cells generates distinct MHC class II-restricted cytotoxic T lymphocytes. *Nat Immunol* **14**, 281-289 (2013).

41. Perez-Diez, A. *et al.* CD4 cells can be more efficient at tumor rejection than CD8 cells. *Blood* **109**, 5346-5354 (2007).

42. Vincent, J. *et al.* 5-Fluorouracil selectively kills tumor-associated myeloid-derived suppressor cells resulting in enhanced T cell-dependent antitumor immunity. *Cancer research* **70**, 3052-3061 (2010).

43. Aghi, M., Vogelbaum, M. Surgical Trial Results: Tocagen. Journal of Neuro-Oncology; 2015; Washington D.C.; 2015. p. 611-619.

44. Aghi, M. *et al.* AT-02. Intratumoral Delivery of the Retroviral Replicating Vector (RRV) Toca 511 in Subjects with Recurrent High Grade Glioma: Interim Report of a Phase I Study (NCT 01156584). *Neuro Oncol* **16 (suppl 5)**, v8 (2014).

45. Delamarre, L., Mellman, I. & Yadav, M. Cancer immunotherapy. Neo approaches to cancer vaccines. *Science* **348**, 760-761 (2015).

46. Kalkanis, S. *et al.* AT-29. Intravenous Administration of Toca 511 in Patients with Recurrent Glioblastoma. *Neuro Oncol* **16 (suppl 5)**, v15 (2014).

47. Stupp, R. *et al.* Effects of radiotherapy with concomitant and adjuvant temozolomide versus radiotherapy alone on survival in glioblastoma in a randomised phase III study: 5-year analysis of the EORTC-NCIC trial. *The Lancet. Oncology* **10**, 459-466 (2009).

48. Weil, R.J., Palmieri, D.C., Bronder, J.L., Stark, A.M. & Steeg, P.S. Breast cancer metastasis to the central nervous system. *The American journal of pathology* **167**, 913-920 (2005).

49. Virasch, N. & Kruse, C.A. Strategies using the immune system for therapy of brain tumors. *Hematol Oncol Clin North Am* **15**, 1053-1071 (2001).

50. Paul, D.B. & Kruse, C.A. Immunologic approaches to therapy for brain tumors. *Curr Neurol Neurosci Rep* **1**, 238-244 (2001).

51. Kruse, C.A., Kong, Q., Schiltz, P.M. & Kleinschmidt-Demasters, B.K. Migration of activated lymphocytes when adoptively transferred into cannulated rat brain. *J Neuroimmunol* **55**, 11-21 (1994).

52. Fleshner, M., Watkins, L.R., Redd, J.M., Kruse, C.A. & Bellgrau, D. A 9L gliosarcoma transplantation model for studying adoptive immunotherapy into the brains of conscious rats. *Cell Transplant.* **1**, 307-312 (1992).

53. Kruse, C.A., Lillehei, K.O., Mitchell, D.H., Kleinschmidt-DeMasters, B. & Bellgrau, D. Analysis of interleukin 2 and various effector cell populations in adoptive immunotherapy of 9L rat gliosarcoma: allogeneic cytotoxic T lymphocytes prevent tumor take. *Proc Natl Acad Sci USA* **87**, 9577-9581 (1990).

54. Redd, J.M., Lagarde, A.C., Kruse, C.A. & Bellgrau, D. Allogeneic tumor-specific cytotoxic T lymphocytes. *Cancer immunology, immunotherapy : CII* **34**, 349-354 (1992).

55. Kulprathipanja, N.V. & Kruse, C.A. Microglia phagocytose alloreactive CTL-damaged 9L gliosarcoma cells. *J Neuroimmunol* **153**, 76-82 (2004).

56. Kruse, C.A. *et al.* Treatment of recurrent glioma with intracavitary alloreactive cytotoxic T lymphocytes and interleukin-2. *Cancer immunology, immunotherapy : CII* **45**, 77-87 (1997).

57. Kruse, C.A. & Rubinstein, D. Cytotoxic T Lymphocytes Reactive to Patient Major Histocompatibility Proteins for Therapy of Recurrent Primary Brain Tumors. In: Liau, L.M., Cloughesy, T.F., Becker, D.P. & Bigner, D.D. (eds). *Brain Tumor Immunotherapy*. Humana Press: Totowa, 2001, pp 149-170.

58. Gomez, G.G. & Kruse, C.A. Subsets within alloreactive CTL (aCTL) exhibit upregulated proinflammatory cytokine secretion: aCTL response to coincubation with irrelevant and relevant parental and immunoresistant (IR) gliomas *FASEB J* **20**, LB120-LB121 (2006).

59. Adler, A.J. Mechanisms of T cell tolerance and suppression in cancer mediated by tumor-associated antigens and hormones. *Curr Cancer Drug Targets* **7**, 3-14 (2007).

60. Flavell, R.A., Sanjabi, S., Wrzesinski, S.H. & Licona-Limon, P. The polarization of immune cells in the tumour environment by TGFbeta. *Nat Rev Immunol* **10**, 554-567 (2010).

61. Zitvogel, L., Tesniere, A. & Kroemer, G. Cancer despite immunosurveillance: immunoselection and immunosubversion. *Nat Rev Immunol* **6**, 715-727 (2006).

62. Zou, W. Regulatory T cells, tumour immunity and immunotherapy. *Nat Rev Immunol* **6**, 295-307 (2006).

63. Kruse, C.A. *et al.* Systemic chemotherapy combined with local adoptive immunotherapy cures rats bearing 9L gliosarcoma. *J Neurooncol* **15**, 97-112 (1993).

64. Burrows, F.J. *et al.* Purified herpes simplex virus thymidine kinase retroviral particles: III. Characterization of bystander killing mechanisms in transfected tumor cells. *Cancer gene therapy* **9**, 87-95 (2002).

65. Kruse, C.A. *et al.* Purified herpes simplex thymidine kinase retroviral particles. II. Influence of clinical parameters and bystander killing mechanisms. *Cancer gene therapy* **7**, 118-127 (2000).

66. Kruse, C.A. *et al.* Purified herpes simplex thymidine kinase Retrovector particles. I. In vitro characterization, in situ transduction efficiency, and histopathological analyses of gene therapy-treated brain tumors. *Cancer gene therapy* **4**, 118-128 (1997).

67. Ram, Z., Culver, K.W., Walbridge, S., Blaese, R.M. & Oldfield, E.H. In situ retroviral-mediated gene transfer for the treatment of brain tumors in rats. *Cancer research* **53**, 83-88 (1993).

68. Rainov, N.G. A phase III clinical evaluation of herpes simplex virus type 1 thymidine kinase and ganciclovir gene therapy as an adjuvant to surgical resection and radiation in adults with previously untreated glioblastoma multiforme. *Human gene therapy* **11**, 2389-2401 (2000).

69. Rainov, N.G. & Ren, H. Clinical trials with retrovirus mediated gene therapy--what have we learned? *J Neurooncol* **65**, 227-236 (2003).

70. Kikuchi, E. *et al.* Delivery of replication-competent retrovirus expressing Escherichia coli purine nucleoside phosphorylase increases the metabolism of the prodrug, fludarabine phosphate and suppresses the growth of bladder tumor xenografts. *Cancer gene therapy* **14**, 279-286 (2007).

71. Logg, C.R. & Kasahara, N. Retrovirus-mediated gene transfer to tumors: utilizing the replicative power of viruses to achieve highly efficient tumor transduction in vivo. *Methods Mol Biol* **246**, 499-525 (2004).

72. Paar, M. *et al.* Effects of viral strain, transgene position, and target cell type on replication kinetics, genomic stability, and transgene expression of replication-competent murine leukemia virus-based vectors. *Journal of virology* **81**, 6973-6983 (2007).

73. Kawasaki, Y. *et al.* Replication-competent retrovirus vector-mediated prodrug activator gene therapy in experimental models of human malignant mesothelioma. *Cancer gene therapy* **18**, 571-578 (2011).

74. Wang, W. *et al.* Use of replication-competent retroviral vectors in an immunocompetent intracranial glioma model. *Neurosurgical focus* **20**, E25 (2006).

75. Gomez, G.G. & Kruse, C.A. Isolation and culture of human brain tumor cells. *Methods Mol Med* **88**, 101-109 (2004).

76. Gomez, G.G., Hickey, M.J., Tritz, R. & Kruse, C.A. Immunoresistant Human Glioma Cell Clones Selected with Alloreactive Cytotoxic T Lymphocytes: Downregulation of Multiple Proapoptotic Factors. *Gene Ther Mol Biol* **12**, 101-110 (2008).

77. Gomez, G.G., Varella-Garcia, M. & Kruse, C.A. Isolation of immunoresistant human glioma cell clones after selection with alloreactive cytotoxic T lymphocytes: cytogenetic and molecular cytogenetic characterization. *Cancer genetics and cytogenetics* **165**, 121-134 (2006).

78. Zhang, J.G. *et al.* Antigenic profiling of glioma cells to generate allogeneic vaccines or dendritic cell-based therapeutics. *Clinical cancer research : an official journal of the American Association for Cancer Research* **13**, 566-575 (2007).

79. Kruse, C.A. & Beck, L.T. Artificial-capillary-system development of human alloreactive cytotoxic T-lymphocytes that lyse brain tumours. *Biotechnol Appl Biochem* **25 (Pt 3)**, 197-205 (1997).

80. Tai, C.K. *et al.* Antibody-mediated targeting of replication-competent retroviral vectors. *Human gene therapy* **14**, 789-802 (2003).

81. Lamers, C.H., Willemsen, R.A., Luider, B.A., Debets, R. & Bolhuis, R.L. Protocol for gene transduction and expansion of human T lymphocytes for clinical immunogene therapy of cancer. *Cancer gene therapy* **9**, 613-623 (2002).

82. Gomez, G.G. & Kruse, C.A. Cellular and functional characterization of immunoresistant human glioma cell clones selected with alloreactive cytotoxic T lymphocytes reveals their up-regulated synthesis of biologically active TGF-beta. *Journal of immunotherapy (Hagerstown, Md. : 1997)* **30**, 261-273 (2007).

83. Fabre, J.W. The allogeneic response and tumor immunity. *Nat Med* **7**, 649-652 (2001).

84. Kranz, D.M. Incompatible differences: view of an allogeneic pMHC-TCR complex. *Nat Immunol* **1**, 277-278 (2000).

85. Suchin, E.J. *et al.* Quantifying the frequency of alloreactive T cells in vivo: new answers to an old question. *J Immunol* **166**, 973-981 (2001).

86. Hedfors, I.A., Beckstrom, K.J., Benati, C., Bonini, C. & Brinchmann, J.E. Retrovirus mediated gene transduction of human T-cell subsets. *Cancer immunology, immunotherapy : CII* **54**, 759-768 (2005).

87. Marktel, S. *et al.* Immunologic potential of donor lymphocytes expressing a suicide gene for early immune reconstitution after hematopoietic T-cell-depleted stem cell transplantation. *Blood* **101**, 1290-1298 (2003).

88. Koning, F.A. *et al.* Defining APOBEC3 expression patterns in human tissues and hematopoietic cell subsets. *Journal of virology* **83**, 9474-9485 (2009).

89. Stopak, K.S., Chiu, Y.L., Kropp, J., Grant, R.M. & Greene, W.C. Distinct patterns of cytokine regulation of APOBEC3G expression and activity in primary lymphocytes, macrophages, and dendritic cells. *J Biol Chem* **282**, 3539-3546 (2007).

90. Chiu, Y.L. & Greene, W.C. APOBEC3G: an intracellular centurion. *Philos Trans R Soc Lond B Biol Sci* **364**, 689-703 (2009).

91. Cole, C. *et al.* Tumor-targeted, systemic delivery of therapeutic viral vectors using hitchhiking on antigen-specific T cells. *Nat Med* **11**, 1073-1081 (2005).

92. Stupp, R. *et al.* Radiotherapy plus concomitant and adjuvant temozolomide for glioblastoma. *The New England journal of medicine* **352**, 987-996 (2005).

93. Wen, P.Y. & Kesari, S. Malignant gliomas in adults. *The New England journal of medicine* **359**, 492-507 (2008).

94. Weiss, T., Weller, M. & Roth, P. Immunotherapy for glioblastoma: concepts and challenges. *Current opinion in neurology* **28**, 639-646 (2015).

95. Sampson, J.H. *et al.* Immunologic escape after prolonged progression-free survival with epidermal growth factor receptor variant III peptide vaccination in patients with newly diagnosed glioblastoma. *Journal of clinical oncology : official journal of the American Society of Clinical Oncology* **28**, 4722-4729 (2010).

96. Phuphanich, S. *et al.* Phase I trial of a multi-epitope-pulsed dendritic cell vaccine for patients with newly diagnosed glioblastoma. *Cancer immunology, immunotherapy : CII* **62**, 125-135 (2013).

97. Lu, C.W. & Roth, M.J. Functional characterization of the N termini of murine leukemia virus envelope proteins. *Journal of virology* **75**, 4357-4366 (2001).

98. Hudrisier, D., Oldstone, M.B. & Gairin, J.E. The signal sequence of lymphocytic choriomeningitis virus contains an immunodominant cytotoxic T cell epitope that is restricted by both H-2D(b) and H-2K(b) molecules. *Virology* **234**, 62-73 (1997).

99. Boulter, J.M. *et al.* Potent T cell agonism mediated by a very rapid TCR/pMHC interaction. *European journal of immunology* **37**, 798-806 (2007).

100. Yang, I. *et al.* Modulation of major histocompatibility complex Class I molecules and major histocompatibility complex-bound immunogenic peptides induced by interferon-alpha and interferon-gamma treatment of human glioblastoma multiforme. *Journal of neurosurgery* **100**, 310-319 (2004).

101. Chesebro, B. & Wehrly, K. Different murine cell lines manifest unique patterns of interference to superinfection by murine leukemia viruses. *Virology* **141**, 119-129 (1985).

102. Rein, A. Interference grouping of murine leukemia viruses: a distinct receptor for the MCF-recombinant viruses in mouse cells. *Virology* **120**, 251-257 (1982).

103. Slingsby, J.H. *et al.* Analysis of 4070A envelope levels in retroviral preparations and effect on target cell transduction efficiency. *Human gene therapy* **11**, 1439-1451 (2000).

104. Miller, D.G. & Miller, A.D. A family of retroviruses that utilize related phosphate transporters for cell entry. *Journal of virology* **68**, 8270-8276 (1994).

105. Roe, T., Reynolds, T.C., Yu, G. & Brown, P.O. Integration of murine leukemia virus DNA depends on mitosis. *The EMBO journal* **12**, 2099-2108 (1993).

106. Albright, L., Madigan, J.C., Gaston, M.R. & Houchens, D.P. Therapy in an intracerebral murine glioma model, using Bacillus Calmette-Guerin, neuraminidase-treated tumor cells, and 1-(2-chloroethyl)-3-cyclohexyl-1-nitrosourea. *Cancer research* **35**, 658-665 (1975).

107. Takeda, E. *et al.* Mouse APOBEC3 restricts friend leukemia virus infection and pathogenesis in vivo. *Journal of virology* **82**, 10998-11008 (2008).